Continued optimization of a microelectrolysis treatment process for removal of arsenic from landfill gas condensate, characterization of materials, and evaluation of Fe as a predictor of treatment monitoring

Geneva Lynne Schlepp

A thesis
submitted in partial fulfilment of the
requirements for the degree of

Master of Science in Civil Engineering

University of Washington
2024

Committee:
Gregory Korshin
Jessica Ray

Program Authorized to Offer Degree:
College of Engineering

University of Washington

Abstract

Continued optimization of a microelectrolysis treatment process for removal of arsenic from landfill gas condensate, characterization of materials, and evaluation of Fe as a predictor of treatment monitoring

Geneva Lynne Schlepp

Chair of the Supervisory Committee:

Gregory Korshin

Department of Civil and Environmental Engineering

Landfill gas condensate is formed during landfill gas (LFG) purification that must be carried out to produce pipeline-quality renewable natural gas. LFG condensates (LGC) are known to contain high levels of arsenic whose presence may result in exceeding applicable discharge limits. Arsenic speciation in LGC is dominated by organo-As compounds that are difficult or impossible to remove by conventional methods. This difficulty may be circumvented via microelectrolysis (ME) treatment that uses a combination of zero-valent iron (ZVI) and granular activated carbon (GAC). This study compared the performance of alternative types of ZVI/GAC media and examined effects of other treatment variables including pH, agitation methods, and media cycling. This study also addressed the significance of iron release as a treatment indicator. Experimental results

showed the ME treatment reliably removes up to >90% of arsenic from LGC in several consecutive treatment cycles. Release of dissolved iron from the treatment media tends to be correlated with arsenic removal and the quantification of iron release in ME treatment may be a suitable option to monitor the efficiency of arsenic removal in field conditions.

Acknowledgments

Writing this thesis filled me with so much gratitude for my time spent at the University of Washington. I am incredibly grateful for Dr. Korshin's invitation to join his research group which changed the trajectory of my master's education wholly for the better. I have thoroughly enjoyed working with Dr. Korshin and will dearly miss hearing the many languages he uses to direct group meetings, viewing and discussing art, and receiving his mentorship. Thank you, Dr. Korshin, for the great care you have taken in guiding my research efforts and for your encouragement. I am extremely fortunate to have had my education sponsored by the King County Solid Waste Division and am very grateful to have been entrusted to work on this very special project. Thank you to Said Seddiki, Laura Belt, Kris McArthur, Joan Kenton, and other KC SWD staff for their support of this research. I'm grateful for my involvement with WSP's consulting engineers working on this project: Karen Budgell, McBride Galt, and Scott Keen. Thank you, Dr. Ray, for your time and efforts to be on my thesis committee, and for being a wonderful instructor. I want to give a very special thank you to Ivette Pinochet-Troncoso for setting an incredible standard in the laboratory and for her efforts in training me when I joined the group. Over bench testing, cleaning glassware, and spending many hours at ICP, we became not only good colleagues but also friends. Thank you Annapaola Panico for your sunny disposition, Italian sayings (which make everything better), and friendship. You're a joy to work alongside, I admire your work ethic and attitude, and I cannot wait for a Napoli adventure with you. Thank you Wanyu Mao for being such a sweet labmate. I will miss your homemade cooking, admiring your beautiful art, and working together in the lab. Thank you Yak Yerbich-Louman for being an amazing colleague. And finally, thank you Mom, Dad, Mya, Beau, and all my family and friends who have supported me during my graduate school journey. I feel incredibly blessed and am very excited to see where the Lord leads my next chapter.

1. Table of Contents

ABSTRACT **2**

ACKNOWLEDGMENTS **1**

LIST OF FIGURES **5**

LIST OF TABLES **13**

LIST OF ABBREVIATIONS **15**

1 LITERATURE REVIEW AND INTRODUCTION **16**

1.1 THE ARSENIC CYCLE: SOURCES, SPECIATION, AND MOBILIZATION 16

1.2 LANDFILL GAS GENERATION, COLLECTION, AND PROCESSING 21

1.3 LANDFILL GAS CONDENSATE COMPOSITION AND TREATMENT TECHNOLOGIES 25

1.4 LFG AS A SOURCE OF RENEWABLE NATURAL GAS 29

1.5 LANDFILL CHARACTERIZATION 32

1.6 DEVELOPMENT OF MICROELECTROLYSIS TREATMENT (I.E., PREVIOUS WORK) 35

1.7 GOALS OF THIS STUDY 37

2 MATERIALS AND EQUIPMENT **39**

2.1 EXPERIMENTAL CHEMICALS AND MATERIALS 39

2.1.1 ICP-MS Standards *39*

2.1.2 Chemicals and gases *39*

2.1.3 Active media for microelectrolysis treatment *40*

2.1.4 Laboratory consumables *44*

2.2 MATERIALS AND EQUIPMENT USED FOR COLUMN REACTOR CONSTRUCTION 44

2.3 LFG CONDENSATE SAMPLING SUPPLIES AND PPE 45

2.4 ME TREATMENT AND ASSOCIATED EXPERIMENTS EQUIPMENT/MATERIALS 45

2.5 PIPETTES 46

3 MICROELECTROLYSIS (ME) REACTOR DESIGN AND ASSEMBLY **48**

3.1 ME REACTOR BACKGROUND 48
3.2 REACTOR RE-DESIGN AND CONSTRUCTION 49
3.2.1 3D design and printing 50
3.2.2 Reactor assembly 50
4 METHODS 52
4.1 LFG CONDENSATE SAMPLING 52
4.2 ME TREATMENT 53
4.2.1 Safety and waste disposal 53
4.2.2 ME treatment operations 54
4.2.3 Active media dosing Calculations 58
4.3 ANALYTICAL METHODS 58
4.3.1 Analytical balances 58
4.3.2 ICP-MS 58
4.3.3 ORP measurements 60
4.3.4 Determination of particles sizes of the active media by sieving 61
4.3.5 BET measurements of specific surface area 62
4.3.6 Mixing speed determination 63
4.4 HAZARDOUS WASTE MANAGEMENT 64
5 EXPERIMENTAL RESULTS & DISCUSSION 65
5.1 MATERIAL CHARACTERIZATION 65
5.1.1 Sieving 65
5.1.2 BET 66
5.1.3 Settling time 69
5.1.4 Quantifying activation effects of active media through pH drift 69
5.1.5 Comparison of As & Sb removal using alternative ZVI types 73
5.1.6 Effects of GAC type on As and Sb removal 74
5.2 ME TREATMENT OPTIMIZATION 77

5.2.1 Variations in active media dose *77*
5.2.2 Effects of pH variations on As/Sb removal *82*
5.2.3 Effects of variations of mixing conditions: axial flow and mixing intensity *88*
5.3 ME TREATMENT CYCLING 95
5.3.1 Delayed cycling *95*
5.3.2 Examination of effects of an extended number of cycling *103*
5.3.3 Variations of the top-offs compositions *105*
5.3.4 Typical up flow cycles *109*
5.3.5 Variations in pH *111*
5.3.6 Comparing efficiencies of ME treatment using alternative top-off compositions and doses *113*
5.4 IRON AS A PREDICTOR OF AS REMOVAL IN ME TREATMENT 115
6 CONCLUSIONS AND SUGGESTIONS FOR FUTURE WORK 122
6.1 MATERIAL CHARACTERIZATION CONCLUSIONS 122
6.2 ME TREATMENT OPTIMIZATION CONCLUSIONS 123
6.3 ME TREATMENT CYCLING CONCLUSIONS 124
6.4 IRON AS A TREATMENT PREDICTOR CONCLUSIONS 126
6.5 SUGGESTIONS FOR FUTURE WORK 126
7 APPENDIX 129
7.1 SAMPLE ROUND COMPOSITION QUANTIFIED BY UW ICP-MS ANALYSIS 129
7.2 CONFIRMATION OF UW ICP-MS ANALYSIS WITH KCEL 129
7.2.1 September 2023 samples *129*
7.2.2 December 2023 samples *134*
8 REFERENCES 140

List of figures

Figure 1.1 Effects of pH on the speciation of arsenite [As(III)] (EPA, 2003) 17

Figure 1.2 Effects of pH on the speciation of arsenate [As(V)] (EPA, 2003) 18

Figure 1.3 The Arsenic Cycle: natural and anthropogenic mobilization (Mudhoo et al., 2011) ... 19

Figure 1.4 The Challenger Pathway for biomethylation of arsenic species (Challenger, 1947) 20

Figure 1.5 Total MSW generated in the U.S. in 2018, by material. Organic content includes Paper and Paperboard, Yard Trimmings, Food, and Wood. (EPA, 2023) 21

Figure 1.6 Profile of working landfill with LFG collection and conveyance to a LFG-to-energy processing plan (Wasatch Integrated Waste Management District, n.d.) 22

Figure 1.7 Changes of LFG composition over time (Waga Energy, n.d.) 23

Figure 1.8 LFG processing stages and end uses (LMOP, 2024a) 24

Figure 1.9 organo-As removal from LFG condensate treated by SBR and RO (Zhao et al. 2013) 28

Figure 1.10 U.S. primary energy consumption by energy source, 2022 (EIA, 2023) 29

Figure 1.11 LMOP proposed candidate landfills for LFG-to-energy processes (LMOP, 2023a) .. 31

Figure 2.1 ZVI Particle Size Distribution, by mass 41

Figure 2.2 GAC Particle Size Distribution, by mass 42

Figure 2.3 Estimated ZVI Specific Surface Area, by diameter 42

Figure 3.1 General view of BC2 ME reactor with annotated design elements and dimensions. .. 51

Figure 4.1 Visual of ME treatment experimental operations set up with BC4..... 55

Figure 5.1 BET adsorption plot for IPW GAC 68

Figure 5.2 BET adsorption plot for Thermo Scientific GAC 68

Figure 5.3 Overall pH drift from 3.0 versus time since addition of active media for 50 g/L ZVI & GAC (2:1) dose 71

Figure 5.4 Overall pH drift from 3.0 versus time since addition of active media for 16 g/L ZVI and variable GAC dose..... 72

Figure 5.5 Initial pH drift (t = 0 to 1 minute) from 3.0 versus time since addition of active media for 16 g/L ZVI and variable GAC dose..... 73
Figure 5.6 Comparison of As/Sb removal for varying ZVI types with ME treatment conditions of 2L of SR 17 in BC3 with 50 g/L ZVI & IPW GAC (2:1) dose, continually mixed for 30-minutes at 1000 RPM at pH 3.0 with pre-treatment CO2 purging..... 74
Figure 5.7 Comparison of As/Sb concentration versus contact time for varying GAC types with ME treatment conditions of 2L of SR 17 in BC3 with 50 g/L LC Plus ZVI & GAC (2:1) dose, continually mixed for 30-minutes at 1000 RPM at pH 3.0 with pre-treatment CO2 purging..... 75
Figure 5.8 Comparison of As/Sb removal for varying GAC types with ME treatment conditions of 2L of SR 17 in BC3 with 50 g/L LC Plus ZVI & GAC (2:1) dose, continually mixed for 30-minutes at 1000 RPM at pH 3.0 with pre-treatment CO2 purging 75
Figure 5.9 Comparison of As removal for cycles with varying GAC types with ME treatment conditions of 2L of SR 19 in BC2 with initial 50 g/L CR ZVI & GAC (2:1) dose and 1 g/L GAC top-offs, continually mixed for 3- 30-minute cycles at 1000 RPM at pH 3.0 with continuous 1 LPM CO2 purging..... 76
Figure 5.10 Comparison of As removal for varying active media doses (2:1) with ME treatment conditions of 2L of SR 17 in BC3 with variable LC Plus ZVI & IPW GAC (2:1) dose, continually mixed for 1-hr at 1000 RPM at pH 3.0 with pre-treatment CO2 purging 78
Figure 5.11 Comparison of Sb removal for varying active media doses (2:1) with ME treatment conditions of 2L of SR 17 in BC3 with variable LC Plus ZVI & IPW GAC (2:1) dose, continually mixed for 1-hr at 1000 RPM at pH 3.0 with pre-treatment CO2 purging 78
Figure 5.12 Comparison of As log-normalized removal for varying active media doses (2:1) with ME treatment conditions of 2L of SR 17 in BC3 with variable LC Plus ZVI & IPW GAC (2:1) dose, continually mixed for 1-hr at 1000 RPM at pH 3.0 with pre-treatment CO2 purging 79

Figure 5.13 Comparison of Sb log-normalized removal for varying active media doses (2:1) with ME treatment conditions of 2L of SR 17 in BC3 with variable LC Plus ZVI & IPW GAC (2:1) dose, continually mixed for 1-hr at 1000 RPM at pH 3.0 with pre-treatment CO2 purging 79
Figure 5.14 Comparison of redox potentials, by probe for varying active media doses (2:1) with ME treatment conditions of 2L of SR 17 in BC3 with variable LC Plus ZVI & IPW GAC (2:1) dose, continually mixed for 1-hr at 1000 RPM at pH 3.0 with pre-treatment CO2 purging 80
Figure 5.15 Comparison of As removal for varying GAC doses with ME treatment conditions of 2L of SR 17 in BC3 with constant 33.3 g/L CR ZVI & variable IPW GAC dose, continually mixed for 1-hr at 1000 RPM at pH 3.0 with pre-treatment CO2 purging 81
Figure 5.16 Comparison of Sb removal for varying GAC doses with ME treatment conditions of 2L of SR 17 in BC3 with constant 33.3 g/L CR ZVI & variable IPW GAC dose, continually mixed for 1-hr at 1000 RPM at pH 3.0 with pre-treatment CO2 purging 82
Figure 5.17 Comparison of As removal for varying pH (20 g/L dose) with ME treatment conditions of 2L of SR 17 in BC3 with 20 g/L LC Plus ZVI & IPW GAC (2:1) dose, continually mixed for 30-minutes at 1000 RPM at variable pH with pre-treatment CO2 purging 83
Figure 5.18 Comparison of Sb removal for varying pH (20 g/L dose) with ME treatment conditions of 2L of SR 17 in BC3 with 20 g/L LC Plus ZVI & IPW GAC (2:1) dose, continually mixed for 30-minutes at 1000 RPM at variable pH with pre-treatment CO2 purging 84
Figure 5.19 Comparison of As removal for varying pH (50 g/L dose) with ME treatment conditions of 2L of SR 17 in BC3 with 50 g/L CR ZVI & IPW GAC (2:1) dose, continually mixed for 1-hr at 1000 RPM at variable pH with pre-treatment CO2 purging.....85
Figure 5.20 Comparison of Sb removal for varying pH (50 g/L dose) with ME treatment conditions of 2L of SR 17 in BC3 with 50 g/L CR ZVI & IPW GAC (2:1) dose, continually mixed for 1-hr at 1000 RPM at variable pH with pre-treatment CO2 purging.....86

Figure 5.21 Comparison of As log-normalized removal for varying pH (50 g/L dose) with ME treatment conditions of 2L of SR 17 in BC3 with 50 g/L CR ZVI & IPW GAC (2:1) dose, continually mixed for 1-hr at 1000 RPM at variable pH with pre-treatment CO2 purging 86
Figure 5.22 Comparison of Sb log-normalized removal for varying pH (50 g/L dose) with ME treatment conditions of 2L of SR 17 in BC3 with 50 g/L CR ZVI & IPW GAC (2:1) dose, continually mixed for 1-hr at 1000 RPM at variable pH with pre-treatment CO2 purging 87
Figure 5.23 Comparison of redox potentials, by probe for varying pH (50 g/L dose) with ME treatment conditions of 2L of SR 17 in BC3 with 50 g/L CR ZVI & IPW GAC (2:1) dose, continually mixed for 1-hr at 1000 RPM at variable pH with pre-treatment CO2 purging 88
Figure 5.24 Differentiating degree of mixing based on particle suspension (Dynamix Agitators, 2020).....89
Figure 5.25 Comparison of As removal for varying axial flow patterns with ME treatment conditions of 2L of SR 19 in BC3 with 50 g/L CR ZVI & IPW GAC (2:1) dose and 1 g/L combined top-offs, continually mixed for 3- 1-hr cycles at 1000 RPM at pH 3.0 with pre-treatment CO2 purging..... 91
Figure 5.26 Comparison of As removal for varying mixing intensities with ME treatment conditions of 2L of SR 17 in BC3 with 50 g/L CR ZVI & IPW GAC (2:1) dose, continually mixed for 1-hr at variable RPM at pH 3.0 with pre-treatment CO2 purging.....93
Figure 5.27 Comparison of Sb removal for varying mixing intensities with ME treatment conditions of 2L of SR 17 in BC3 with 50 g/L CR ZVI & IPW GAC (2:1) dose, continually mixed for 1-hr at variable RPM at pH 3.0 with pre-treatment CO2 purging.....93
Figure 5.28 Comparison of As log-normalized removal for varying mixing intensities with ME treatment conditions of 2L of SR 17 in BC3 with 50 g/L CR ZVI & IPW GAC (2:1) dose, continually mixed for 1-hr at variable RPM at pH 3.0 with pre-treatment CO2 purging 94

Figure 5.29 Comparison of Sb log-normalized removal for varying mixing intensities with ME treatment conditions of 2L of SR 17 in BC3 with 50 g/L CR ZVI & IPW GAC (2:1) dose, continually mixed for 1-hr at variable RPM at pH 3.0 with pre-treatment CO2 purging 94
Figure 5.30 Comparison of redox potentials, by probe for varying mixing intensities with ME treatment conditions of 2L of SR 17 in BC3 with 50 g/L CR ZVI & IPW GAC (2:1) dose, continually mixed for 1-hr at variable RPM at pH 3.0 with pre-treatment CO2 purging 95
Figure 5.31 Comparison of As removal for cycles with 2-hr delays and no top-offs with ME treatment conditions of 2L of SR 17 in BC3 with 50 g/L CR ZVI & IPW GAC (2:1) dose, continually mixed for 10- 1-hr cycles, with 2-hour to overnight delays, at 1000 RPM at pH 3.0 with pre-treatment CO2 purging..... 96
Figure 5.32 Comparison of Sb removal for cycles with 2-hr delays and no top-offs with ME treatment conditions of 2L of SR 17 in BC3 with 50 g/L CR ZVI & IPW GAC (2:1) dose, continually mixed for 10- 1-hr cycles, with 2-hour to overnight delays, at 1000 RPM at pH 3.0 with pre-treatment CO2 purging..... 97
Figure 5.33 Comparison of As log-normalized removal for cycles with 2-hr delays and no top-offs with ME treatment conditions of 2L of SR 17 in BC3 with 50 g/L CR ZVI & IPW GAC (2:1) dose, continually mixed for 10- 1-hr cycles, with 2-hour to overnight delays, at 1000 RPM at pH 3.0 with pre-treatment CO2 purging 98
Figure 5.34 Comparison of Sb log-normalized removal for cycles with 2-hr delays and no top-offs with ME treatment conditions of 2L of SR 17 in BC3 with 50 g/L CR ZVI & IPW GAC (2:1) dose, continually mixed for 10- 1-hr cycles, with 2-hour to overnight delays, at 1000 RPM at pH 3.0 with pre-treatment CO2 purging 98
Figure 5.35 Comparison of apparent first order kinetics removal rate for cycles with 2-hr delays and no top-offs with ME treatment conditions of 2L of SR 17 in BC3 with 50 g/L CR ZVI & IPW GAC (2:1) dose, continually mixed for 10- 1-hr cycles, with 2-hour to overnight delays, at 1000 RPM at pH 3.0 with pre-treatment CO2 purging 100

Figure 5.36 Estimations for required treatment (contact) time to achieve 90% As/Sb removal based on apparent first order kinetics for delayed cycling 101
Figure 5.37 Comparison of As removal for cycle with 21-hr delay and 1 g/L GAC top-off with ME treatment conditions of 2L of SR 18 in BC3 with 50 g/L CR ZVI & IPW GAC (2:1) dose and 1 g/L GAC top-off, continually mixed for 2- 1-hr cycles, with a 21-hr delay, at 1000 RPM at pH 3.0 with pre-treatment N2 purging 102
Figure 5.38 Comparison of Sb removal for cycle with 21-hr delay and 1 g/L GAC top-off with ME treatment conditions of 2L of SR 18 in BC3 with 50 g/L CR ZVI & IPW GAC (2:1) dose and 1 g/L GAC top-off, continually mixed for 2- 1-hr cycles, with a 21-hr delay, at 1000 RPM at pH 3.0 with pre-treatment N2 purging 103
Figure 5.39 Comparison of As removal for an extended number of cycles with ME treatment conditions of 2L of SR 18 in BC3 with 50 g/L CR ZVI & IPW GAC (2:1) dose and 1 g/L GAC top-offs, continually mixed for 20- 1-hr cycles, with minimal delays, at 1000 RPM at pH 3.0 with pre-treatment CO2 purging 105
Figure 5.40 Comparison of Sb removal for an extended number of cycles with ME treatment conditions of 2L of SR 18 in BC3 with 50 g/L CR ZVI & IPW GAC (2:1) dose and 1 g/L GAC top-offs, continually mixed for 20- 1-hr cycles, with minimal delays, at 1000 RPM at pH 3.0 with pre-treatment CO2 purging 105
Figure 5.41 Comparison of As removal for cycles with variable top-offs with ME treatment conditions of 2L of SR 19 in BC3 with 50 g/L CR ZVI & IPW GAC (2:1) dose and variable 1 g/L top-offs, continually mixed for 8- 1-hr cycles at 1000 RPM at pH 3.0 with pre-treatment CO2 purging 106
Figure 5.42 Comparison of Sb removal for cycles with variable top-offs with ME treatment conditions of 2L of SR 19 in BC3 with 50 g/L CR ZVI & IPW GAC (2:1) dose and variable 1 g/L top-offs, continually mixed for 8- 1-hr cycles at 1000 RPM at pH 3.0 with pre-treatment CO2 purging 107

Figure 5.43 Comparison of redox potentials, by probe for cycles with variable top-offs with ME treatment conditions of 2L of SR 19 in BC3 with 50 g/L CR ZVI & IPW GAC (2:1) dose and variable 1 g/L top-offs, continually mixed for 8- 1-hr cycles at 1000 RPM at pH 3.0 with pre-treatment CO2 purging.....108
Figure 5.44 Comparison of As removal versus Fe release for cycles with variable top-offs with ME treatment conditions of 2L of SR 19 in BC3 with 50 g/L CR ZVI & IPW GAC (2:1) dose and variable 1 g/L top-offs, continually mixed for 8- 1-hr cycles at 1000 RPM at pH 3.0 with pre-treatment CO2 purging.....108
Figure 5.45 Comparison of acid required to maintain pH 3.0 for cycles with variable top-offs with ME treatment conditions of 2L of SR 19 in BC3 with 50 g/L CR ZVI & IPW GAC (2:1) dose and variable 1 g/L top-offs, continually mixed for 8- 1-hr cycles at 1000 RPM at pH 3.0 with pre-treatment CO2 purging.....109
Figure 5.46 Comparison of As removal for cycles with upflow mixing and 1 g/L GAC top-offs with ME treatment conditions of 2L of SR 18 in BC3 with 50 g/L CR ZVI & IPW GAC (2:1) dose and 1 g/L GAC top-offs, continually mixed for 3- 1-hr cycles at 1000 RPM at pH 3.0 with pre-treatment CO2 purging.....110
Figure 5.47 Comparison of average redox potentials, by cycle for cycles with upflow mixing and 1 g/L GAC top-offs with ME treatment conditions of 2L of SR 18 in BC3 with 50 g/L CR ZVI & IPW GAC (2:1) dose and 1 g/L GAC top-offs, continually mixed for 3- 1-hr cycles at 1000 RPM at pH 3.0 with pre-treatment CO2 purging 111
Figure 5.48 Comparison of As removal for cycles with variable pH with ME treatment conditions of 2L of SR 19 in BC3 with 50 g/L CR ZVI & IPW GAC (2:1) dose and 1 g/L combined top-offs, continually mixed for 6- 1-hr cycles at 1000 RPM at variable pH with pre-treatment CO2 purging.....112
Figure 5.49 Comparison of Sb removal for cycles with variable pH with ME treatment conditions of 2L of SR 19 in BC3 with 50 g/L CR ZVI & IPW GAC (2:1) dose and 1 g/L combined top-offs,

continually mixed for 6- 1-hr cycles at 1000 RPM at variable pH with pre-treatment CO2 purging....113
Figure 5.50 Comparison of As removal for cycles with variable top-off compositions and doses with ME treatment conditions of 2L of variable SR in BC3 with 50 g/L CR ZVI & IPW GAC (2:1) dose and variable top-offs, continually mixed for 3- 1-hr cycles at 1000 RPM at pH 3.0 with pre-treatment CO2 purging....114
Figure 5.51 As removal/Fe release correlations for typical ME treatment at pH 3.0 for Cycles 1 - 3, with tabulated average As removal for ranges of Fe released 118
Figure 5.52 As removal/Fe release correlations for three cycles of typical ME treatment at pH 3.0 in BC4: 2L, SR 19, BC4, 50 g/L CR ZVI & IPW GAC with 2 g/L combined top-offs, pH 3.0 (1M H2SO4), pre-treatment CO2 purging, continuous mixing at 1000 RPM (10-19-2023).....119
Figure 5.53 As removal/Fe release correlations for variable pH experiment for 6 cycles of typical ME treatment: 2L, SR 19, BC3, variable pH 120
Figure 7.1 Comparison of ICP-MS analyses between the UW and KCEL for As, Sb, and Fe.....131
Figure 7.2 Comparison of ICP-MS analyses between the UW and KCEL for As, Sb, and Fe, separated by experiment 132
Figure 7.3 Comparison of UW and KCEL percent removals of As and Sb as determined by ICP-MS analyses (September 2023).... 133
Figure 7.4 Comparison of ICP-MS analyses between the UW and KCEL for As, Sb, Fe, and Cu135
Figure 7.5 Comparison of ICP-MS analyses between the UW and KCEL for As, Sb, and Fe, separated by analysis run 136
Figure 7.6 Comparison of UW and KCEL percent removals of As as determined by ICP-MS analyses (December 2023) 137
Figure 7.7 Comparison of UW and KCEL percent removals of Sb as determined by ICP-MS analyses (December 2023) 138

List of tables

Table 1.1 Treatment efficiency of different physical/chemical technologies for organo-As in SBR effluent (Zhao et al., 2013) 29

Table 2.1 Single element standards used for ICP-MS analyses 39

Table 2.2 Chemicals and purge gases utilized in ME treatment and associated experiments 40

Table 2.3 Specifications of active media products used for ME treatment 40

Table 2.4 Estimations of specific surface area for ME treatment media ZVI, based on sieving data, ranked highest to lowest 43

Table 2.5 BET specific surface area and pore volumes for ME media 43

Table 2.6 Materials used for ME treatment operations and associated experiments 44

Table 2.7 Materials used to build ME treatment column reactor used in this study 45

Table 2.8 Equipment used for ME treatment operations and associated experiments. 46

Table 4.1 Sample round composition quantified by certified laboratories and pH measured prior to ME treatment operations. 53

Table 5.1 ME treatment conditions for varying ZVI types experiment 73

Table 5.2 ME treatment conditions for varying GAC types experiment 74

Table 5.3 ME treatment conditions for cycles with varying GAC types experiment 76

Table 5.4 ME treatment conditions for varying active media doses (2:1) experiment. 77

Table 5.5 ME treatment conditions for varying GAC doses experiment 80

Table 5.6 ME treatment conditions for varying pH (20 g/L dose) experiment 82

Table 5.7 ME treatment conditions for varying pH (50 g/L dose) experiment 85

Table 5.8 ME treatment conditions for varying axial flow patterns experiment 90

Table 5.9 Comparing sulfuric acid (1 M) required to maintain pH 3 for 1-hr treatment cycles for varying axial flow patterns. 91

Table 5.10 ME treatment conditions for varying mixing intensities experiment 92

Table 5.11 ME treatment conditions for cycles with 2-hr delays and no top-offs experiment 96

Table 5.12 Comparison of inter-cycle decrease in As removal for cycles with 2-hr delays and no top-offs. 97
Table 5.13 ME treatment conditions for cycle with 21-hr delay and 1 g/L GAC top-off experiment 101
Table 5.14 ME treatment conditions for an extended number of cycles experiment 103
Table 5.15 ME treatment conditions for cycles with variable top-offs experiment 106
Table 5.16 ME treatment conditions for cycles with upflow mixing and 1 g/L GAC top-offs experiment. 110
Table 5.17 ME treatment conditions for cycles with variable pH experiment 111
Table 5.18 ME treatment conditions for cycles with variable top-off compositions and doses experiment 114
Table 6.1 Comparison of As removal for the first cycle of ME treatment for ME treatment conditions of 2L of LFG condensate sample, 60-minutes treatment length, IPW GAC, and 50 g/L ZVI and GAC (2:1) 124
Table 6.2 Comparison of As removal for cycles of ME treatment for ME treatment conditions of 2L of LFG condensate sample and 50 g/L CR ZVI and IPW GAC (2:1) 126
Table 7.1 Sample round composition quantified by UW ICP-MS analysis 129
Table 7.2 ME treatment conditions for cycles in BC4 with copper catalysis experiment 134
Table 7.3 ME treatment conditions for typical ME treatment cycles in BC4 experiment 134

List of abbreviations

As: arsenic
ASTM: American Society for Testing and Materials
BC: big column
BET: Brunauer Emmett Teller
CFM: cubic feet per minute
CO_2: carbon dioxide
DF: dilution factor
DMA: dimethylarsinic acid
DOE: Department of Ecology
EH&S: Environmental Health & Safety
EIA: Energy Information Administration
EPA: Environmental Protection Agency
Fe: iron
GAC: granular activated carbon
GCCS: gas collection and control systems
GHG: greenhouse gas
GWP: global warming potential
ICP-MS: inductively coupled plasma – mass spectrometry
KCEL: King County Environmental Laboratory
LFG: landfill gas
LGC: landfill gas condensate
LMOP: Landfill Methane Outreach Program
LPM: liters per minute
ME: microelectrolysis
MMA: monomethylarsonic acid
MSW: municipal solid waste
MW: megawatt
N_2: nitrogen
NPDES: National Pollutant Discharge Elimination System
ORP: oxidation-reduction potential
PAC: powder activated carbon
PBR: permeable reactive barrier
PLA: polylactic acid
PNW: Pacific Northwest
POTW: publicly operated treatment works
PPE: personal protective equipment
RNG: renewable natural gas
RO: reverse osmosis
RPM: rotations per minute
RTT: Research Training Testbeds
Sb: antimony
SBR: sequencing batch reactor
SC: small column
SR: sample round
TMA: trimethylarsine
UW: University of Washington
WM: Waste Management
ZVI: zero-valent iron

1 Literature review and introduction

1.1 The Arsenic Cycle: sources, speciation, and mobilization

Arsenic (As) is a naturally occurring ubiquitous element, present in water, air, soil, and food. The element is classified as a semi-metal (or metalloid) due to its variety of redox, protonation and other reactions, as well as for the wide range of its chemical and physical properties. Throughout history, As has been anthropogenically extracted and used for many applications including preparation of pigments and pesticides, wood-preservation, and even chemical warfare. Presently, As is relied upon as a dopant for semiconductor manufacturing, making it a key element in the ever-growing production of electronics. In addition to natural mobilization, As is released to the environment through human activities such as ore mining and smelting, applying fertilizers and pesticides, and burning fossil fuels (Wang et al., 2014). Regardless of its source or purpose, As is a known toxicant/carcinogen with its toxicity/carcinogenicity dependent on its chemical structure. The increased use of As in consumer products, such as semiconductors and wood preservatives, has correspondingly increased the element's anthropogenic mobilization which raises both environmental and human health concerns.

Compounds containing As are classified as either organic (organo-As) or inorganic (inorg-As), meaning they are carbon or non-carbon based, respectively. Also differentiated by its oxidation state, environmental As most often exists in its trivalent (+III) "arsenite" or pentavalent (+V) "arsenate" forms. However, it can also exist in oxidation states of -III and 0 (International Agency for Research on Cancer (IARC), 2012) which, in the case of inorganic As compounds correspond to arsine AsH_3 and elemental arsenic, respectively. Conventionally, when oxidation (or nominal valence) states are quoted, a positive number indicates the loss of electrons, negative for a gain of electrons. Arsenic's valence state is dependent on the local oxidation-reduction conditions. For example, groundwater is often a reductive environment since it is oxygen-depleted which typically promotes the dominance of the reduced form of arsenic: arsenite, H_3AsO_3 and its deprotonated

forms which, in the general context of environmental analytical chemistry, are frequently referred to as As(III). Conversely, surface water is often an oxidative environment, yielding the oxidized form of arsenic: arsenate, H3AsO4 and its deprotonated form, generally referred to as As(V).

Like all acids, arsenite and arsenate's speciation is pH dependent. Arsenite's stepwise deprotonation is shown in Figure 1.1 and that of arsenate in Figure 1.2. The pH, and thus speciation will impact arsenic's treatability since its form dictates the chemical's surface charge. For the treatment of aqueous inorganic arsenic, negatively charged ions tended to be more amenable to removal by adsorption, anion exchange and, in some cases, precipitation. At circumneutral pH ranges (i.e., 6-9), arsenite's dominant species, H3AsO3, is neutral rendering it difficult to remove by treatments which are efficient mostly for anionic forms of the solutes of interest. For this reason, the majority of As treatment processes include oxidation of arsenite to arsenate which at circumneutral pH, is dominated by arsenic anions with charges of -1 or -2. The oxidation of arsenite is often accomplished using chlorine or permanganate (Environmental Protection Agency (EPA), 2003).

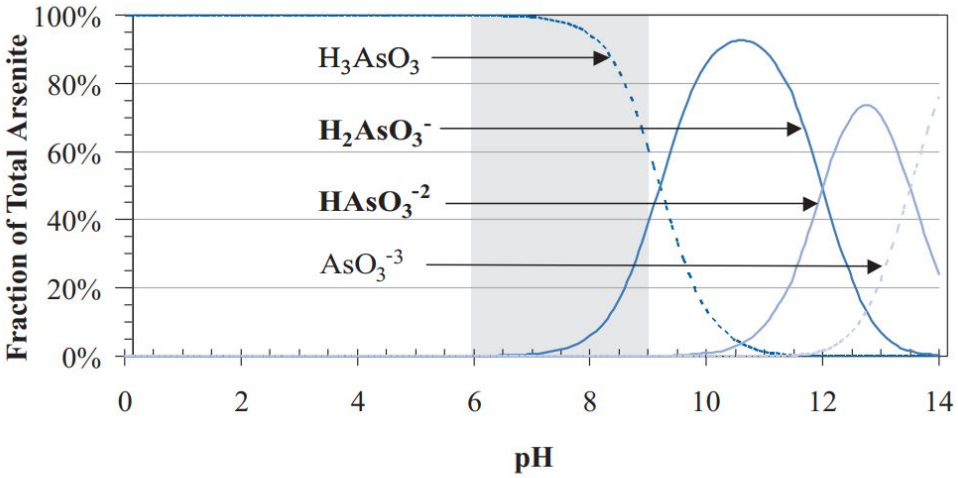

Figure 1.1 Effects of pH on the speciation of arsenite [As(III)] (EPA, 2003)

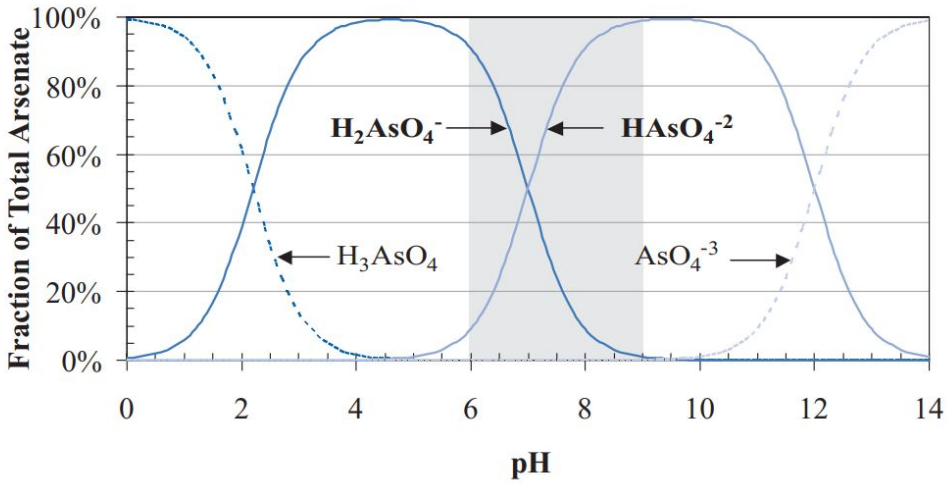

Figure 1.2 Effects of pH on the speciation of arsenate [As(V)] (EPA, 2003)

Inorganic forms of As are deemed to have the highest toxicity and carcinogenicity, and all forms or arsenic are subsequently classified as a human carcinogen. Chronic exposure to inorganic arsenic can cause a variety of cancers including lung, bladder, and skin (American Cancer Society, 2023). Beyond cancer, exposure to inorganic arsenic can result in other adverse health effects impacting the gastrointestinal, cardiovascular, and integumentary systems (Agusa et al., 2011). While organo-As compounds are often regarded as having lower toxicity than inorg-As, common organo-As compounds, for instance dimethylarsinic acid (DMA(V)) and monomethylarsonic acid (MMA(V)), are still classified to be "possibly carcinogenic to humans" by the International Agency for Research on Cancer (IARC). The IARC has also determined that other organo-As compounds should be considered as having unknown carcinogenicity in humans (IARC, 2012). Thus, organo-As compounds are still regarded as hazardous, or potentially hazardous, to human health but with more limited toxicity and carcinogenicity. Beyond the more commonly known DMA and MMA compounds, many other methylated organoarsenic species exist, notably monomethylarsonous acid (MMAs(III)), trimethylarsine (TMAs(III)) and trimethylarsine oxide (TMAsO(V)). In the environment, there are many other organoarsenic compounds which are formed via biomethylation and in some cases bioethylation (Pinel-Raffaitin et al., 2007). Treatment methods for organo-As species are much less frequently reported in prior literature since inorganic As

tends to dominate in aquatic systems requiring treatment (e.g., surface water, groundwater). For this reason, the EPA's guidebook for As treatment methods omits treatment for organic arsenic completely (EPA, 2003). This trend is mirrored in a wide range of academic publications that primarily address the treatment of water contaminated with inorganic forms of arsenic.

In the environment, arsenic is mobilized in numerous ways, for instance via weathering of soils or sediments which contain As-based minerals (e.g., sulfide deposits), biological activity, wet and dry deposition, volatilization, leaching, extraction, run off, precipitation, and anthropogenically (NIH, 1977). These pathways of As mobilization are summarized in Figure 1.3 (Duckworth and Harrington, 2012). As opposed to the natural cycling of As, human-induced mobilization pathways are dominated by (1) mining, (2) metal smelting, and (3) burning fossil fuels, all of which release significant amounts of As to the atmosphere, water bodies, and soil systems (Upadhyay et al., 2019).

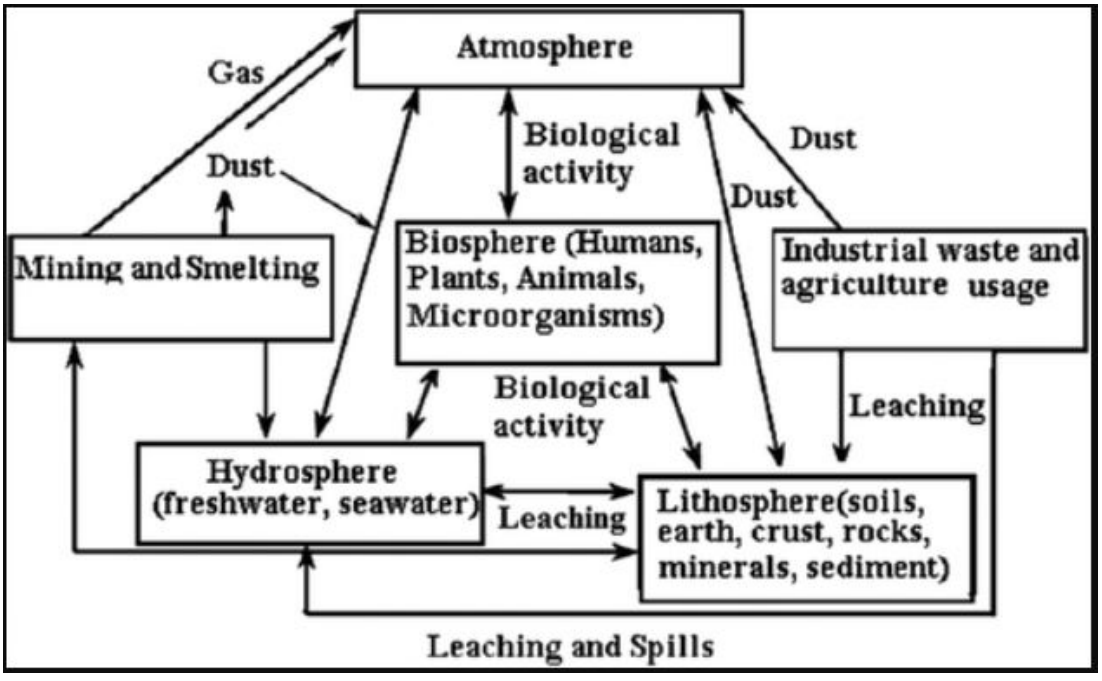

Figure 1.3 The Arsenic Cycle: natural and anthropogenic mobilization (Mudhoo et al., 2011)

Biomethylation is one of the primary pathways by which arsenic is transformed in biological systems, as shown in Figure 1.3 and referred to as "biological activity". Challenger, and then Cullen and Reimer, carried out extensive studies of the methylation of arsenic species (Challenger, 1947; Cullen and Reimer, 1989). In 1945, Fredrick Challenger developed the most likely pathway for arsenic's biological methylation, which is now referred to as the Challenger Pathway. In this pathway, methylation proceeds via oxidation-reduction-methylation reactions driven by microorganisms. These reactions produce a sequence of organo-As species with an increased number of methyl groups attached to the central As atom (Figure 1.4). Biomethylation, and the ensuing transport of As, is further described in Section 1.3 with regards to landfill systems.

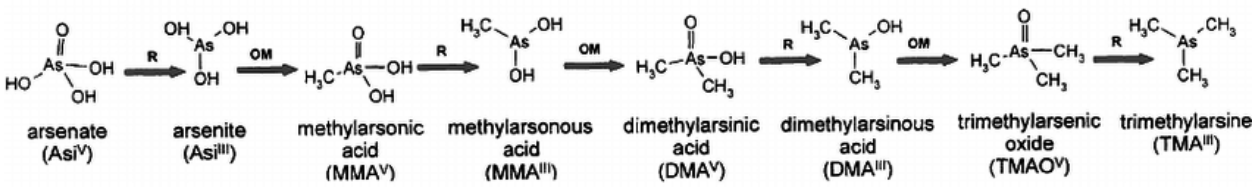

Figure 1.4 The Challenger Pathway for biomethylation of arsenic species (Challenger, 1947)

In the environment, the biomethylation of arsenic, and other metalloids such as antimony, is primarily associated with bacteria, fungi, yeast, and algae (Cullen and Reimer, 1989; Thayer, 2002). Many studies have observed that the occurrence of biomethylation, and volatilization, of As-compounds is enhanced in strongly reducing conditions and also in the presence of reduced sulfur compounds (Frankenberger, 2002). For instance, the generation of volatile sulfur-arseno compounds at Yellowstone's hot springs' is deemed to be enhanced due to the reducing conditions and the presence of hydrogen sulfide (H_2S) in the examined system (Kösters et al., 2003). The methylation of As—and antimony (Sb) whose environmental chemistry has many similarities with that of As—in anaerobic floodplain soil was also correlated with the occurrence of reducing conditions, which also resulted in a notable increase of its volatility (Frohne et al., 2010). Inorganic arsine and stibine can be rapidly oxidized when released to the air (Parris & Brinckman,

1976) but methylated forms of arsines and stibines tend to be more recalcitrant toward oxidation in atmospheric conditions.

1.2 Landfill gas generation, collection, and processing

Nearly everyone generates municipal solid waste (MSW), the technical term for household trash or garbage. The composition of MSW is highly variable. Traditionally, MSW has been sent to landfills. In Europe and some Asian countries, MSW is frequently incinerated but in the US, the vast majority of MSW is landfilled (ACTenviro, 2024). Based on EPA data of MSW generated in 2018(Figure 1.5), about 63% of MSW generated is organic, meaning it was derived from plants or animals (EPA, 2023). Examples of MSW organics include food scraps, wood debris, paper and paperboard, and lawn clippings.

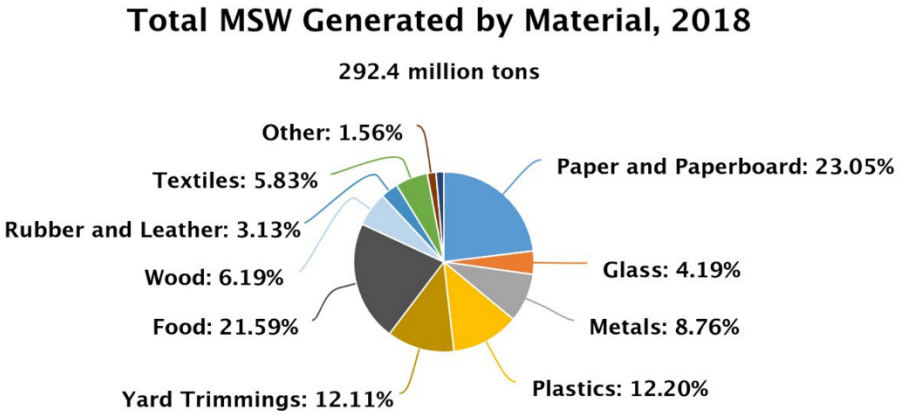

Figure 1.5 Total MSW generated in the U.S. in 2018, by material. Organic content includes Paper and Paperboard, Yard Trimmings, Food, and Wood. (EPA, 2023)

Microorganisms naturally biodegrade (i.e., decompose) organic matter present in MSW, releasing gases such as carbon dioxide, methane, and water vapor as byproducts of their microbial activity. In a landfill, the majority of decomposition occurs anaerobically which fosters a suitable environment for microbially-driven methanogenesis or the generation of methane. Every day, MSW is deposited into organizational landfill units called cells, compacted by tractors, and covered with soil (Figure 1.6). Cells quickly become anaerobic after oxygen is consumed by

decomposers and is scarcely available thereafter. Once completely filled, landfill cells are capped (sealed) with layers of impermeable cover materials effectively trapping evolved gases and minimizing the percolation of water. Gases generated during organics' biodegradation are called landfill gas (LFG).

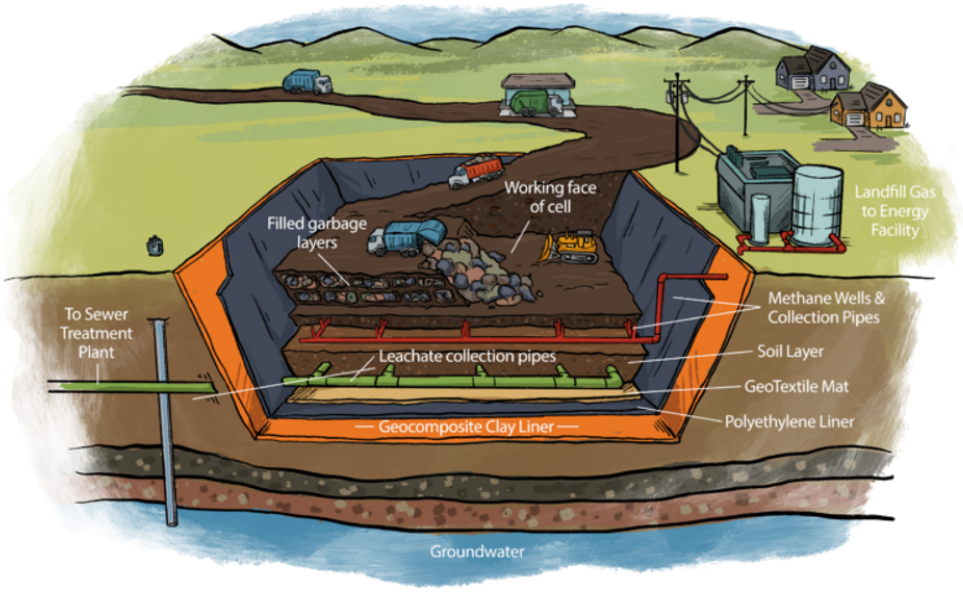

Figure 1.6 Profile of working landfill with LFG collection and conveyance to a LFG-to-energy processing plan (Wasatch Integrated Waste Management District, n.d.)

LFG's composition is variable, but relatively quickly after a cell is covered, all oxygen is consumed (Phase 1 in Figure 1.7) prompting the development of anaerobic, methanogenic microorganisms. During the next phase, a large fraction of LFG is contributed by methane, with a comparable fraction of carbon dioxide and also a range of trace-level contaminants that are found in LFG. After an initial adjustment period (Phases 1-2, > 1 year), methane production tends to plateau and its generation spans decades (+/- 30 years) of a landfill's operation (Waga Energy, n.d.). Over a landfill's lifetime, anaerobic waste degradation dominates and provides a near steady-state stream of methane-rich LFG. Production of LFG does decrease over time, but this is a very gradual process. Furthermore, if a landfill is continually expanding, the newly created cells compensate for the lower gas production of older, less productive cells. Even still, relative to a human's lifespan, LFG can be considered to have near constant, methane-rich gas production.

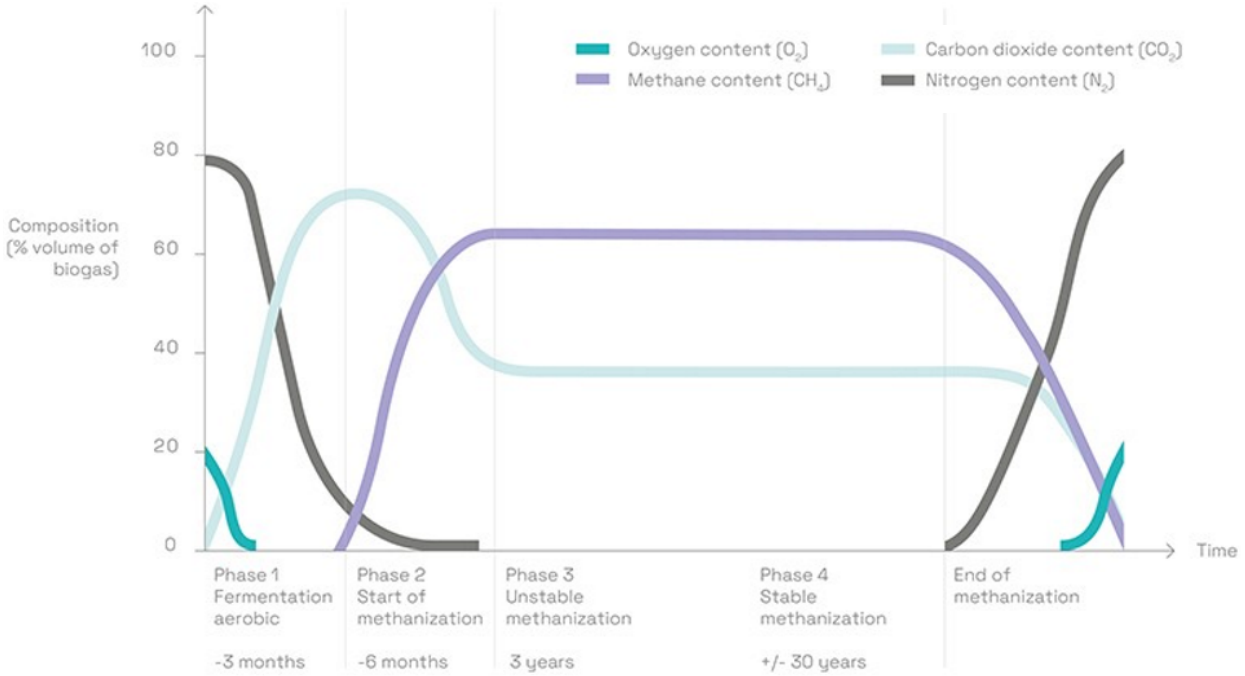

Figure 1.7 Changes of LFG composition over time (Waga Energy, n.d.)

Methane is a very powerful greenhouse gas (GHG), and if it is released directly to the environment, it greatly exacerbates climate change. For this reason, the EPA's Clean Air Act legally requires landfills to collect and manage their LFG through gas collection and control systems (GCCS) (Landfill Methane Outreach Program (LMOP), 2023b). Traditional compliance with the Clean Air Act had landfills burn off the collected LFG in a process called flaring to convert methane to carbon dioxide, thus removing the greenhouse gas impact of the methane generated in MSW landfills. While CO_2 is still a GHG, its global warming potential (GWP) is about 30 to 84 times less powerful than CH4, depending on the global warming timescale considered (European Commission, n.d.). However, flaring LFG is a missed opportunity, especially as society strives to become more creative with sourcing renewable energy. An alternative approach to flaring is to process LFG so it can be used as a source of renewable natural gas (RNG) to support everyday energy needs such as cooking and heating. Or, requiring less processing, energy can be recovered from LFG through combustion engines or gas turbines which generate electricity (LMOP, 2024c). Figure 1.6's illustration of a working landfill's profile includes a GCCS and LFG processing plant.

For LFG-to-RNG projects, collected LFG is conveyed to a processing plant where it is purified through physical processes which remove water and other undesired volatiles based on their boiling points which are sensitive to pressure and temperature (Zhao et al., 2013). LFG processing removes the moisture (water) via condensation thus producing a stream of LFG condensate. A more descriptive term for LFG condensate is "gas derived liquids" which reflects the fact that there are other constituents, notably volatile organic compounds, present in the LFG and then undergo condensation which leads to their presence in the processing wastewater stream (Zhao et al., 2013). Figure 1.8 shows the process flow for LFG-to-RNG treatment which notably includes (1) moisture removal, (2) impurities removal, and (3) advanced treatment for any other composition corrections necessary, notably the removal of carbon dioxide and nitrogen (LMOP, 2024a).

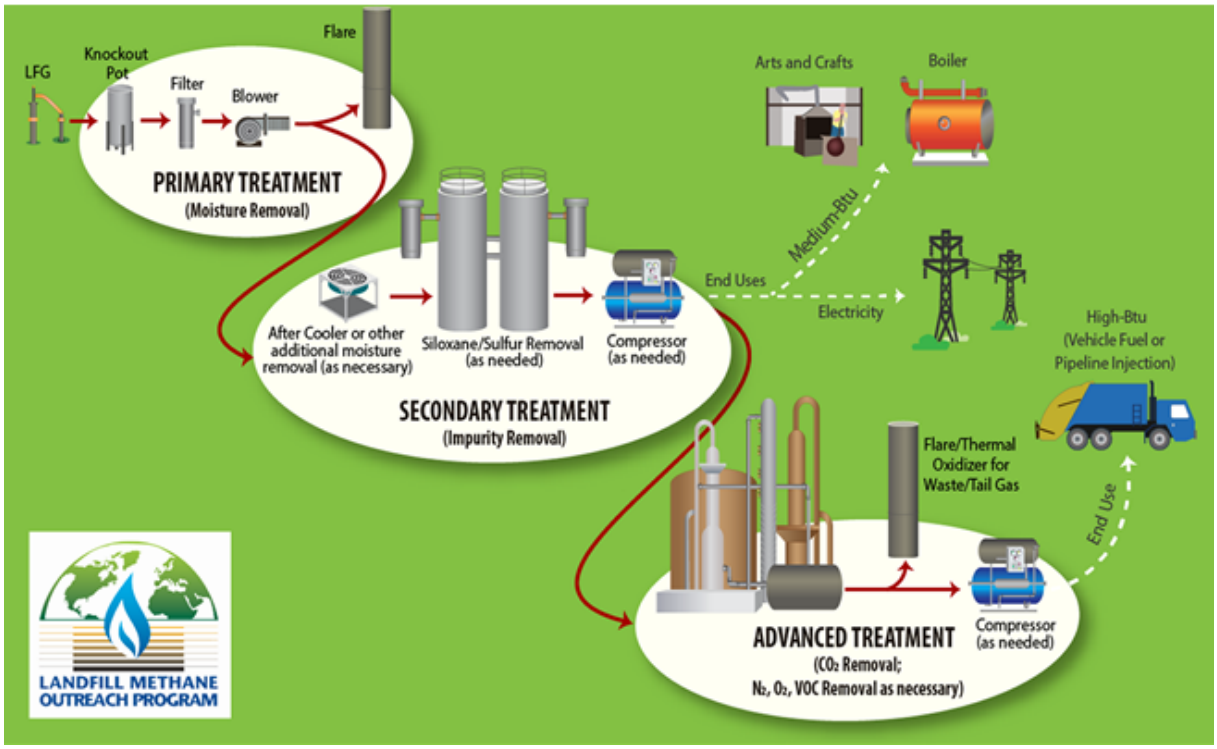

Figure 1.8 LFG processing stages and end uses (LMOP, 2024a)

For pipeline-quality RNG, sufficient moisture must be removed from the LFG to prevent its interference with the other steps of LFG purification and also to prevent corrosion of natural gas pipelines. Beyond its generation within the gas processing facility, condensate is also naturally

generated within the GCCS (e.g., booster blower sumps). This condensate tends to have a composition similar to that of the condensate generated in the processing plant. In summary, LFG condensate is a byproduct formed naturally within the GCCS and also produced during gas processing moisture removal measures (e.g., knockouts, compressors).

1.3 Landfill gas condensate composition and treatment technologies

As described in section 1.2, an unavoidable byproduct of LFG purification is condensate generated during moisture removal processes. A study conducted by the EPA, published in 1988, investigated the typical physical and chemical properties of LFG condensate collected from four American landfills. The study determined that the liquid stream produced during LFG processing is primarily divided into two phases: aqueous and floating hydrocarbon organics. Water and aqueous constituents comprise the aqueous phase. And organics (often floatable) comprise up to 5% of the condensate's volume. Common EPA priority pollutants, found in all LFG condensate sampled, were benzene, toluene, phenol, and ethyl benzene (Briggs, 1988).

Due to the reducing conditions in a landfill, many compounds volatilize alongside decomposing garbage, similar to the reduction induced As volatilization described in section 1.1. Volatiles are conveyed with the LFG stream to the gas processing plant and condensed out of the gaseous phase and into the liquid condensate, largely simultaneously with the condensation of water vapor. That is, when water is removed from LFG, it brings a range of other contaminants with it. Condensate has been described as containing a "chemical dictionary" since the overall LFG stream integrates all the off-gassing streams from all types of waste in a landfill (Bio Energy Washington (BEW), 2023).

In the past, As was believed to be stable when discharged in its inorganic forms, and consequently it used to be classified as "inert, immobile, relatively nontoxic" in landfill conditions (Parris & Brinckman, 1976). However, the dominant environments in landfills are both reductive and anaerobic. This results in the occurrence of "bio-decomposition [processes that] combine with complex chemical-physical processes, providing a condition for inorganic arsenic transformation

through bio-alkylation and hydride generation" (Zhao et al., 2013, p. 2). This unique condition facilitates the release of As and Sb volatiles via biomethylation.

As shown by the Challenger Pathway (Figure 1.4), As can be transformed via biomethylation from an inorganic form to mobile forms that include organo-arsines which can be conveyed to the environment together with the major components of LFG: methane and carbon dioxide. A recent investigation of the composition of a Florida landfill's LFG determined the release of volatile As and Sb to be much greater than previously estimated, indicating increased mobility of these elements (Oliveira et al., 2022). While inorganic forms of As and Sb volatiles occur (as AsH_3 and SbH_3, respectively), the speciation of As and Sb volatiles in LFG is dominated by methylated forms of As and Sb volatiles such as the mono-, di-, or tri-methylated arsine or stibine (Oliveira et al., 2022), with trimethylarsine (TMA) being dominant in LFG (Pinel-Raffaitin et al., 2007). As mentioned above, the generation of these organic volatile As and Sb species is mediated by microbial processes (Oliveira et al., 2022). Biomethylation and ensuing partial volatilization of As and Sb transfer organic As and Sb compounds into LFG condensate. As a result, many MSW landfills' waste streams that contain LFG condensate may be unfit for direct discharge to a publicly operated treatment works (POTW) (i.e., wastewater treatment facility).

Across the country, there may be many landfills which produce condensate containing high levels of As. However, the vast majority of, indeed practically all, landfills do not publish or otherwise make available detailed data on the composition of their LFG condensates so at present it is difficult to understand the extent of this issue (Briggs et al., 1988).

While the treatment of inorganic As has been studied extensively, there is limited previous research on the removal of organo-As compounds from aqueous matrices, notably from LFG condensate. The following options for LFG condensate waste management have been suggested (Briggs et al., 1988):

1. Evaporation
2. Incineration

3. Hazardous waste disposal, off-site
4. Deep-well injection
5. Treatment (e.g., air-stripping, aeration) and disposal to POTW
6. Landfill, on-site (state regulation permitting)

However, given the difficulties of removing organo-As compounds from LFG condensate, their largely unknown speciation, and the little information of the occurrence of such compounds at different sites where LFG is collected and used for energy generation and/or RNG production, the conventional options for the treatment, and ultimately management, of As-containing LFG condensate are inadequate (Brookshire, 1995).

In all, LFG condensate treatment, let alone removing organic arsenic, is a relatively unprecedented area of research. In terms of prior published research, the only available source is a 2013 study that compared the performance of treatment methods to remove organo-As from LFG condensate from a Pennsylvania landfill which was prohibited from direct discharge of its condensate waste stream to a POTW.

The study tested treatment techniques to remove organo-As from LFG condensate that had arsenic levels similar to those (7-40 mg/L As) relevant to this thesis's work. The methods examined in Zhao et al. 2013 included biological, physical, and chemical treatment in a sequencing batch reactor (SBR), and by coagulation, permanganate oxidation, Fenton's reagent oxidation, carbon adsorption, and membrane separation. This study showed that the organo-As species present in LFG condensate were stable and largely resistant to their conversion to inorganic As species by conventional and advanced chemical oxidation. Activated carbon showed only a limited capability to treat organo-As.

Membrane separation (reverse osmosis, RO) was found to be the most promising technology for removal of organo-As. This approach resulted in a removal of 95.8% As from the SBR effluent (Figure 1.9). However, no information was given in Zhao et al. 2013 concerning the resistance of the RO membrane to organic solvents such as benzene and toluene typically present in LFG

condensates, and the occurrence of reversible and irreversible fouling that always takes place in membrane operations.

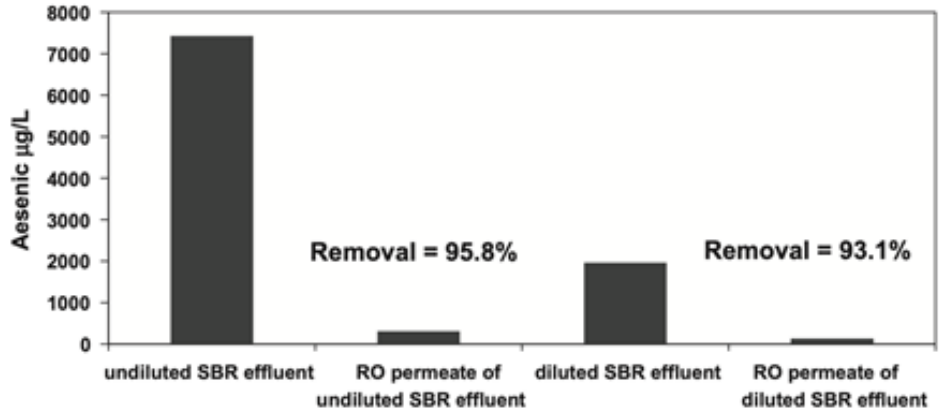

Figure 1.9 organo-As removal from LFG condensate treated by SBR and RO (Zhao et al. 2013)

No other modes of treatment tested removed greater than 20% of As, making the SBR to RO treatment method the most likely candidate for practical implementation (Table 1.1). As mentioned above, drawbacks inherent to operating RO systems include their large energy requirements, tendency for membrane fouling, costs, and yet unknown suitability of conventional RO membrane materials for treatment of LFG condensates (Sharma et al., 2016). Furthermore, the Zhao et al. (2013) study only tested RO after a sequencing batch reactor pre-treatment.

Table 1.1 Treatment efficiency of different physical/chemical technologies for organo-As in SBR effluent (Zhao et al., 2013)

Treatment method	Max. As removal (%)
Coagulation/flocculation (FeCl3)	8.0
Oxidation + coagulation (KMnO4 + FeCl3)	5.6
Advanced oxidation (Fenton's reagent)	15.1
Carbon adsorption	6.5
Membrane separation (reverse osmosis)	95.8

These results show that the only alternative to RO treatment is the microelectrolysis technology which has been tested by the UW research group. This technology was further explored in this thesis, as presented in the sections that follow.

1.4 LFG as a source of renewable natural gas

While renewable energy sources such as solar and wind have been popular since the 1970s, LFG is an alternative, consistently available energy source which is much less susceptible to fluctuations with environmental factors such as weather. In 2022, 33% of the United States' primary energy consumption was sourced from natural gas, second only to petroleum (Figure 1.10) (EIA, 2023). Augmenting the crucial, fossil fuel-based source of energy with RNG will assist in meeting energy needs as well as reduce fossil fuels released to the environment.

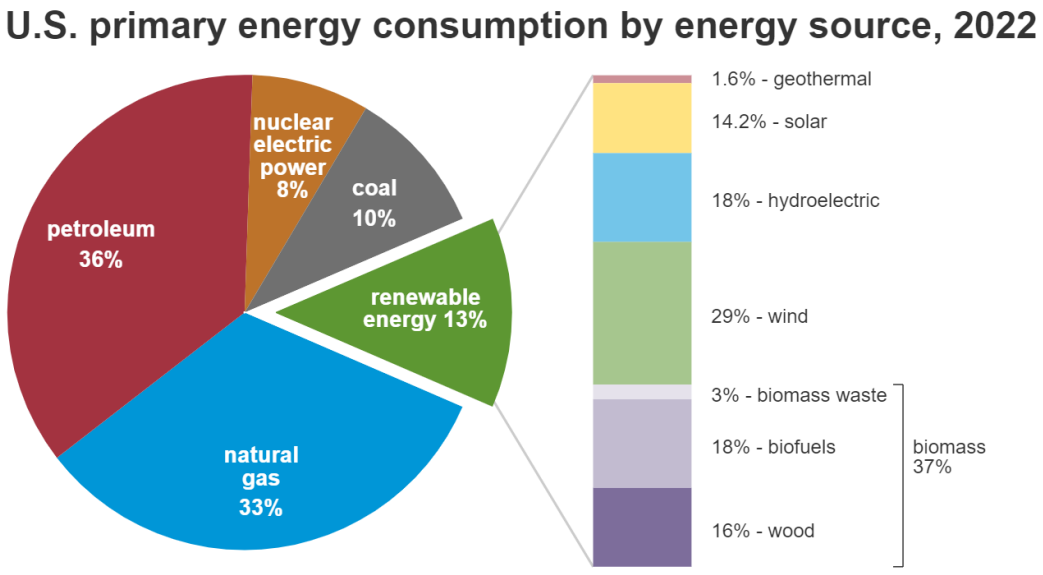

Figure 1.10 U.S. primary energy consumption by energy source, 2022 (EIA, 2023)

Historically, LFG has been a nuisance to waste off through flaring. However, with current and emerging technologies, LFG is now viewed as a methane-rich resource. When managed well, LFG can also be quite lucrative for waste purveyors (LMOP, 2024c). LFG-to-RNG is an excellent example of a closed-loop system which recaptures available energy that would otherwise be wasted making it a truly sustainable operation. Treating the contaminated condensate to discharge-quality furthers this sustainability, recapturing water resources that would otherwise also be wasted.

LFG should be considered as a part of local energy portfolios, to augment consumers of fossil fuel natural gas or potentially serve as a replacement. Renewable energy resources are defined by the Energy Information Administration (EIA) as "energy resources that are naturally replenishing but flow limited. They are virtually inexhaustible in duration but limited in the amount of energy that is available per unit of time" (EIA, n.d.). Since the source of LFG is waste organics, which are steadily produced by humankind, the methane source is qualified as renewable. LFG is flow-limited since its production is dependent on the natural generation of methane by bacterial activity, which is fairly stable. In other words, LFG production cannot be accelerated on-demand. LFG as a source of RNG is relatively easily integrated into the existing electricity portfolio if the community already utilizes natural gas.

The initial investment in LFG to RNG requires a gas conveyance system, gas processing and treatment, and integration into natural gas pipelines. If a facility is already flaring gas, then the initial investment in a conveyance system should be relatively minor, only needing to connect their existing LFG conveyance into a plant for processing.

Apparent constraints for LFG-to-RNG include, but are not limited to:

1. Initial investment in extension of gas conveyance system
2. Investment in gas processing and purification, including waste management (which this thesis investigates)

3. Partnership with gas receiving entity (i.e., energy purveyor) and/or gas processing entities (i.e., private 3rd party)

LFG-to-energy projects provide an opportunity to integrate a renewable energy source into the grid, removing societal dependence on traditional, fossil fuel energy sources. Pursuing LFG-to-energy is critical to meet the current, and future, energy supply and demand in the United States as the success of our modern lifestyle becomes increasingly dependent on reliable energy sources. End uses of RNG include vehicle fuel, electricity and thermal applications (e.g., heat) (ARI, n.d.). RNG sourced from LFG can be integrated into local energy needs and also serve regional energy needs through pipeline injection. Furthermore, research pertaining to RNG is a beneficial investment since high-quality RNG products are fairly easily integrated into the grid, via existing natural gas pipelines. There is a tremendous opportunity for LFG-to-RNG projects to serve up to 10% of the nation's natural gas demand (IEA, 2020; Marconi & Rosa, 2023). While more than 500 landfills have already implemented LFG-to-energy projects, the EPA has identified 463 more as candidates, shown in Figure 1.11.

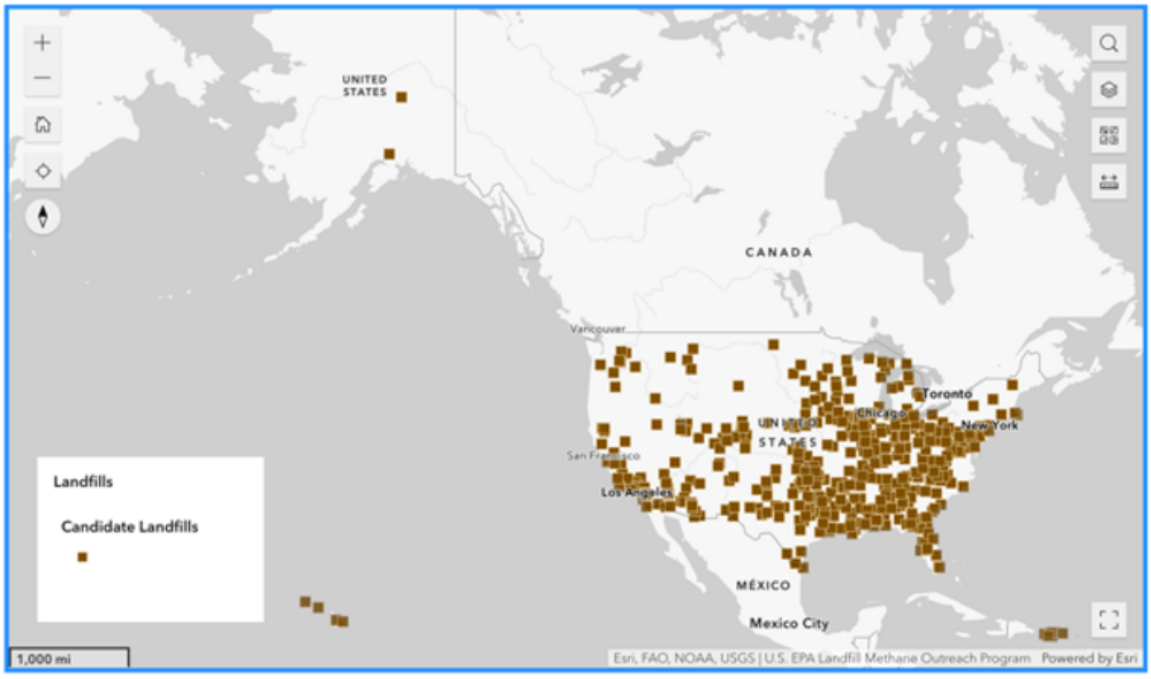

Figure 1.11 LMOP proposed candidate landfills for LFG-to-energy processes (LMOP, 2023a)

One state over, the Columbia Ridge Landfill in Arlington, Oregon also runs a landfill gas to energy facility that differs slightly from the landfill's operations. The Waste Management (WM) operated landfill states benefits of landfill gas to energy being the generation of a renewable energy source, a reduction in GHG emissions, and a means of odor control. LFG-to-energy is strategically included in WM's plan to "extract value from waste" (Waste Management, 2015). This landfill captures and conveys 9,400 CFM LFG, the majority of which is sent for on-site gas processing, with a small amount flared-off (Waste Management, n.d.a). Columbia Ridge's operation produces 12.8 MW of electricity via combustion generators, powering 12,500 Seattle homes through a contract with the City of Seattle (Waste Management, n.d.b). This closes the loop on available energy in waste since Seattle also relies on Columbia Ridge to manage the city's solid waste (Waste Management, n.d.b). Finally, this project shows the opportunity for landfill gas spans beyond sourcing renewable natural gas. Using combustion engines, a non-selective energy source can be generated for direct consumption.

Each renewable energy source has constraints and the strategies implemented to mitigate these challenges are critical to their success. With regards to LFG-to-energy, waste management for the often heavily contaminated (polluted) condensate by-product is key. The coming years will require creativity, adaptability, and persistence to satisfy the nation's growing energy needs with RE in-lieu of traditional energy sources which exacerbate climate change through their harmful greenhouse gas emissions.

1.5 Landfill characterization

This project involves a local landfill which is owned and operated by the county-level solid waste division which is the municipal waste purveyor for the majority of a highly populated county (the "landfill"). The facility captures generated LFG with horizontal collection wells which "pull" the gas out of landfill cells. Rather than flare the energy-rich gas, the landfill conveys the gas to a third party for on-site gas processing to generate a pipeline-quality RNG methane. The purified gas is sold to the local energy purveyor to meet local and regional energy demand.

The LFG condensate produced naturally within the landfill's gas distribution system, and by the 3rd party's processing, have observed levels of arsenic which exceed the allowable levels for discharge to the publicly owned treatment works (POTW), or the environment. Historically, the landfill has conveyed the LFG condensate waste stream to the local POTW facility for processing. However, the landfill has been in exceedance in terms of the allowable As loading rate as set by the county's industrial waste program (Mirfendereski, 2023). In recent years, the maximum allowable As for receipt by the POTW was 5 mg/L As, as set by the National Pollutant Discharge Elimination System (NPDES) permit for the landfill (BEW, 2023). This thesis documents LFG condensate having concentrations of from about 13 to 20 mg/L As. Daily loading limits for As discharge to the POTW were set at 0.27 lbs As per day and are monitored per a leachate monitoring plan to comply with their permit requirements (Facility Engineering & Science Section, King County Solid Waste Division (KCSWD), 2019). In addition to the environmental compliance rules set by the industrial waste department, two other public health agencies also regulate release of As by the landfill.

The cost to transport the condensate to a landfill capable of receiving hazardous waste has been estimated to be on the order of millions of dollars annually making an alternative solution desirable (BEW, 2023). Deep-well injection requires lengthy hauling routes to transport the waste to a state which can accept waste of this kind. Beyond aqueous disposal, the Puget Sound Clean Air Agency regulates airborne As emissions to 5 ppm (Puget Sound Clean Air Agency, 2019). So, flaring LFG is also not an acceptable long-term option due to these elevated levels of As present in the LFG. Thus, treatment of the condensate was the most logical step to continue LFG-to-RNG operations.

Since 2018, the landfill has sought to characterize the As exceedance problem, by investigating the source of As within the landfill and how it transforms into volatile and liquid forms (KCSWD, 2019). In 2019, the solid waste division engaged with the University of Washington (UW) to initiate research to investigate, and develop, a suitable treatment technology to remediate As-

contaminated LFG condensate. Since then, Dr. Korshin and his research team have worked to develop a novel treatment technique based on the combination of reductive, adsorptive and other processes driven by zero-valent iron (ZVI) and granular activated carbon (GAC) solid media at appropriate reaction conditions, to remove organic As from LFG condensate, remediating the wastewater to As levels which can be discharged to the local POTW. The target contaminant is arsenic, but the technology referred to as microelectrolysis (ME) is also applicable to treating other contaminants of emerging concern. Organic forms of arsenic that are dominant in LFG condensate are highly recalcitrant to removal by conventional methods. In contrast, ME has been determined as a feasible technology to remove organic arsenic from the aqueous matrix. The team's prototypes have been used for bench scale remediation of the contaminated wastewater to a threshold that meets requirements for safe disposal.

Prior investigations of the speciation of As in LFG condensate showed that it is dominated by methylated and/or sulfur containing compound (i.e., thiolated) (Chen et al., 2023). These methylated/thiolated-arsenic compounds are likely to be formed by the reactions between hydrogen sulfide (H_2S) and possibly other volatile sulfur-containing gases and As volatiles and solutes present in the MSW leachate and LFG. While organo-As is reported to be hundreds of times less toxic than inorg-As, it must still be removed from the condensate to meet a total As limit specified by federal, state, and/or local environmental protection agencies (Hughes, 2002 and Cullen & Bentley, 2005).

Potential sources of As in the landfill may include treated wood, soils, electronic waste (i.e., e-waste), and possibly historical contamination from the Asarco copper smelting plant that operated from 1890 to 1986 in Ruston (Tacoma), WA. Asarco operations were a notable source of arsenic contamination in western Washington widespread due to transport via smokestacks (King County, n.d.). Background sources of As include natural soils, especially those used for soil cover. The Washington State Department of Ecology (DOE) and the United States Geological Survey (USGS) report the natural background levels of arsenic in the Puget Sound's soil as 7 ppm (King

County, n.d.). In summary, due to a naturally higher level of arsenic in the PNW, historical As contamination, and arsenic containing MSW, the landfill's LFG has heightened levels of As.

1.6 Development of microelectrolysis treatment (i.e., previous work)

As stated in section 1.5, since 2019, the University of Washington research team have led an investigation into determining a suitable treatment technology to remove As from LFG condensate. After conducting an alternatives analysis of prospective treatment process for organo-As removal, an ME treatment process was determined to be the optimal approach (Malik, 2020; Rifkin, 2021; Walters, 2022; Pinochet-Troncoso, 2023). The novel ME treatment process is achieved by interacting particles of ZVI) and (GAC), together referred to as "active media", in an acidic and oxygen-free environment (Malik, 2020; Rifkin, 2021; Walters, 2022). ZVI is the reducing agent in ME treatment which can be oxidized, releasing (donating) electrons by the formula:

$$Fe \rightarrow Fe^{2+} + 2e^{-}$$

The standard reduction potential, E_o (V), of the iron half-reaction is -0.409 V, with the negative signifying the reductive nature of the reaction (Yokogawa, 2014). GAC removes a wide variety of dissolved constituents which makes it a popular choice for treatment applications (Nowicki, 2016); its high surface area makes GAC a common choice for remediation work, since it can retain a relatively large amount of contamination per its mass (Mohan and Pittman, 2007).

In ME treatment, the combination of GAC with ZVI catalyzes this electrochemical corrosion –that is the oxidation of ZVI – thus creating a highly dynamic reducing environment which is conducive to organo-As removal. The galvanic cells strip arsenic and other compounds from the contaminated water and retain them on the solids' surface (Liu et al., 2022). This method of treatment has successfully, and consistently, removed the majority of organic arsenic from the landfill's LFG condensate (Pinochet-Troncoso, 2023).

Since the completion of the alternatives analysis and initial development of ME treatment, the team has furthered the technology by optimizing the ME treatment process for specific

operational variables (Walters, 2022; Pinochet-Troncoso, 2023). Experimental ME treatment was conducted within fixed bed and fluidized column reactors (Walters, 2022). Performance optimization was conducted for the fluidized column reactor involving a number of treatment variables including pH, recycling of media (i.e., cycling), length of treatment time, anaerobic conditions, carrier gas, reactor headspace, mode of process activation, and method of media agitation (Pinochet-Troncoso, 2023).

For initial ME treatment investigations, LFG condensate was filtered prior to treatment; this practice was abandoned after ME treatment was proven to be successful for unfiltered condensate, thus removing the need for any condensate pre-treatment filtering (Pinochet-Troncoso, 2023). A notable development in the ME process was the transition away from fine active media (i.e., powder activated carbon, PAC) to coarser media which has multiple benefits including ease of reuse for active media cycling and/or regeneration, ease of clean up due to particle settling velocities and characteristics (Pinochet-Troncoso, 2023). Supplementary doses of active media were found to increase the useful life of media, allowing for multiple rounds of LFG condensate batch treatment (Pinochet-Troncoso, 2023). A notable effect of the amount of reactor's headspace on the ME treatment efficiency was observed, affirming that ME treatment is best conducted in anoxic conditions. ME treatment successfully removed As at a variety of temperatures, affirming its efficacy for field operations with temperature variability (Pinochet-Troncoso, 2023).

With regards to operational pH, ME treatment efficacy was affirmed for a range of pH (Walters, 2022; Pinochet-Troncoso, 2023). Oxidation reduction potential (ORP) of the aqueous matrix were measured during the ME process to monitor treatment. Correlations between ORP and arsenic removal were investigated as a potentially helpful variable when looking forward to a real-time operational variable to be used for monitoring treatment of in-field operations (Pinochet-Troncoso, 2023). Larger scale reactors were developed and were shown to typically perform better than the smaller reactors. Their use also provided a better approximation of the conditions expected for planned pilot- and full-scale ME operations. The larger-scale ME treatment initially

used reactors in which the removal of As was facilitated by the presence of a carrier gas (typically CO_2) (Walters, 2022; Pinochet-Troncoso, 2023). That modus operandi was replaced by mechanical mixing which proved to be sufficient to agitate active media in ME reactors (Pinochet-Troncoso, 2023). The ME treatment mechanism's mass balance for arsenic removal determined that GAC retains the majority of the removed arsenic (Pinochet-Troncoso, 2023; Panico, 2023). This result was obtained by magnetically separating the ZVI/GAC phases and performing separate digestions for them (Panico, 2023). However, the mass balance for As removed by ME treatment needs further investigation to determine the extent of As volatilization in ME reactors.

1.7 Goals of this study

This thesis documents the progress of the ME treatment process optimization to remove arsenic from LFG condensate, making it a continuation of the experimental goals of prior work of the UW group. The overall focus of this thesis' work was geared towards envisioning and implementing practical engineering design, based on the previous and concurrent technological advancements of the group.

This thesis focuses on furthering and developing the following:

1. The exploration of recycling, or "cycling", active media in which multiple rounds of ME batch treatment are conducted consecutively to minimize waste generated and materials necessary. With cycling, extending the useful life of media was investigated using smaller, supplementary doses, also called "top-offs".
2. Operational pH for ME treatment was further investigated, seeking to optimize the conditions for As removal while balancing acid requirements and subsequent effluent neutralization for discharge to a POTW.
3. Preliminary exploration into the mixing mode (or media agitation) was conducted to better understand the impacts of hydrodynamics on ME treatment.
4. Following the transition away from fine particle size active media, the performance of different commercially available particle size media was investigated.

5. Active media dosing was further optimized.
6. Approaches were developed to quantify As removal without relying on lengthy and expensive laboratory analyses.
    6.1. ORP was further explored as a direct-measurement surrogate parameter to predict As removal.
    6.2. ORP's ambiguity spurred a new investigation into using concentrations of dissolved iron (Fe) released from the ZVI phase as a better predictor of ME treatment efficiency. This investigation into Fe was conducted on the basis of pH, length of treatment time, and dose of media.

Determining the optimal operational conditions was essential to provide a basis of design for the pilot plant and subsequent full-size ME operations.

2 Materials and equipment

The following chapter details the materials and equipment utilized in this thesis. The first section pertains to the chemicals and materials utilized in ME treatment and associated experiments including: ICP-MS standards, chemicals and gases, active media for ME treatment, and laboratory consumables. The second section details the materials and equipment which were required for constructing ME treatment column reactors. The third section lists PPE and supplies required for LFG condensate field sampling, followed by a fourth section dedicated to materials and equipment necessary for ME treatment and associated experiments. Finally, the fifth section lists pipettes utilized in this experimental work.

2.1 Experimental chemicals and materials

2.1.1 ICP-MS Standards

Table 2.1 summarizes the single element standards used to develop calibration standards for ICP-MS quantitative elemental analysis, as described in section 4.3.2. All standards were procured from an International Organization for Standardization (ISO) accredited reference material producer (RMP) which adheres to the ISO 17034 quality standard for reference materials.

Table 2.1 Single element standards used for ICP-MS analyses

Analyte	Brand	Product	CAS	Concentration (µg/mL)
As	Agilent	ICP-033	1327-53-3	1,000
Cu	Agilent	ICP-029	10031-43-3	1,000
Fe	Agilent	ICP-026	7782-61-8	1,000
Sb	Agilent	ICP-151	7440-36-0	10,000
Y	Agilent	IMS-115	1314-36-9	100

2.1.2 Chemicals and gases

Table 2.2 summarizes chemicals and purge gases utilized for ME treatment operations and associated experiments.

Table 2.2 Chemicals and purge gases utilized in ME treatment and associated experiments

Chemical / Gas	Supplier	CAS	Specifications
Carbon Dioxide	Linde, Inc.	124-38-9	50 lb Carbon dioxide gas cylinder, UN: 1013
Hydrochloric Acid	Sigma-Aldrich	7647-01-0	ACS Grade Hydrochloric Acid, 36.5-38.0% assay
Nitric Acid	Fisher	7697-37-2	Nitric Acid (TraceMetal™ Grade) appropriate for ICP-MS analysis, 67-70% assay
Nitrogen, compressed	Linde, Inc.	7727-37-9	Nitrogen gas cylinder, 304 cubic feet, UN: 1066
Nitrogen, liquid	--	7727-37-9	Cryogenic liquid nitrogen
Sulfuric Acid	VWR	7664-93-9	ACS Grade Sulfuric Acid, 95-98% assay

2.1.3 Active media for microelectrolysis treatment

Table 2.3 summarizes active media products utilized to carry out ME treatment. All zero valent iron products are identified by CAS: 7439-89-6 and all carbon by CAS: 7440-44-0. The media denoted "typical" were the most utilized products for ME treatment experiments in this thesis.

Table 2.3 Specifications of active media products used for ME treatment

Product (Media Type) – Supplier	Apparent Density (g/cm^3)	Manufacturer Sieve Analysis
CR-15 (ZVI, typical) - Höganäs	1.5	Percent Retained +40 mesh (+425μ): 9.1% +60 mesh (+250μ): 22.2% +100 mesh (+150μ): 38.8% +200 mesh (+75μ): 28.4% -200 mesh (-75μ): 1.5%
CR Plus (ZVI) – Höganäs	1.5	*Same as CR-15*
LC Plus (ZVI) – Höganäs	1.25 – 1.6	Sieve Analysis -20/+60 mesh (-841μ/+250μ): 70% -20/+100 mesh (-841/+150μ): 93%
LC Plus Fine (ZVI) – Höganäs		Percent Retained +100 mesh (+150μ): 0.1% +140 mesh (+106μ): 30% -140 mesh (+106μ): 70%
PRB (ZVI) – Höganäs	1.4 – 1.6	Percent Passing Sieve #4 (4.75 mm): 100% Sieve #8 (2.36 mm): 100% Sieve #16 (1.18 mm): 75-90% Sieve #30 (0.6 mm): 25-45% Sieve #50 (0.3 mm): 0-10% Sieve #100 (0.15 mm): 0-5%
Coconut Shell Granular Activated Carbon Charcoal (GAC, Typical) – IPW Industries	--	12- 40 mesh

Activated charcoal, Norit ® (GAC) – Thermo Scientific	--	12-40 mesh: ≤ 5% (>12 mesh) and ≤ 4% (<40 mesh)
Activated charcoal, granular, Norit ® (GAC) – Sigma-Aldrich	--	4 – 14 mesh
Activated charcoal, untreated, granular (GAC) – Sigma-Aldrich	--	8 – 20 mesh

As reported by the manufacturer, the CR-15 product has a chemical composition of 98.2% Fe, 0.74% H_2, and 0.20% acid – insoluble (Höganäs, 2021); it is described as a porous and irregularly shaped reduced iron powder which increases its surface area and lowers its bulk density. The CR Plus product is a washed, or "activated", version of CR-15 and is characteristically orange in color. The PRB product was designed for permeable reactive barrier (PRB) in situ chemical reduction (ISCR) applications and is stated to have >99% iron purity (Höganäs, 2023). The Thermo Scientific GAC product was formerly distributed by Acros Organics and is specified to contain less than 2% water. The IPW GAC product is acid washed, and the resulting particle size distributions for the dried ME treatment active media that are listed in Table 2.3. These distributions were determined by sieve analyses, with methods described in section 4.3.4.

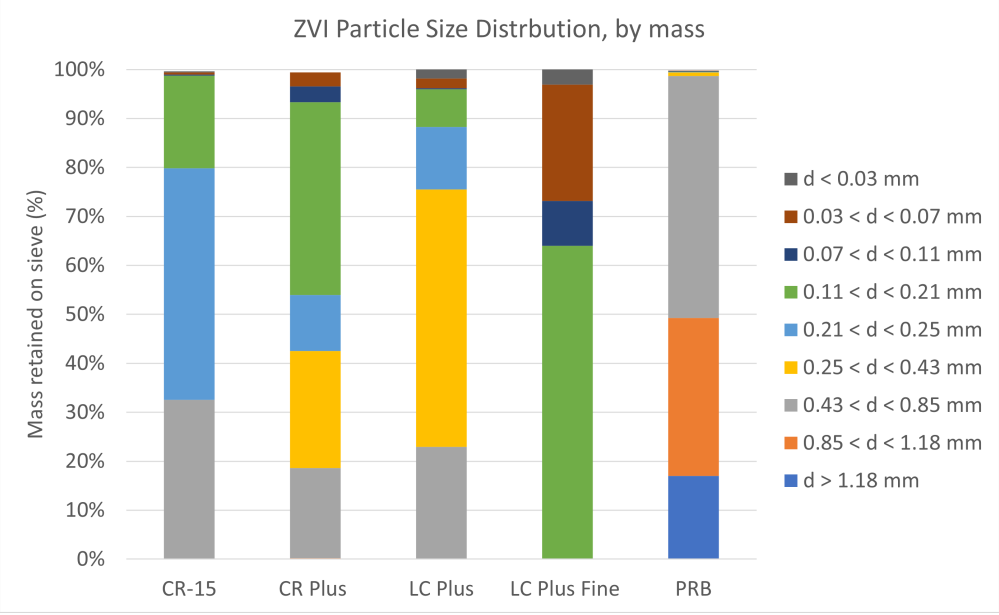

Figure 2.1 ZVI Particle Size Distribution, by mass

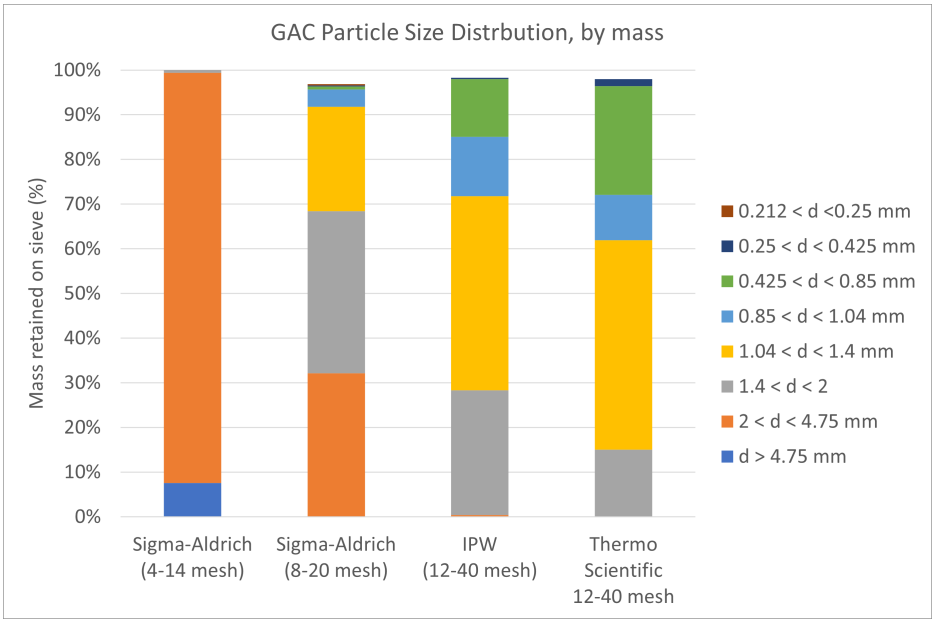

Figure 2.2 GAC Particle Size Distribution, by mass

The particle size distribution results, and bulk densities, were used to estimate specific surface areas of the ZVI, shown in Figure 2.3. The bulk densities for ZVI were specified by the manufacturer and shown in Table 2.3. An estimate for typical GAC bulk density (between 0.4 to 0.6 g/cm^3) was utilized (Zhulin Carbon, n.d.). Specific surface area was not estimated for GAC due to its porous and irregular shape which makes it ill-suited for an assumption of spherical particles.

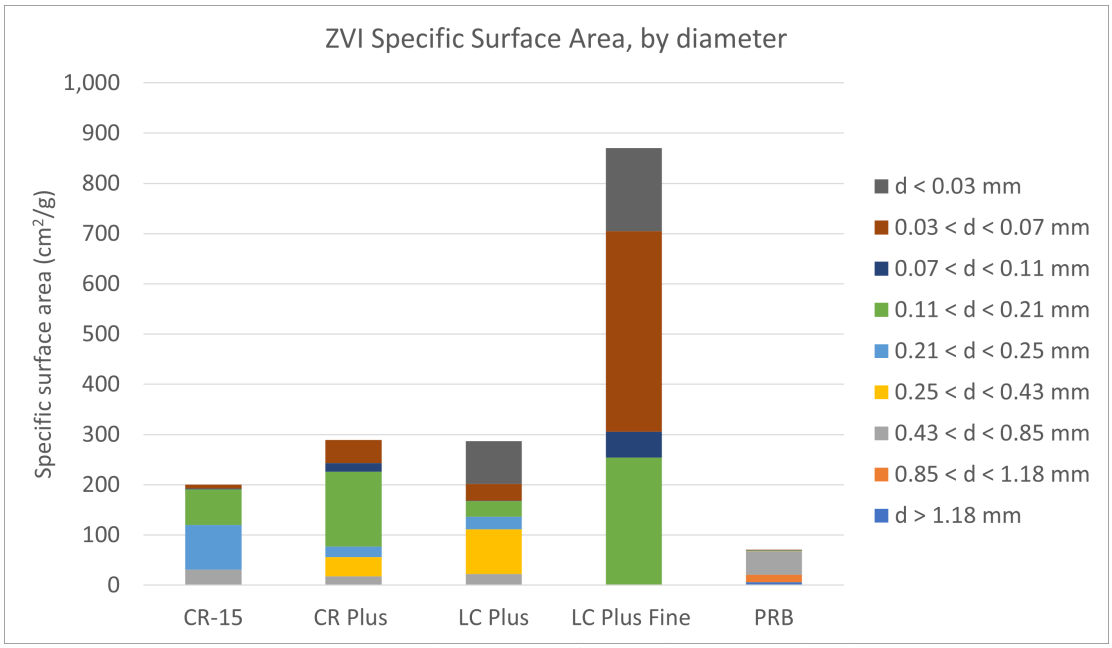

Figure 2.3 Estimated ZVI Specific Surface Area, by diameter

The particles' surface area data (Figure 2.3) was utilized to estimate the products' specific surface areas, per method in section 4.3.4, and tabulated in Table 2.4, ranked from highest to lowest.

Table 2.4 Estimations of specific surface area for ME treatment media ZVI, based on sieving data, ranked highest to lowest

Product	Specific surface area (cm^2/g)
LC Plus Fine	870
CR Plus	289
LC Plus	287
CR	200
PRB	70

Select media were analyzed by BET, as described in section 4.3.5, and the resultant specific surface areas and pore volumes are summarized in Table 2.5.

Table 2.5 BET specific surface area and pore volumes for ME media

Product	Specific Surface Area (m^2/g)	Pore Volume (cm^3/g)
IPW (12-40 mesh)	939	0.23
Thermo Scientific (12-40 mesh)	884	0.48
LC Plus	4	0.02
CR	0.5	--

2.1.4 Laboratory consumables

Table 2.6 summarizes consumable materials utilized for ME treatment operations and associated experiments.

Table 2.6 Materials used for ME treatment operations and associated experiments

Material	Supplier	Model / CAT #	Specifications
Aluminum foil	--	--	--
Buffer pH 10.0	VWR BDH Chemicals	BDH5072	Buffer, Reference Standard, pH 10.00 ± 0.01 at 25 °C (Color Coded Blue)
Buffer pH 4.0	Ricca	CAT: 1501-16	Buffer, Reference Standard, pH 4.00 ± 0.01 at 25 °C
Buffer pH 7.0	Supelco	BX1632-1	Buffer pH 7.0, Yellow
Filter paper	--	--	15 cm diameter, Grade 415
Kimwipes	Kimtech Science	CAT: 06-666A	1-ply, delicate task wipes
Labeling tape	--	--	--
Laboratory film	Bemis Company, Inc.	Model: PM992	Parafilm M: Laboratory film
Membrane filter	--	--	15 cm diameter, 0.45 μm filter
Nitrile gloves	Kimtech	Product code: 55082	Nitrile gloves
ORP Calibration Solution	Gain Express	SOL-ORP-256MV	256 mV oxidation-reduction potential calibration solution
pH/ORP storage solution	Hanna Instruments	HI70300	pH and ORP electrode storage solution
Syringe	BD	Model #: 302995	10-mL Luer-Lok plastic syringe
Syringe filters	VWR	CAT: 76479-032	0.45 μm nylon membrane Luer Lock syringe filter tip, 25 mm diameter
Test Tubes	VWR	21008-936	10 mL Falcon tubes
Vacuum Grease	Dow Corning	Cat. No. 970 V	Non-melting silicone lubricant
Valve, Check/One-Way	Mudder	Mudder-Check Valve-01	Polyvinyl chloride check valve, fuel gas liquid air
Weighing boats	Fisher	--	--
Weighing paper	Fisher	--	--

2.2 Materials and equipment used for column reactor construction

Table 2.7 summarizes materials utilized for ME treatment column reactor assembly, with methods described in Section 0. Reactor assembly was achieved using common tools and, in some cases, more specialized tools such as a heat gun, Dremel rotary tool, and band saw.

Table 2.7 Materials used to build ME treatment column reactor used in this study

Material	Supplier	Model / Part #	Specifications
Barb fittings	--	--	Plastic, various diameters
Bearings	ANCIRS	608 2RS	Double rubber sealed ball bearings. 22 mm OD, 8 mm ID, 7 mm width
Heat shrink tubing	Wirefy	Wirefy-DW41-190-B-R	Polyolefin dual wall, marine grade heat shrinking tubing
Liquid rubber	Dicor	501LSW-1	Self-leveling lap sealant
Marine Weld	J-B Weld	SKU: 50172	Adhesive epoxy resin
O-ring	Sterling Seal & Supply Inc.	421	Buna-nitrile O-ring, 4" ID
Polylactic Acid (PLA), Silk	Amazon	ESilk-PLA175CO1A	3D printer filament,1.75 mm (0.069 in) diameter, 1 kg spool
PVC Tube	Tennessee Valley Products	SKU: 4IND-CPVC-2FT	4" ID (4.5" OD) clear PVC Schedule 40 pipe
Rubber stoppers	--	--	Various sizes
Silicone	GE Sealants	GE500	Clear, 100% silicone sealant
Spray paint	Rust-oleum	7718830	General purpose spray paint
Stainless steel mesh	--	--	Approximate mesh size of typical ZVI
Steel rod	VI-CHAN	VC-LMR6	6 mm x 600 mm C45 steel rod
Tubing	--	--	Various diameters
Water-Gas-Oil valve	DERNORD	DERNORD-782	1/4" stainless steel ball valves

OD = Outer Diameter
ID = Inner Diameter

2.3 LFG condensate sampling supplies and PPE

The following supplies and personal protective equipment (PPE) were utilized to minimize and prevent contact with LFG condensate during sampling trips to the landfill.

- Carboys (i.e., large sampling containers)
- Disposable gloves and/or biohazard gloves
- Disposable pants
- Funnels
- Laboratory coat or disposable jacket
- Paper towels
- Plastic trash bags

2.4 ME treatment and associated experiments equipment/materials

Table 2.8 lists equipment utilized for ME treatment and associated experiments.

Table 2.8 Equipment used for ME treatment operations and associated experiments.

Equipment	Supplier	Model #	Specifications
Air pump	EcoPlus USA	ECOair 1	793 gph output, 2.9 psi, 0.25 A current, 120 V input, ¼" tube size
Buchner Funnel	--	--	Porcelain, perforated funnel
Electric Mixer	MXBAOHENG	JJ-1	Variable speed mixer, 3000 RPM capacity, 100 W DC motor
Gas Flow Meter	N/A	N/A	1.5 LPM flow meter
Glassware	--	--	Various laboratory glassware
ME Reactor	N/A	N/A	Described in following section
ORP Data Logger	Dataq Instruments	DI-2108	USB based instrument with WinDaq Acquisition software for data logging with measurement bounds of ± 100 V
ORP Probes	Gain Express	B07KXKR8C9	Single cylinder ORP electrodes, ± 1999 mV range, 1 mV resolution
Overhead Stirrer	JOAN LAB	OS-15S	Variable speed mixer, 100-2000 RPM capacity with RPM readout, mixing volume up to 10L
pH Controller	Bluelab	SKU: CONTPH	Programmable pH controller, 10 mL/min peristaltic pump for chemical dosing with 0.1 pH tolerance
pH Probe	Bluelab	SKU: PROBPH	Double-junction pH probe
Programmable timer	Nearpow	T19S	Digital timer outlet
Respirator	3M	B01CSPTIFW	NIOSH-approved respirator
Sieves	--	--	ASTM E-11 standard sieves, numbers 16 through 500
Support stands	--	--	Variable height support stands
Utility knife	--	--	Standard box cutter

2.5 Pipettes

Various pipettes, and pipette tips, were utilized in experiments reported in this thesis, as described in more detail in section 4.3.2. The equipment utilized are shown in Table 2.9.

Table 2.9 Pipette and pipette tip models and brands used.

Volume Dispensed	Brand (Model)	Pipette Tip
5 – 50 µL	Socorex (Acura 825)	Fisher, Sure One, 50 µL Filter, Sterile *and* Thermo Scientific ART™ 50 µL Aerosol Resistant Tip
20 – 200 µL	Socorex (Acura 825)	VWR Universal Pipet Tips, 200 µL
100 – 1000 µL	Socorex (Acura 825)	Fisher, Sure One, 1000 µL Filter *and* Neptune 1000 µL Blue Traditional Shaped Tip
0.5 – 5 mL	Socorex (Acura 835)	Fisher, Maxi Pipet Tips, 1000-5000 µL
1 – 5 mL	Fisher (Finnpipette)	Fisher, Maxi Tips, 1-5 mL
100 – 1000 µL	Four E's Scientific	Fisher, Sure One, 1000 µL Filter *and* Neptune 1000 µL Blue Traditional Shaped Tip
1000 – 5000 µL	ONiLAB (MicroPette Plus)	Fisher, Maxi Pipet Tips, 1000-5000 µL

3 Microelectrolysis (ME) reactor design and assembly

The following section details the ME reactor's design and assembly. It includes a subsection on the background of ME reactor development and a subsection on the redesign and construction of improved ME reactors.

3.1 ME reactor background

Column reactors to carry out ME treatment have been under development in Dr. Korshin's lab group since 2019. The design and operations of these reactors have been revised several times as the ME process has matured. Modifications have been carried out to investigate different modes of treatment as well as improve upon previous iterations. In late 2022, a reactor was prototyped, transitioning ME treatment facilitated by gas flow to ME treatment performed in the presence of mechanical mixing only (Pinochet-Troncoso, 2023). Two reactors were commissioned to investigate treatment by mechanical mixing and were operationally called "Big Column 2" and "Big Column 3" and will be referred to henceforth as BC2 and BC3 for short. These two column reactors were preceded by BC1 which relied upon CO_2 gas flow which was used for the fluidization of the ZVI/GAC phases, mixing and, partly, for As transfer to the gas phase. BC2 and BC3 utilized only mechanical mixing during ME treatment and CO_2 gas was used only to flush out the atmospheric oxygen from the system.

In September 2023, a new column reactor – referred to henceforth as BC4 – was designed and assembled, with the help of Zachary (Yak) Yerbich-Louman who is pursuing master's studies in Prof. Korshin's group. The design of this reactor closely followed that of BC 2/3 but was improved upon to better facilitate experiments of interest. Specific aspects of its design are given in the section that follows. Two smaller column reactors – CR9 and CR10 – were designed and operated by previous researchers, similar in design to BC2/3 but on a smaller scale with slight differences (Walters, 2022; Pinochet-Troncoso, 2023). In this thesis, CR9 and CR10 were utilized for a few preliminary experiments. BC3 was utilized for the bulk of ME experimentation from March to

September 2023. BC2 was utilized for gas phase experiments. BC4 was utilized for ME treatment from September 2023 onwards.

3.2 Reactor re-design and construction

Efforts to redesign column reactors were prompted by the need to better control ME treatment and optimize As removal. Design elements of BC4 which were maintained from BC2/3 are as follows:

- PVC reactor body
- Conical bottom
- ORP probes' placement
- pH probe placement
- Acid dosing port
- Mixing impeller's shaft length and diameter

BC4 design improvements and modifications are as follows.

1. Mounting the reactor against a reinforced wooden backboard improved reactor stability and standardized the reactor's position. Other equipment was mounted to improve organization within the laboratory hood.
2. The mixing shaft was stabilized by securing the shaft into the reactor cap with bearings at a particular height to maintain consistent depth of impellers across experiments.
3. The airtightness of the reactor cap was improved with a rubber gasket (i.e., O-ring) and bearings.
4. Gas effluent ports were installed in the top of the reactor and the cap and fitted with air control valves.
5. A dedicated condensate dosing port was installed in the top of the reactor next to a dedicated media dosing port with the intent to separate the liquid and media dosing.
6. A dedicated gas influent port was installed in the reactor bottom, alongside a media discharge port and effluent discharge port.

7. Aside from the media discharge port, stainless steel screens were installed in the reactor bottom to minimize media losses during cycling. The intent of the designated media discharge port was to improve ZVI/GAC media exchanges.

All valves utilized were tested for airtightness. Water-oil-gas valves were installed on ports with liquid dosing or discharges to ensure liquid and airtightness (i.e., sampling, condensate influent/effluent, and gas influent port). pH and ORP ports were installed per previous designs, with the omission of a redundant top ORP probe (i.e., 3 ORP ports in BC4 as opposed to 4 ports in BC3).

3.2.1 3D design and printing

Custom ME reactor components were previously designed for BC2 and 3 in Autodesk software (Pinochet-Troncoso, 2023). Custom designed reactor parts include the reactor cap, ORP/pH probe ports, mixing impellers, and conical reactor bottom. The cap design was modified by Yak Yerbich-Louman, blending elements of the senior design course with previous iterations and optimized 3D printing parameters. After design in AutoCAD, components were printed using PLA filament on Creality Ender 3 and Flashforge Adventurer 4 3D printers.

3.2.2 Reactor assembly

All pieces were secured to the column using waterproof silicone, marine adhesive sealant, and a self-leveling “lap” sealant. PVC tubing was cut to size using a bandsaw, courtesy of UW’s The 8 wood and metal shop. Port holes were drilled in the PVC using a Dremel tool. A heat gun was used to soften PLA printed impellers and fix them to a stainless-steel shaft. Impellers were further secured in place with heat shrink tubing, shrunk to either side of impellers. Figure 3.1 shows specific technical information of BC2 components.

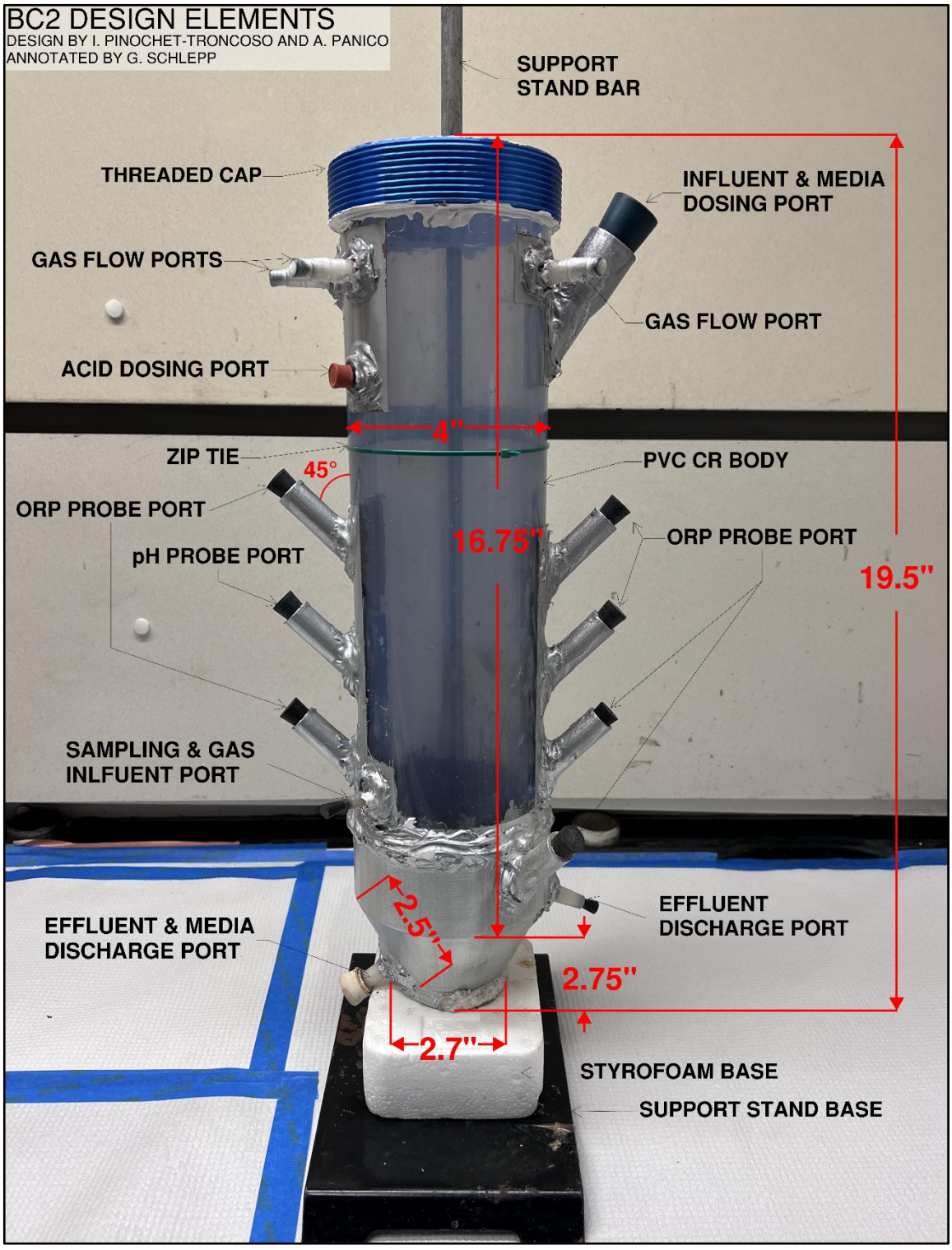

Figure 3.1 General view of BC2 ME reactor with annotated design elements and dimensions.

4 Methods

The following chapter describes the methods followed for the experiments reported in this thesis. Relevant protocols are described in the LFG condensate sampling, ME treatment, and Hazardous waste management sections. The Analytical Methods section details procedures for Analytical balances, ICP-MS, ORP, Determination of particles sizes of the active media by sieving, BET, and Mixing speed determination. Reference Chapter 2 for materials and equipment specified in the following methods.

4.1 LFG condensate sampling

Prof. Korshin's research team visited the landfill's site periodically, coordinated with the landfill, to collect LFG condensate from a tote which was filled with fresh condensate ("sample") by the third-party which treats the LFG. The desired volume of LFG sample was transferred from the tote to carboy containers with funnels. It was transported to the UW laboratory within one or two hours and stored in a cold room at approximately 5 °C until needed for ME experimentation. Section 2.3 describes the materials and PPE utilized in the sampling. Each sampling trip was referred to as a sample round (SR). ME treatment experiments were denoted by SR followed by sample round's number (i.e., sampling trip since start of research). This thesis' experimental work pertains to SR 17 through SR 19. The date of sampling rounds and the concentrations of analytes are shown in Table 4.1, determined by ICP-MS at certified laboratories. SR 19 was analyzed by KCEL and Fremont Analytical laboratories. SR 18 was analyzed by KCEL. SR 17 was sampled on March 10, 2023 (initial pH = 4.4) but was not sent for analysis by a certified laboratory. Appendix Section 7.1 includes sample round composition for SR 17-19, as quantified by the UW ICP-MS instrument.

Table 4.1 Sample round composition quantified by certified laboratories and pH measured prior to ME treatment operations.

Sample Round	Date	As, mg/L	Sb, mg/L	Fe, mg/L	pH
SR 18	May 12, 2023	15.4	2.4	301	--
SR 19	June 13, 2023	13.1 ± 0.3	2.3 ± 0.4	39 ± 28	5.3

LFG condensate sample ranged from orange to relatively clear in color with some rounds being more clear or opaque. The levels of organics were variable as well as the amount of grease and oil which is visible on the top of the sample. Floating hydrocarbons are the result of grease and oils used to lubricate LFG processing equipment. While the majority of hydrocarbons are skimmed from the condensate by the LFG processors, a small amount is retained in the condensate waste stream.

4.2 ME treatment

The following section describes the typical methodology for how ME treatment experiments were conducted in the laboratory. Each ME treatment experiment explored unique variables, but the overarching method was standardized. ME treatment was primarily differentiated by:

- Sample round (pretreatment)
- Treatment volume
- Reactor
- Length of treatment
- Gas flow
- Agitation
- Media dosing
- pH controlling acid
- Sampling frequency

4.2.1 Safety and waste disposal

All ME experiments were performed with the appropriate PPE: lab coat, goggles, mask (if desired), gloves, pants, and closed toe shoes. All work with LFG condensate was conducted under the hood to minimize contact with volatile species or other fumes off gassed from condensate. As stated in section 4.2.1, all wastewater and contaminated materials generated during ME treatment were properly disposed of through UW's EH&S Hazardous Waste collection service.

4.2.2 ME treatment operations

4.2.2.1 Reactor setup

The ME reactor and mixer were securely stabilized either by a support stand and adjustable holder or backboard. If a backboard was utilized, the reactor was secured via hose clamps and mixer was secured via U-shaped pipe clamp and wing nuts (Figure 4.1). The mixing shaft was fitted through the reactor cap and placed into the reactor. The cap was screwed tightly in place and the mixing shaft was secured into the overhead mixer's motor shaft via adjustable chuck (i.e., shaft coupling). Mixer height was adjusted until the mixing shaft was positioned optimally, by height and vertical alignment. The pH controlling unit was secured to a backboard. The pH probe was calibrated with pH 4 and 7 buffers prior to each experiment was secured in-place with multiple layers of Parafilm to create a liquid-tight seal between probe and reactor. Acid intake tubing was placed into a vessel of acid; for acid expenditure tracking, acid was dosed from a graduated cylinder. The acid feed line was connected to the reactor's acid dosing port. ORP probes were likewise calibrated with 256 mV ORP buffer and secured in-place with Parafilm in their designated ports. A gas delivery hose was connected to a gas influent port.

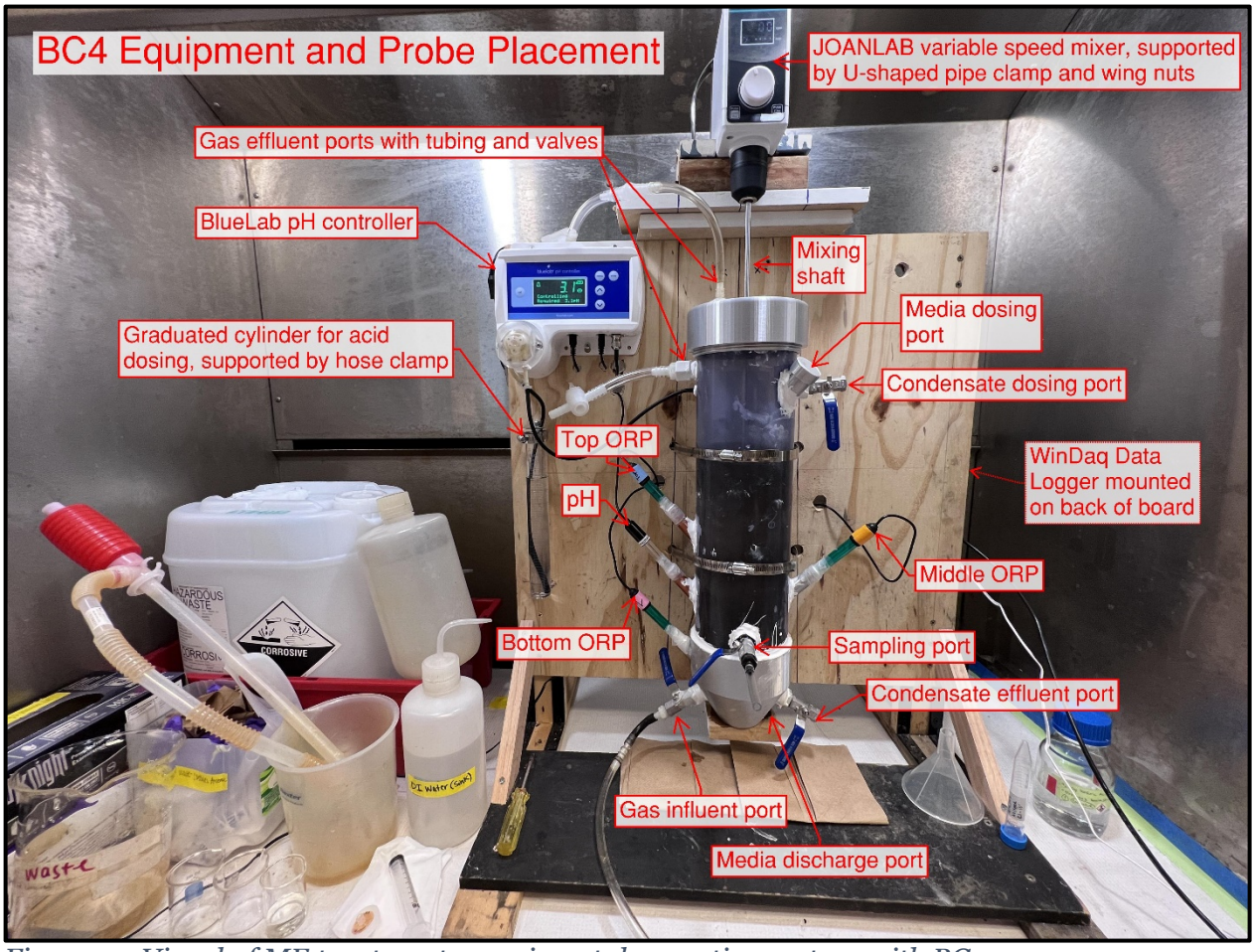

Figure 4.1 Visual of ME treatment experimental operations set up with BC4.

4.2.2.2 Experimental start-up

The reactor's headspace was flushed with CO_2 or N_2 gas, at approximately 1 L/min regulated via gas flow meter, to evacuate atmospheric oxygen. Stored condensate was retrieved from the cold room, the desired treatment volume was transferred into a secondary container via a hand pump. The desired aliquot of the LFG condensate was carefully poured into the reactor through the dosing port using a funnel. The mixer was turned on to approximately 100 RPM; acid was manually dosed (using the pH controller's override function) until the condensate was adjusted to the desired starting pH. The mixer was turned off and a small beaker of pH adjusted condensate (approx. 50 mL aliquot) was discharged for media flushing. Active media were weighed using an analytical balance (See section 4.2.3 for example media dosing calculations). The data acquisition

system was setup and ORP measurements were started. Media were poured into the reactor's dosing port via funnel and flushed with the aliquot of condensate. No pretreatment or activation of the active media prior to their dosing to the ME reactor was used.

The mixer was turned on to the desired speed and a timer was started, with the mixing of media and condensate denoting the official start of ME treatment. The dosing port was sealed with a rubber stopper, gas egress valves were closed, and gas flow was quickly turned off. Vacuum grease was applied to the space between the mixing shaft and reactor cap to reduce ingress of oxygen into the reactor. Due to the initial catalytic action of the media, acid was manually dosed at the beginning of treatment (approx. 5-minutes) to maintain desired pH and reduce risk of overdosing acid using the control feature. Once the pH equilibrated at the desired acidity, the pH controller was set into "controlling" mode to maintain pH throughout the rest of treatment with automatic acid additions. Controller settings were modified, as necessary, based on dosing frequency (typically 1-minute) and dosing time (typically 4 to 6 seconds). Note that periods of quiescence (i.e., no mixing) were minimized as they led to acid overdoses, since acid was not fully incorporated into the liquid matrix during these times.

4.2.2.3 Sampling

Throughout treatment, ME-treated effluent was sampled periodically. Initial samples (i.e., untreated condensate) were drawn up from the condensate storage bottle via syringe and filtered into a test tube. For treatment samples, the mixer was briefly paused (15 to 30 seconds) to allow suspended media to settle. Via the reactor sampling port, condensate was briefly flushed (1 second) into a waste beaker to expel dead volume. Then, 5 to 10 mL of effluent was discharged into a clean beaker, drawn up by a syringe, and filtered into a test tube for ensuing ICP-MS analysis. Mixing was resumed.

4.2.2.4 Post-treatment.

Once the ME treatment time concluded, the mixer was turned off, pH controller was set to "monitor" mode (i.e., conclusion of acid dosing), and the final treatment sample was taken. The volume of dosed acid was recorded. The ORP data was saved and exported to Excel. If desired, an effluent sample was taken and stored for further experimentation (e.g., titration).

If cycling of ME treatment media was desired, treated effluent was drained via the *effluent discharge valve* and disposed of, while maintaining the settled media in the bottom of the reactor. The next batch of condensate was added to the reactor along with any desired additional media doses. Smaller, supplementary doses of active media were added with the next cycle's fresh condensate with the intention to extend the useful life of the initial active media dose. These supplementary media doses are henceforth referred to as "top-offs". The next cycle of treatment was then initiated, per Section 4.2.2.2's methodology, thus recycling the original treatment media for another round (cycle) of treatment with fresh condensate.

The primary differences between the first treatment cycle and subsequent cycles were:

1. Longer manual acid dosing at beginning of subsequent cycles
2. Dosing of supplementary media (i.e., top-offs)
3. Returning media lost during sampling or draining to the reactor

If no more cycles of treatment were required, the reactor was drained via the *media discharge port*, draining a slurry of media and effluent. The mixer was often turned on during this drainage to assist with the removal of media from the reactor. After draining, the reactor's probes were removed, cleaned and stored. If probe electrodes appeared particularly dirty (e.g., residual media, discoloration) they were soaked in 0.1 M HCl or 0.1 M H_2SO_4 for a few hours, thoroughly rinsed, and stored in fresh buffer solution. Then, the reactor was rinsed and dried with paper towels to remove residual media from reactor sidewalls.

4.2.3 Active media dosing Calculations

ME treatment media were dosed in a mass ratio and were most frequently dosed in a two-to-one (2:1) mass dosing ratio of ZVI to GAC, respectively. Typical supplementary doses (i.e., top-offs) ranged from 1 to 2 g/L, with various compositions of media (e.g., ZVI only, GAC only, combined). An example calculation for active media dosing is performed below:

Treatment volume (V): 2 L
Dose (d): 50 g/L ZVI and GAC, 2:1 dosing ratio (by mass, respectively)

$$Total\ mass\ media\ (M) = V \times d$$

$$M = 2\ L\ \times\ 50\frac{g}{L} = 100\ g$$

$$Total\ mass\ ZVI\ (Z) = \frac{M}{3} \times 2$$

$$Z = \frac{100\ g}{3} \times 2 = 66.7\ g$$

$$Total\ mass\ GAC\ (G) = \frac{M}{3} \times 1$$

$$G = \frac{100\ g}{3} = 33.3\ g$$

4.3 Analytical Methods

4.3.1 Analytical balances

Unless stated otherwise, all masses weighed were performed on an analytical balance. For mass less than 310 g, a Mettler Toledo MonoBloc analytical balance was used and reported a precision of ± 0.001 g. For pipette calibration affirmations, a Mettler AE 100 analytical balance was used, had a maximum allowable weight of 109 g, and reported a precision of ± 0.0001 g.

4.3.2 ICP-MS

Inductively coupled plasma mass spectrometry (ICP-MS) is an industry standard analytical method which atomizes aqueous samples to determine trace levels of elements with precision and accuracy (PerkinElmer, n.d.). During the ICP-MS analysis, a liquid sample is nebulized, and the generated aerosol is conveyed by argon gas to a plasma torch. Plasma atomizes the stream of sample droplets producing ions which are separated by skimmers, interference cones, and

extraction lenses (Elemental Analysis Core, n.d. and EPA, 2024). A mass spectrometer then sorts ionized elements based on their mass-to-charge (m/z) ratio. A detector counts ions, and this measurement is converted to an analyte's concentration. The EPA's Method 6020B was adapted for this research and specifies ICP-MS to be suitable for the determination of As, Sb, and Fe. This research's ICP-MS analysis was conducted on a PerkinElmer Nexion 2000B ICP-MS instrument, maintained by the UW's Research Training Testbeds (RTT) facility and located in the Nanoengineering and Sciences Building (NanoES). The Nexion ICP-MS instrument was best operated in the KED mode to minimize interference between analytes of interest. This was particularly important for Fe determination since argon complexes with oxygen to create ArO+ which has the same mass as Fe (56 amu).

A range of four to seven ICP-MS calibration standards were prepared from ICP-MS grade standards (Section 2.1.1) to adequately span the typical analyte concentrations found in research samples. All standards were prepared with 2% nitric acid concentration, by volume. Calibration standards were continually optimized to improve the accuracy of analyte determination and were redeveloped based on sample dilution factors (DF). Primarily, ME treatment effluent samples were prepared for ICP-MS analysis. These samples were filtered with 0.45-μm Nylon filters tips to prevent particulate matter (PM) from entering the ICP-MS atomizer. Filtered samples were diluted with Milli-Q ultrapure water and trace metal grade nitric acid to a 2% acid concentration, by volume. Additionally, a known concentration of Yttrium was added to all calibration standards and samples as a quality control check. See Section 2.5 for pipettes utilized for ICP-MS sample preparation.

ICP-MS determination accuracy strongly depends on careful sample and calibration standard preparation. To confirm the reliability of ICP-MS analysis at the Research Training Testbeds (RTT), the UW sent a selection of samples to the King County Environmental Lab (KCEL) which is accredited by the Washington State Department of Ecology (DOE). The UW's As and Sb removal trends were confirmed by KCEL's analysis, as discussed in the sections that follow (Section 7.1).

4.3.3 ORP measurements

Oxidation reduction potential (ORP) is a measure of oxidative or reductive capability. ORP can be measured by an electrode and the reported voltage is proportional to the solution's tendency to transfer electrons, through either a gain or loss (Phidgets. 2023). The ORP of an environment is represented in millivolts with positive and negative ORP values tending to indicate an oxidizing or reducing environment, respectively. As opposed to pH probes, which are selective to the activity of H^+ ions, ORP is non-ion specific and provides a measure of the redox state of the solution, as defined by all its components, notably dissolved oxygen, presence of ZVI and other redox-active reactants.

ORP electrodes were utilized to track the development of sufficiently reducing conditions during ME treatment (Table 2.8). Potential complications regarding ORP data capture included imprecision of the used electrodes, sampling frequency, limitations with electrode calibration, frequency of probe replacement, and difficulty to capture data in a continuously mixed environment (Phidgets. 2023). Section 4.2.2 provides additional details for description of ORP data acquisition setup.

Four Gain Express ORP electrodes were used to monitor ORP during ME treatment using a data logger, providing measurements from three distinct reactor locations: top, middle, and bottom. The electrode positioned at the top of the ME reactor provided redundant ORP measurements. The data logger's default for continuous ORP monitoring was 100 measurements per second generating enormous datasets for 1-hr of ME treatment. A number of data processing methods were explored to manage and process the ORP datasets including MATLAB and JupyterHub (Python). Due to the high sampling frequency and mixing employed during ME treatment, raw ORP data was noisy. This noise was mitigated by applying a moving (or rolling) average function which smoothed the trends in ORP. Smoothed data still showed some undulation in ORP. Periodic peaks in ORP coincided with sampling times when the mixer was paused, and the probes equilibrated with the still liquid matrix.

Inter-electrode differences in ORP, which tended to be prominent, were hypothesized to be caused by the settling out of ZVI which has a lower natural ORP than GAC. When ZVI settled to the bottom of the reactor, due to its greater density, it would be anticipated that the top and middle reactor probe readings would rise due to the primary influence of still-suspended GAC particles (or micro-GAC, created upon mixing). Critical review of ORP data questioned the accuracy of the probes and discussion for more frequent probe calibration and use of alternative probes. Most ORP calibration solutions are for calibration to +256 mV. The ME process predominantly occurred in the negative, reductive ORP range, so calibrating with these standards may not have been the optimal calibration technique.

All told, while extensive ORP measurements were carried out it this study, their results were concluded to be of a generally indicative rather than of a precisely measured nature. As such, results of ORP measurements were interpreted in the context of the development of an alternative concept of correlating Fe release and As removal in ME treatment, as explained in more detail later in this thesis.

4.3.4 Determination of particles sizes of the active media by sieving

Sieve analysis is a conventional method to characterize a solid sample's distribution of particle sizes which provides insight to a medium's properties, such as specific surface area. In this research, ZVI and GAC were the media of interest and multiple products' particle distributions were compared and used to estimate specific surface area (Table 2.3). Specific surface area is a metric which may be useful when considering available surface area for reaction or contaminant retention. This thesis' sieve analysis followed ASTM sieving protocol and utilized a variety of sieve sizes to develop a distribution of particle sizes on a basis on mass retained on each sieve.

To perform the sieve analysis, the masses of solid media passing through a set of ASTM E-11 standard sieves, numbers 16 through 500, were weighed and recorded. For this scale of sieve sizes, the smallest number ASTM sieve corresponded to the largest opening and vice versa. A 10 g mass

of each sample tested was weighed in a weigh boat. From largest opening size to smallest, each sample was sieved, and the weight of the sieve and mass retained was recorded. The mass of sample retained on each sieve was calculated by subtracting the mass of the sieve from the mass of the sieve and sample retained. The percentage of sample passing through each sieve was calculated to determine the distribution of particle sizes. The sieving data was then utilized to estimate specific surface areas of the media by assigning a typical density associated with each media type or using the supplier's reported media density (Table 2.3). The mass of particles retained on each sieve was multiplied by the media's bulk density to estimate the volume of particles retained. This volume was divided by the estimated volume per particle, based on the sieve's opening diameter and assuming particles were spherically shaped, to estimate the number of particles withheld on each sieve. Then, the estimated number of particles was multiplied by the estimated surface area per particle, also based on sieve opening size. All sieve's surface areas of particles retained were summed to determine the total surface area of particles; this was divided by the sample mass to estimate each sample's specific surface area, or surface area of particles available to react on a per mass basis.

4.3.5 BET measurements of specific surface area

Specific surface areas of the solids used in ME treatment were determined by the standard Brunauer, Emmett and Teller (BET) method. The BET theory determines a material's specific surface area and characterizes micro and/or mesopores based on gas adsorption analysis (Particle Technology Labs (PTL), n.d.). Sample pores are typically grouped in the classes of micropores (pore diameter, $d < 2$ nm), mesopores ($2 < d < 50$ nm), macropores ($d > 50$ nm). Additionally, super (ultra) micropores are $d < 1$ nm may be present (PTL, n.d.). BET analysis is conducted by vacuum-drying a sample, cooling the material to cryogenic temperatures, and measuring the sorption of an inert gas (typically nitrogen) to the sample's surface. Specific surface area is

calculated using the sample's mass differential, between the adsorption and desorption phases, and the sample's adsorption isotherms measured by the analyzer.

The UW's Scale-Up & Characterization Testbed facility, located in the Bowman Building, houses a Micromeritics 3Flex physisorption analyzer which calculates surface area, pore size, and adsorption properties of solids and powders. The instrument was used to perform BET analysis to characterize media utilized in ME treatment.

Empty Micromeritics glass sample tubes (with caps) were weighed on an analytical balance, using a deionizer to reduce static which interferes with accurate weight measurements. 50 to 100 mg of samples were weighed on weighing sheets, were added to the glass tubes, and the tubes were re-weighed. The initial weight readings' accuracy was critical, as the rest of the analysis hinged upon the samples' measured changes in mass. The tubes were secured to a VacPrep machine with metal fittings and O-rings. An analysis method was developed on the equipment's software using the Surface Area and Pore Size determination platform. Degassing conditions were specified as having a gas evacuation rate of 5 mmHg/s, temperature of 300 ^{o}C, and evacuation time of 12 hours for GAC and 48 hours for ZVI (Bounab et al., 2021). The samples were then degassed. Once complete, the sample vials were removed from the VacPrep instrument and reweighed. Then, samples were secured to the Micromeritics instrument and placed inside a vessel of liquid nitrogen to maintain sample temperature of 77 K to facilitate an adsorbing environment. Nitrogen was then dosed to the sample vials and the relative changes in pressure were measured by the instrument during both adsorption and desorption. Once this analysis was complete, the software generated a report which included properties of interest such as specific surface area, pore sizes, and adsorption/desorption isotherms.

4.3.6 Mixing speed determination

A Neiko digital tachometer (Model: 20713A) with a 999,999-rpm measurement capacity was utilized to estimate the mixing speed of the JJ-1, variable speed electric mixer. Unlike the Joanlab mixer, the JJ-1 mixer did not display mixing speed. Thus, the tachometer was used to determine

different mixing speeds on the JJ-1 mixer which was useful for investigating ME treatment's dependence on rate of agitation. To operate the tachometer, a small piece of reflective tape was placed on the mixing chuck. The mixer was turned onto the desired speed and the tachometer was activated, shining a detection laser onto the reflective tape. The tachometer output the tape's rate of rotation which corresponded to the mixing speed.

4.4 Hazardous waste management

The More Hall Environmental Engineering laboratory utilized UW's Chemical Waste Disposal service, provided by the department of Environmental Health & Safety (EH&S). A routine chemical waste collection was developed for regular pickup of the typical waste generated by ME operations. This solid-liquid waste stream was disposed of in EH&S provided carboys, labeled with an approximation of its volumetric composition, and collected by EH&S for proper hazardous waste disposal. Labeled constituents included: water, oil (contaminated), iron (ZVI), carbon (GAC), arsenic (organic), antimony, sulfuric acid, etc. In addition to the typical waste generated by ME operations, other chemicals utilized for research were also properly disposed of using EH&S's chemical waste disposal services.

5 Experimental results & discussion

5.1 Material characterization

The following section characterizes the active media employed in ME treatment testing and optimization. The CR ZVI product was determined to be a suitable alternative for the previously utilized LC Plus, procured from the same trusted vendor (Höganäs) (Section 5.1.5). The IPW GAC product, while slower at catalyzing ME treatment, was a suitable and less expensive alternative for the previously utilized Thermo Scientific product (Section 5.1.6).

5.1.1 Sieving

A sieve analysis was performed to determine ME treatment media particle size distributions, per Section 4.3.4. LC Plus was the previously utilized ZVI product but was discontinued, so an acceptable alternative needed to be identified. Prior to LC Plus, LC Plus Fine was utilized with PAC. However, coarser media was desired to improve particle settling time for ease of ME treatment cycling with the same media. An alternative, less expensive GAC product was also desired since the research team had been utilizing a high-purity, research-grade product (Thermo Scientific) which would be too costly for pilot and full-scale treatment.

Five Höganäs ZVI products listed below were sieved. Their specifications are listed in Table 2.3:

- LC Plus
- LC Plus Fine
- CR
- CR Plus
- PRB

In addition to ZVI, four GAC products were sieved, with their specifications also listed in Table 2.3:

- Thermo Scientific 12-40 mesh (nominal size range 1,700 to 425 μm)
- Sigma-Aldrich 4-14 mesh nominal size range 4,750 to 1,400 μm)
- Sigma-Aldrich 8-20 mesh (nominal size range 2,360 to 850 μm)
- IPW 12-40 mesh (nominal size range 1,700 to 425 μm)

The sieve analysis affirmed the products' specified mesh and determined their particle size distributions (Figure 2.1 and Figure 2.2). The LC Plus Fine product had the finest, and most uniform, particle size distribution. CR Plus was the next finest product, had the least uniform particle sizes, and was recommended to be discarded from further testing due to orange hue left on the liquid (i.e., manufacturer's acid washing "activation" residue). The LC Plus and CR products had similar mid-range, fairly uniform particle size distributions. PRB was the coarsest ZVI, with a fairly uniform particle size distribution, and was recommended to be omitted from further testing due to its potential to wear down or damage to mixing equipment.

The GAC analysis determined the Sigma-Aldrich 4-14 mesh product to be the coarsest, as expected. The IPW product had a very similar distribution to the Thermo Scientific product, which was expected since they both were specified as 12-40 mesh products.

Due to the nature of GAC, the spherical particle surface area assumption was deemed to be inappropriate. Rather, GAC products were analyzed using the BET method for a more accurate measurement of their total surface area, including pore volumes.

5.1.2 BET

Surface area and pore volumes were measured using the BET method for the two 12-40 mesh GAC products utilized for large particle active media ME treatment: Thermo Scientific and IPW. Table 2.3 lists their specifications and Section 4.3.5 provides more information about BET methodology. The BET instrument's software reported findings for both the adsorption and desorption phases of the analysis, reporting measurements during the increasing pressure step (adsorption of Nitrogen) and decreasing pressure step (desorption of Nitrogen), respectively. Errors may be introduced to the reported BET surface areas and volumes based on the weight measurements taken using an analytical balance. Care was taken to ensure the most accurate and stable weight readings possible using an anti-static gun. If the mass measurements were erroneous by 10%, for example, then the reported BET surface area would also be erroneous by the same factor, since the BET surface area is normalized per gram of material tested.

5.1.2.1 ZVI

The typical BET analysis method, optimized for analyzing materials such as GAC, failed to report an accurate surface area for ZVI samples analyzed. Despite modifying the BET methodology to better suit ZVI's physical properties, all BET analyses to quantify ZVI products' surface areas and pore volumes failed. This was likely due to the ZVI media's inherently low surface area and the lack of micro- and meso- pores. Given the general absence of pores and unsuitability of ZVI for reliable BET measurements, estimates of the surface area of ZVI materials based on their size distribution determined by sieving can be used.

5.1.2.2 GAC

The BET analysis reported that the IPW GAC product had a BET surface area of 926 m^2/g, cumulative pore volume of 0.226 cm^3/g, and average pore radius as 6.7 nm (per the adsorption isotherm, Figure 5.1). The BET analysis reported that the Thermo Scientific GAC product had a BET surface area of 884 m2/g, cumulative pore volume of 0.482 cm3/g, and average pore radius as 4.9 nm (per the adsorption isotherm, Figure 5.2). In summary, the IPW GAC product has a larger BET surface area than the Thermo Scientific product, but a smaller pore volume area. This difference in pore volume could contribute to why the Thermo Scientific product appears to perform better than the IPW GAC product (Section 5.1.6).

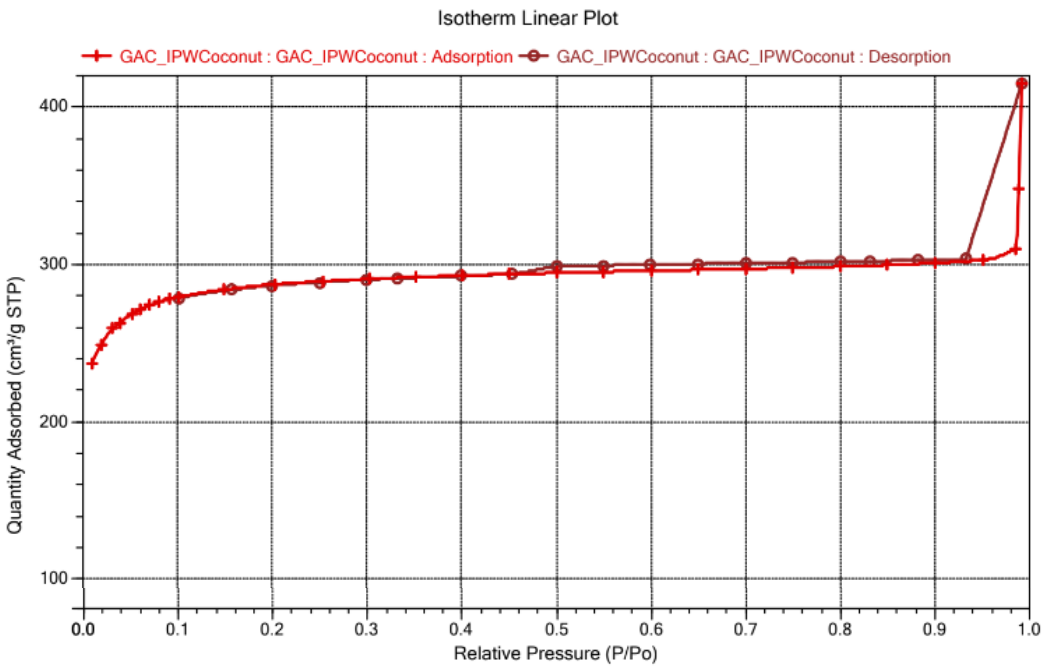

Figure 5.1 BET adsorption plot for IPW GAC

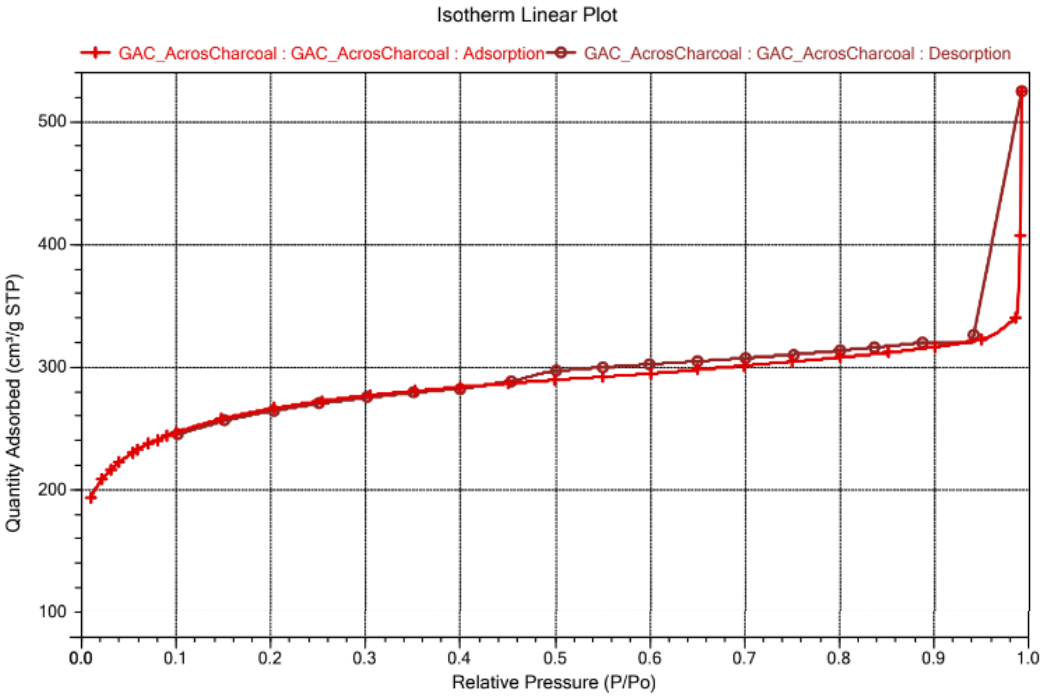

Figure 5.2 BET adsorption plot for Thermo Scientific GAC

5.1.3 Settling time

An experiment to quantify settling time was conducted by suspending active media products in water via mechanical mixing in a larger beaker. In water, all Höganäs ZVI products and both 12-40 mesh GAC settled within approximately 15 seconds. When ZVI and GAC were mixed together, ZVI were observed to ballast GAC settling. PAC did not settle within the experimentation time, further affirming its incompatibility for cyclical ME treatment utilizing the same media.

Post-ME treatment, with the active media suspended in treated LFG condensate, suspended particles largely settled after 5-minutes of settling time, a relatively short period for inter-cycle processes. All ZVI particles were observed to settle well and only a fraction of GAC particles remained suspended, likely due to the carbon's air entrainment.

Observations generated in the settling experiments resulted in several recommendations for further exploration, as stated as follows:

- Investigate two or three alternative impeller designs, sized to be approximately 1/3 of the reactor vessel's diameter; seek to utilize impellers which promote particle suspension (likely via axial flow) and minimize air entrainment
- Investigate an optimal off-bottom distance for the reactor's bottom impeller, and standardize this set-up, ideally utilizing only one impeller
- Optimize mixing speed to achieve sufficient particle suspension

5.1.4 Quantifying activation effects of active media through pH drift

5.1.4.1 pH Drift: 50 g/L ZVI:GAC (2:1) active media dose, small column

To better understand the individual, and combined, catalytic effects of active media in their consumption of protons, an experiment was conducted to monitor the increase in pH (or drift) from pH 3.0 at which most ME experiments were carried out. The speed at which protons were consumed, as tracked by the rise in pH upon addition of active media, was thought to indicate the speed of ME treatment activation, and thus, As removal kinetics. In a small column, 0.5 L of LFG

condensate sample (SR 17) was corrected to pH 3.0 using 1 M sulfuric acid, per normal operations (Section 4.2.2). The reactor was purged with CO2 prior to experimentation to remove oxygen and achieve a near-anoxic environment. Different combinations of active media were added to the pH-corrected sample, mechanical mixing was applied, and the resultant increase in pH (i.e., drift) was recorded. CR brand ZVI and IPW brand GAC were utilized for this experiment. Three variables were separately tested: GAC only, ZVI with GAC added sequentially, and ZVI & GAC.

The GAC only experiment was conducted by adding 16.6 g/L GAC alone and observing the resultant drift in pH. The ZVI with GAC added sequentially experiment was conducted by first adding 33.3 g/L of ZVI and observing the resultant drift in pH. Once pH stabilized, 16.6 g/L of GAC was added, and pH was further monitored for any additional drift catalyzed by the GAC. The ZVI & GAC experiment was conducted by adding 50 g/L of ZVI and GAC (2:1, by mass) together, per normal experimental conditions, and observing the resultant drift in pH.

As shown in Figure 5.3, GAC only was very slow at raising pH and the overall change of pH was much less pronounced than that in the case of ZVI, as GAC by itself does not consume protons although carboxyl-type surface functional group can have some proton-binding capacity. For ZVI with GAC added sequentially, pH drift induced by ZVI by itself stabilized after approximately 22 minutes; upon the addition of GAC (at 22 minutes), there was a secondary small increase in pH. ZVI & GAC added together induced the fastest and largest drift from pH 3.0. This experiment confirmed that, as judged by the consumption of protons that results in pH increases, the combination of ZVI & GAC together induces a greater catalytic effect than for media on their own. While ZVI alone does induce a near-same pH drift, the considerably faster increase of pH for the combined media indicates their greater activity together, based on their interparticle interactions that result in the galvanic coupling of iron and carbon particles and thus increased rate of the oxidation of the iron phase by the protons. However, this effect was most prominent for the first few minutes of ME treatment. Decreases in Figure 5.3 pH readings were hypothesized to be due

to the limitations of the pH probe to accurately monitor pH in a continuously mixed environment with suspended particulates.

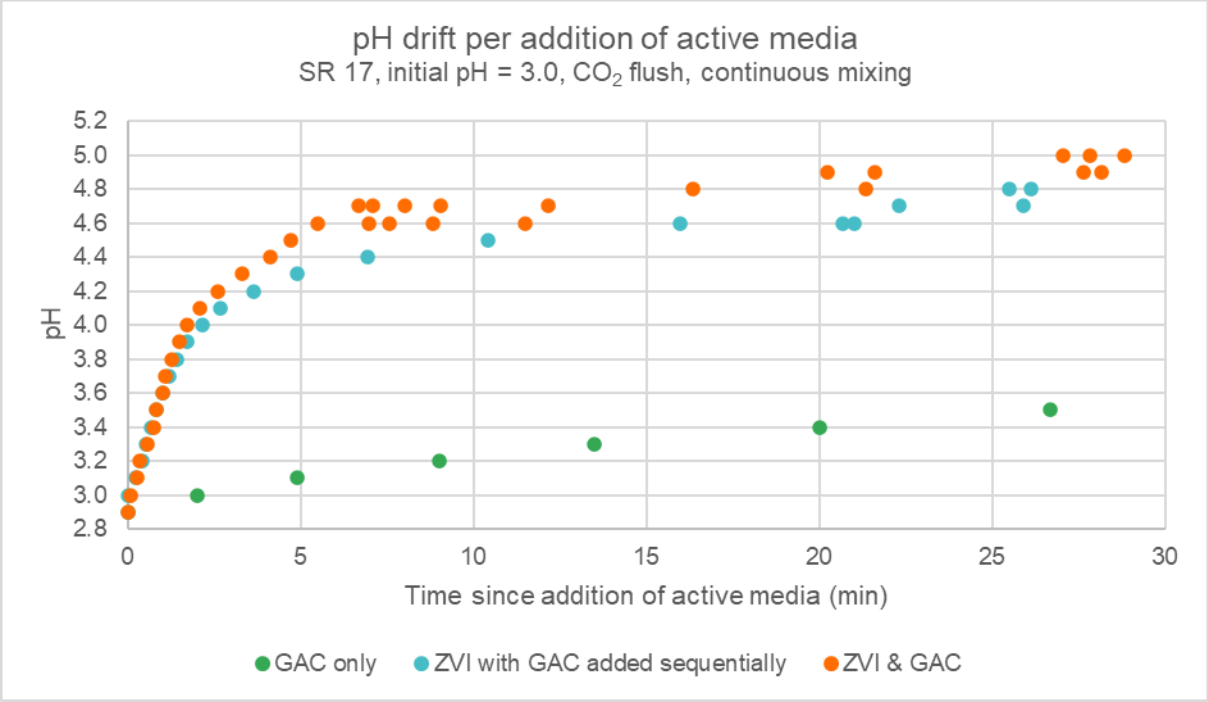

Figure 5.3 Overall pH drift from 3.0 versus time since addition of active media for 50 g/L ZVI & GAC (2:1) dose

5.1.4.2 pH Drift: 16 g/L ZVI:GAC (2:1) active media dose, big column

To better quantify the initial catalytic effect of active media, the pH drift experiment was repeated using varying Fe/C doses. In the 50 g/L active media experiment, the catalytic action was most prominent during the initial 5 minutes of reaction (Section 5.1.4.1). The experiment was expanded using variable GAC doses (2.5, 5, 8, and 12 g/L), to investigate the impact of GAC dose on the catalysis of ZVI. This experiment was conducted in a large column (BC3) with 2 L of LGC condensate sample (SR 18), adjusted to pH 3.0 with 1 M sulfuric acid. CR brand ZVI and IPW brand GAC were utilized for this experiment.

As shown in Figure 5.4, there was a strong effect of the amount of GAC added on the rate of the immediately observed increase of pH from the initial 3.0 value to approximately 3.7. Measurements of pH drift for ZVI only and ZVI with 5.0 g/L GAC test resulted in smooth pH drift

curves. The other three tests showed the presence of some stepwise changes of pH versus time. This may be attributed either to limitations of the pH probe to respond sufficiently rapidly to changing pH, and/or instabilities of mixing of the Fe/C media in a relatively large reactor. It is unclear as to why at contact times above ca. 2 minutes, the test with 5 g/L of GAC consumed protons faster than the other tests. This indicates that while the overall trend is clear, some of the experiments may need to be repeated in the context of further investigation of catalytic effects in Fe/C systems.

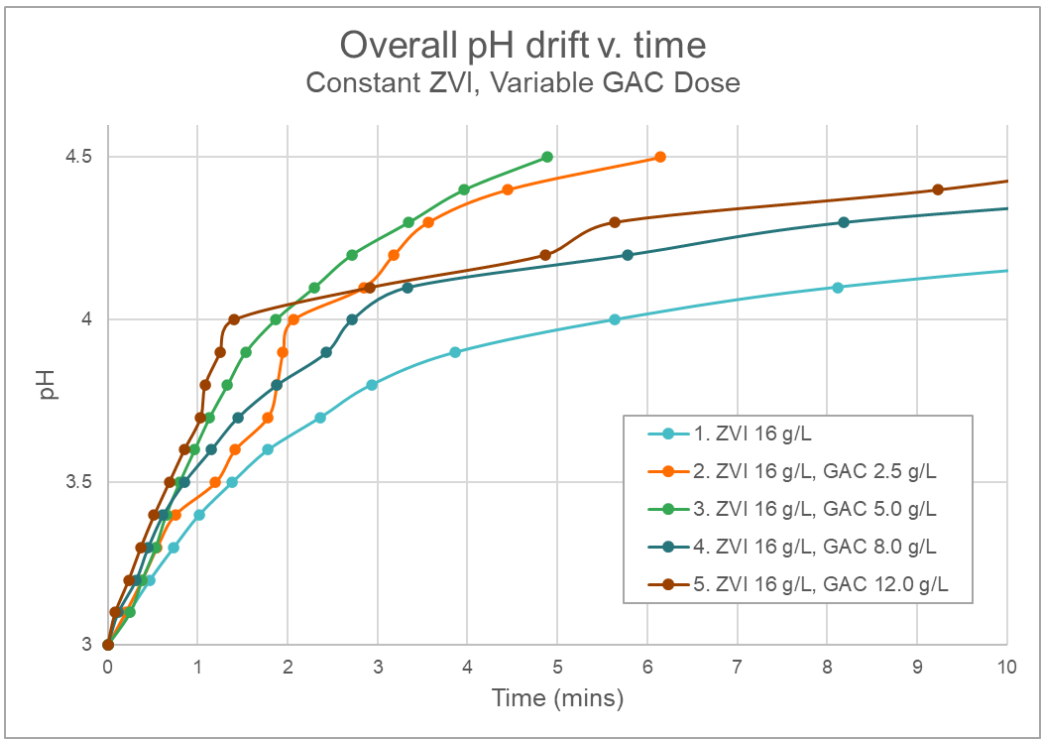

Figure 5.4 Overall pH drift from 3.0 versus time since addition of active media for 16 g/L ZVI and variable GAC dose.

Over the first minute, ZVI only had the slowest initial proton consumption, as would be expected for an "uncatalyzed" ME treatment (i.e., no GAC) (Figure 5.5). ZVI with 12.0 g/L of GAC 12.0 g/L, the highest GAC dose tested, had the fastest initial proton consumption, as was expected for ME treatment with the greatest concentration of GAC catalyst. There was some variability between pH changes observed for GAC concentration varying from 2.5 to 8 g/L. Nonetheless, the data

indicate that the higher the dose of GAC, the faster the consumption of protons in the examined Fe/C systems.

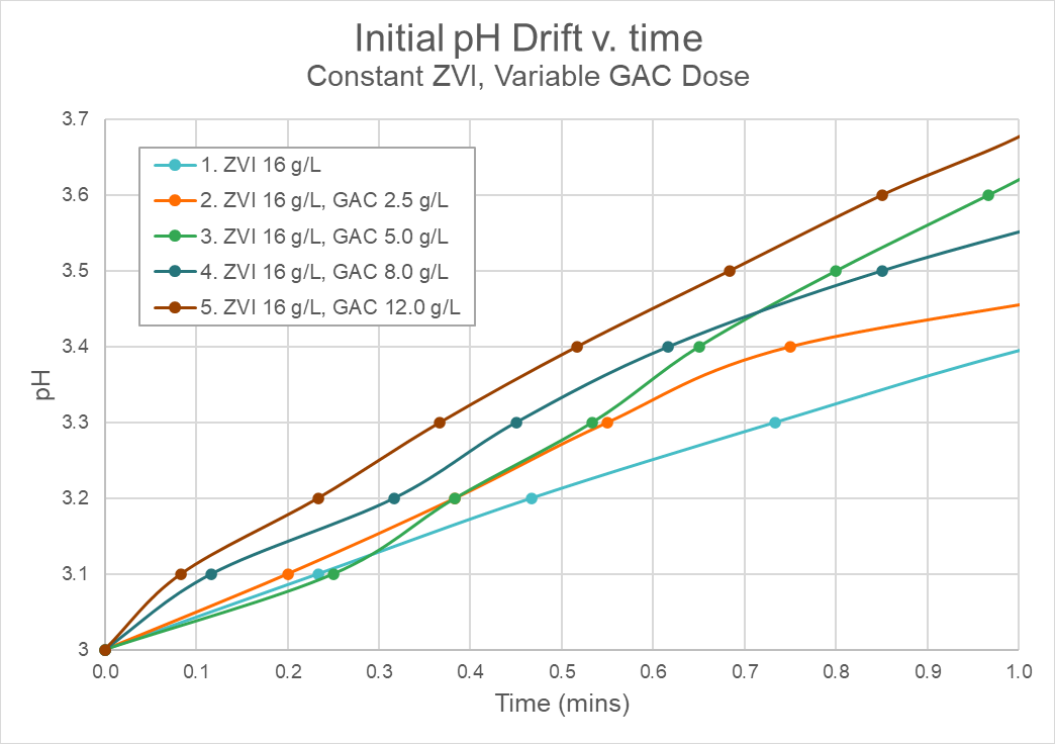

Figure 5.5 Initial pH drift (t = 0 to 1 minute) from 3.0 versus time since addition of active media for 16 g/L ZVI and variable GAC dose

5.1.5 Comparison of As & Sb removal using alternative ZVI types

ME treatment was conducted with several types of ZVI at a constant dose of 50 g/L ZVI and GAC (2:1, by mass). The goal of these experiments was to compare their performance to remove As and Sb. ME treatment conditions are summarized in Table 5.1:

Table 5.1 ME treatment conditions for varying ZVI types experiment

V	SR	Reactor	Dose	pH	Agitation	Purging	Length
2 L	17	BC 3	50 g/L (2:1, variable ZVI & IPW GAC)	3	Continuous mixing, ~1000 RPM	pre-treatment, CO2 at ~ 1 LPM	30-minutes

Results of these experiments affirmed that the use of CR and CR Plus ZVI materials resulted in nearly the same As and Sb removal as LC Plus within 30-minutes of ME treatment (Figure 5.6).

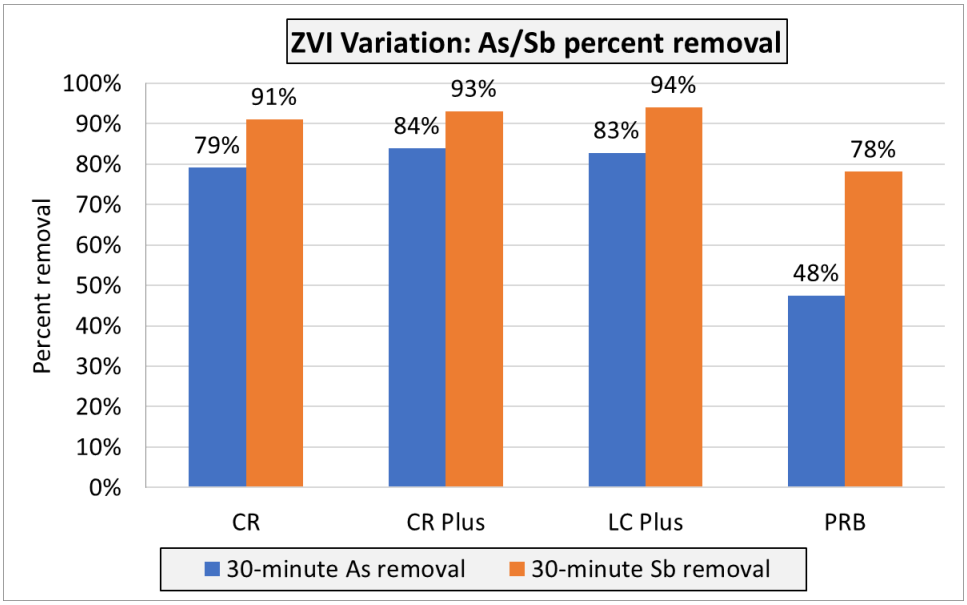

Figure 5.6 Comparison of As/Sb removal for varying ZVI types with ME treatment conditions of 2L of SR 17 in BC3 with 50 g/L ZVI & IPW GAC (2:1) dose, continually mixed for 30-minutes at 1000 RPM at pH 3.0 with pre-treatment CO2 purging

A disadvantage associated with using CR Plus as the ME treatment ZVI medium was that the red-orange stain which rapidly developed during treatment indicated the comparatively lower stability of this type of ZVI. Additionally, this product is notably more expensive than the CR product.

5.1.6 Effects of GAC type on As and Sb removal

5.1.6.1 IPW v. Thermo Scientific, 30-minute ME treatment

An experiment was conducted to compare the performance of two GAC products, seeking to determine whether the IPW GAC product was a suitable substitute for Thermo Scientific GAC product. ME treatment conditions are summarized in Table 5.2:

Table 5.2 ME treatment conditions for varying GAC types experiment

V	SR	Reactor	Dose	pH	Agitation	Purging	Length
2 L	17	BC 3	50 g/L (2:1, LC Plus ZVI & variable GAC)	3	Continuous mixing, ~1000 RPM	pre-treatment, CO2 at ~ 1 LPM	30-minutes

Results indicated that the IPW GAC product catalyzes the ME process slower than the Thermo Scientific GAC (Figure 5.7).

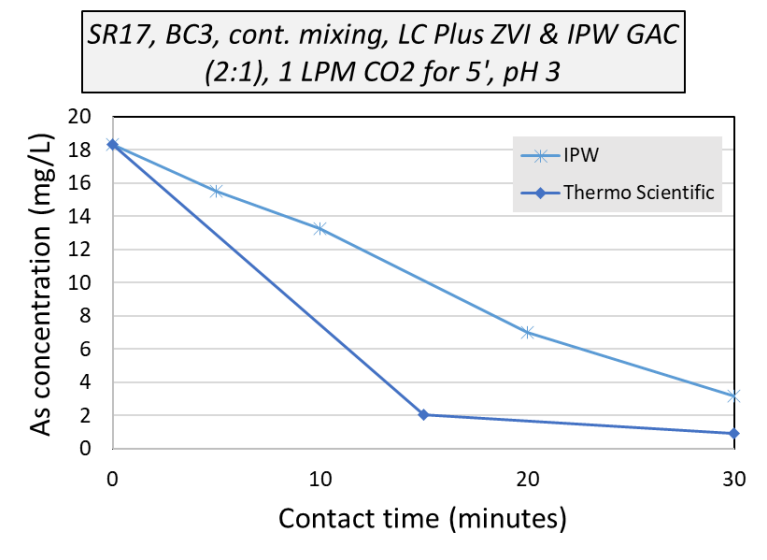

Figure 5.7 Comparison of As/Sb concentration versus contact time for varying GAC types with ME treatment conditions of 2L of SR 17 in BC3 with 50 g/L LC Plus ZVI & GAC (2:1) dose, continually mixed for 30-minutes at 1000 RPM at pH 3.0 with pre-treatment CO2 purging

However, the overall removal of As and Sb was still adequate and warranted testing for 1-hour of ME treatment (Figure 5.8).

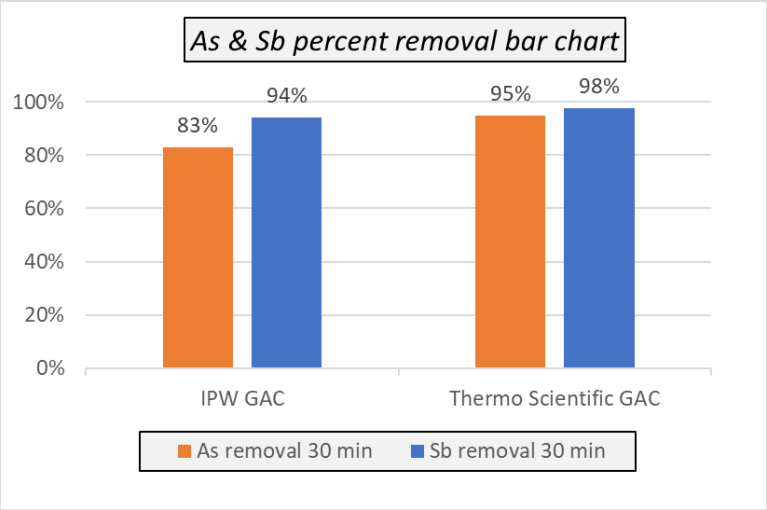

Figure 5.8 Comparison of As/Sb removal for varying GAC types with ME treatment conditions of 2L of SR 17 in BC3 with 50 g/L LC Plus ZVI & GAC (2:1) dose, continually mixed for 30-minutes at 1000 RPM at pH 3.0 with pre-treatment CO2 purging

5.1.6.2 IPW v. Thermo Scientific, 30-minute ME treatment cycles with top-offs

The GAC performance test was expanded further with the goal of comparing the performance of the two GAC products over the course of three, 30-minute ME treatment cycles with GAC top-

offs. For these experiments, the reactor was continuously purged with CO2 (~1 LPM) throughout the treatment cycles to accommodate gas sampling requirements. Gas sampling results are not a part of this thesis. BC2 was used in lieu of BC3 since BC2 is better equipped for gas phase analysis, with gas ports located at the top of the column. ME treatment conditions are summarized in Table 5.3:

Table 5.3 ME treatment conditions for cycles with varying GAC types experiment

V	SR	Reactor	Dose	pH	Agitation	Purging	Length
2 L	19	BC 2	50 g/L (2:1, CR ZVI & variable GAC) with 1 g/L GAC top-offs	3	Continuous mixing, ~1000 RPM	Continuous, CO2 at ~ 1 LPM	30-minutes

Within 30-minutes of ME treatment, the IPW GAC product consistently removed greater than 80% As (Figure 5.9). The IPW product's performance treating SR 17 (83% As removal, Figure 5.8) was similar to that of SR 19 (89% As removal, Figure 5.9).

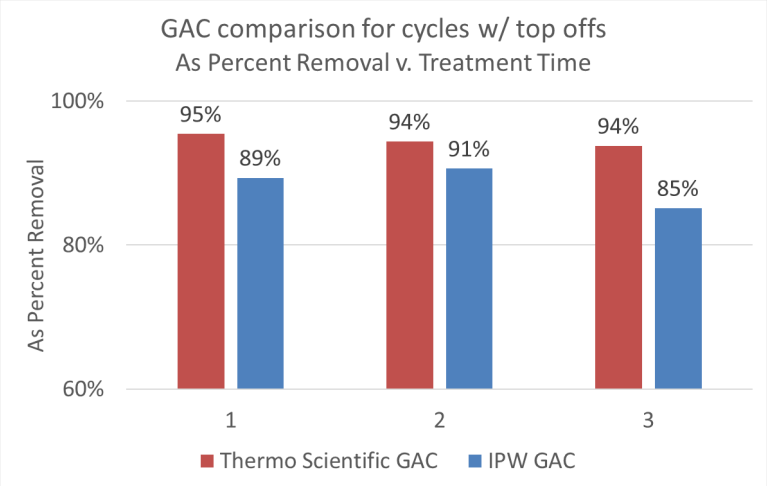

Figure 5.9 Comparison of As removal for cycles with varying GAC types with ME treatment conditions of 2L of SR 19 in BC2 with initial 50 g/L CR ZVI & GAC (2:1) dose and 1 g/L GAC top-offs, continually mixed for 3- 30-minute cycles at 1000 RPM at pH 3.0 with continuous 1 LPM CO2 purging

The Thermo Scientific product did result in better, and faster treatment, supporting the transition to a typical ME treatment length of 1-hr for the CR ZVI and IPW GAC combination. There was a slight increase in treatment for IPW GAC's performance from Cycle 1 to 2 (i.e., 89 to 91 % As removal). This was hypothesized to be a result of treatment media already being activated from

Cycle 2 and resulting in faster Cycle 2 performance. This phenomenon is also observed with the Thermo Scientific product's 15-minute Cycle 1 and Cycle 2 performance (78 to 85 % As removal).

5.2 ME treatment optimization

5.2.1 Variations in active media dose

The following experiments investigated the impacts of active media dose on ME treatment efficiency. Two variations of treatment conditions were examined:

- Effects of active media dose, constant 2:1 dosing ratio
- Effects of GAC dose in the presence of a constant ZVI dose

5.2.1.1 Active media dose variations, 2:1 dosing ratio

This investigation explored changes in ME treatment efficiency caused by variations of active media dose. Additionally, this investigation sought to further confirm the efficacy of the IPW GAC product as a replacement for the Thermo Scientific GAC and its compatibility with LC Plus ZVI, with motivation described in Section 5.1. Five active media doses were tested, maintaining the typical 2:1 dosing ratio between ZVI and GAC: 20, 30, 40, 50, and 60 g/L. ME treatment conditions are summarized in in Table 5.4.

Table 5.4 ME treatment conditions for varying active media doses (2:1) experiment.

V	SR	Reactor	Dose	pH	Agitation	Purging	Length	Other
2 L	17	BC 3	Variable (2:1, LC Plus and IPW)	3	Continuous mixing at ~1000 RPM	pre-treatment, CO2 at ~ 1 LPM	1-hr	Testing IPW GAC as replacement

These experiments determined that active media dosage strongly affects the kinetics of ME treatment, in agreement with prior data reported in Pinochet-Troncoso, 2023. 20 g/L of coarse (large particle) active media removed 16% of As in 30-minutes. However, 60 g/L coarse active media removed 94% of As in the same amount of time (Figure 5.10). This experiment affirmed the initial active media dose of 50 g/L to be sufficient for achieving greater than 90% As removal by ME treatment within ca. 30 minutes of contact time.

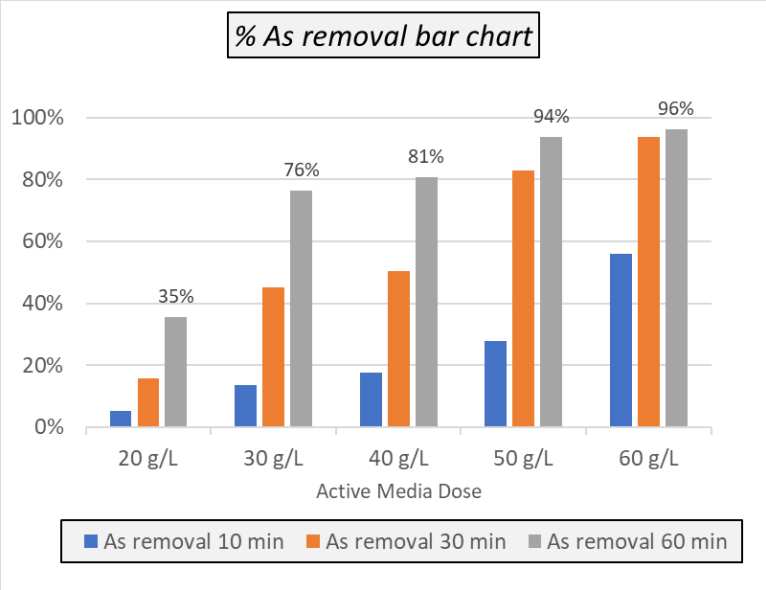

Figure 5.10 Comparison of As removal for varying active media doses (2:1) with ME treatment conditions of 2L of SR 17 in BC3 with variable LC Plus ZVI & IPW GAC (2:1) dose, continually mixed for 1-hr at 1000 RPM at pH 3.0 with pre-treatment CO2 purging

The effect of active media dose on Sb removal was less prominent than with As, mostly due to a considerably faster removal of Sb by microelectrolysis. Largely the same trend was observed, with Sb removal increasing with increasing active media dose (Figure 5.11).

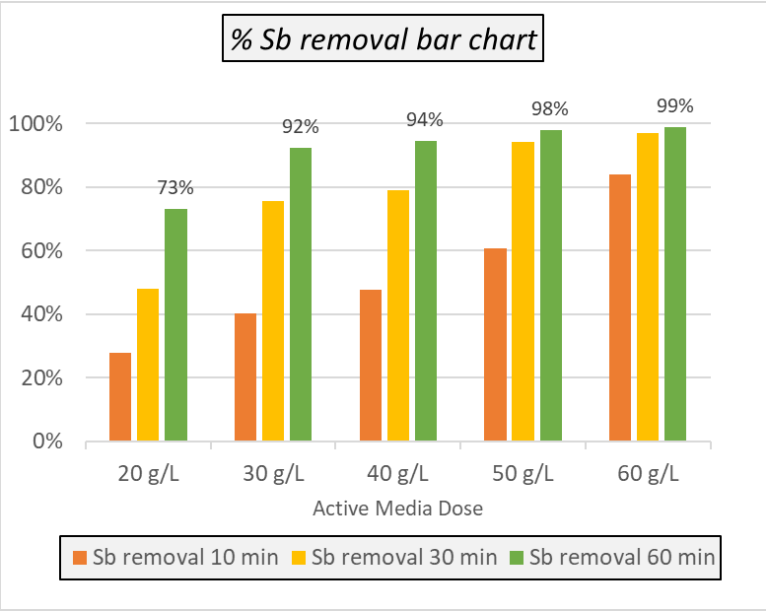

Figure 5.11 Comparison of Sb removal for varying active media doses (2:1) with ME treatment conditions of 2L of SR 17 in BC3 with variable LC Plus ZVI & IPW GAC (2:1) dose, continually mixed for 1-hr at 1000 RPM at pH 3.0 with pre-treatment CO2 purging

Logarithmic plots of the normalized As and Sb concentrations confirm the finding that Fe/C dosage strongly affects ME treatment efficiency (Figure 5.12 and Figure 5.13).

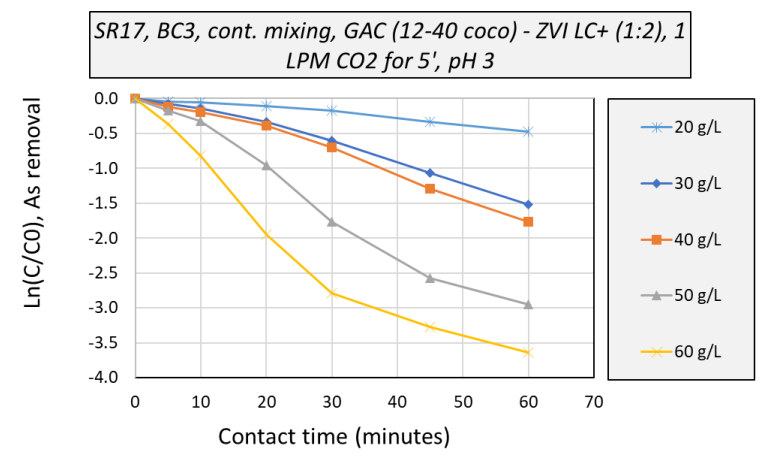

Figure 5.12 Comparison of As log-normalized removal for varying active media doses (2:1) with ME treatment conditions of 2L of SR 17 in BC3 with variable LC Plus ZVI & IPW GAC (2:1) dose, continually mixed for 1-hr at 1000 RPM at pH 3.0 with pre-treatment CO2 purging

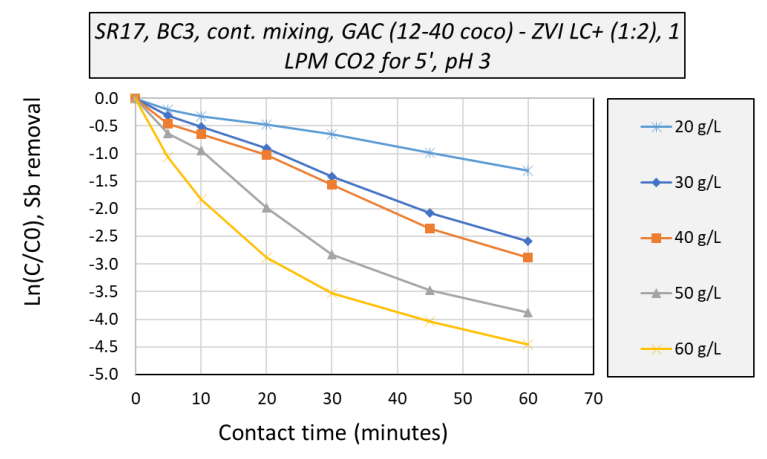

Figure 5.13 Comparison of Sb log-normalized removal for varying active media doses (2:1) with ME treatment conditions of 2L of SR 17 in BC3 with variable LC Plus ZVI & IPW GAC (2:1) dose, continually mixed for 1-hr at 1000 RPM at pH 3.0 with pre-treatment CO2 purging

Measured redox potential trends generally confirmed the removal trends since the 20 g/L (lowest) dose resulted in the highest redox potentials corresponding to the least As/Sb removed. And, the 60 g/L dose resulted in the lowest redox potential corresponding to the most As/Sb removed (Figure 5.14).

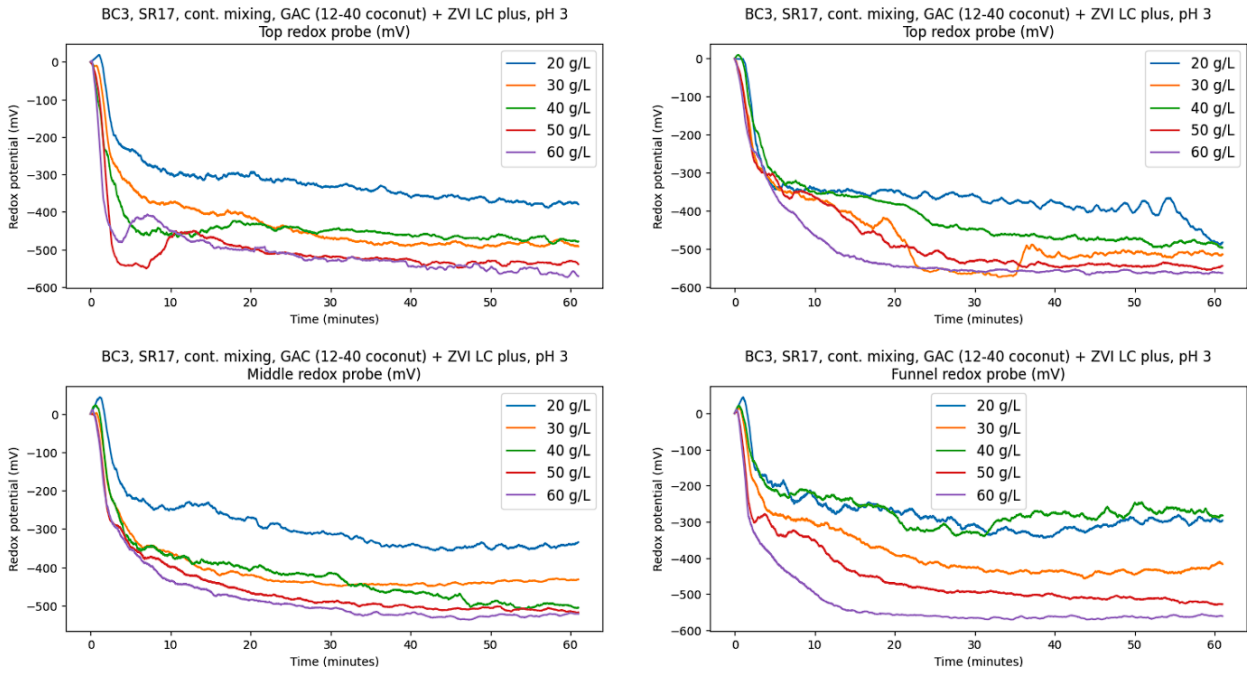

Figure 5.14 Comparison of redox potentials, by probe for varying active media doses (2:1) with ME treatment conditions of 2L of SR 17 in BC3 with variable LC Plus ZVI & IPW GAC (2:1) dose, continually mixed for 1-hr at 1000 RPM at pH 3.0 with pre-treatment CO2 purging

5.2.1.2 GAC dose variations

Variations in GAC dose was investigated to determine their impact on ME treatment efficiency. In these experiments, ZVI dose was maintained constant at 33.3 g/L ZVI CR, the typical amount of ZVI used for 50 g/L active media doses (2:1 mass ratio). Four GAC doses were tested: 5, 10, 16.7 (typical), and 25 g/L. ME treatment conditions are summarized in Table 5.5:

Table 5.5 ME treatment conditions for varying GAC doses experiment

V	SR	Reactor	Dose	pH	Agitation	Purging	Length
2 L	17	BC 3	33.3 g/L CR, variable IPW	3	Continuous mixing at ~1000 RPM	pre-treatment, CO2 at ~ 1 LPM	1-hr cycles

Figure 5.15 shows the results for this experiment. 5 g/L of GAC resulted in dramatically poorer treatment than the other GAC doses, indicating that this amount of GAC is insufficient to achieve desired treatment. 10 g/L of GAC resulted in As and Sb removal which was comparable to the two highest doses tested but resulted in slower treatment than the typical 16.7 g/L dose. There were

only slight differences in As and Sb removal achieved by the 16.7 and 25 g/L GAC doses with the typical 16.6 g/L GAC dose resulting in slightly faster treatment after 10 minutes but slightly slower treatment after 30 and 60 minutes. Thus, there was a trend of accelerated As/Sb removal observed for increasing GAC dose and constant ZVI. Because only a slight increase in As/Sb removal performance was observed between the 16.7 and 25 g/L GAC doses, a 16.6 g/L GAC dose was maintained as the optimal ME treatment GAC dose in combination with 33.3 g/L ZVI for a combined media dose of 50 g/L. These findings were mirrored with Sb removal (Figure 5.16).

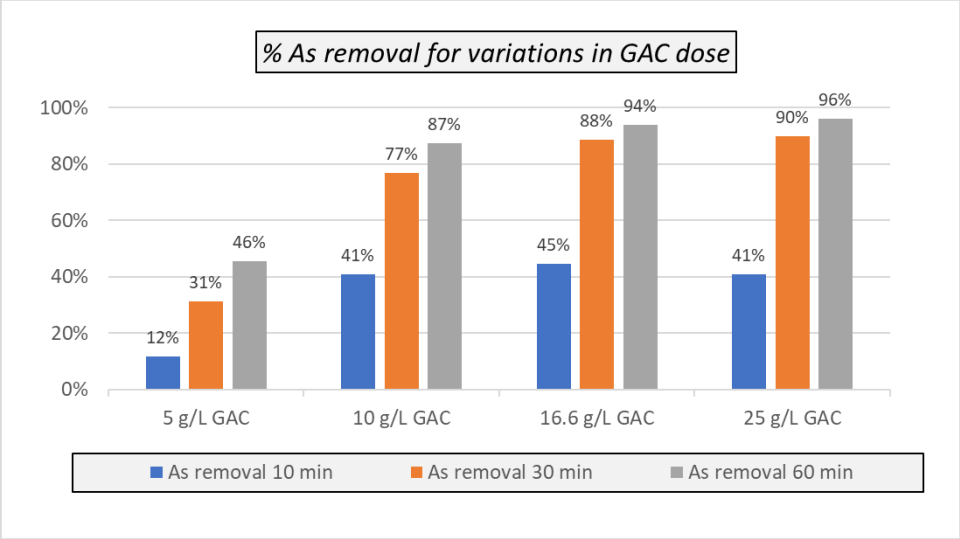

Figure 5.15 Comparison of As removal for varying GAC doses with ME treatment conditions of 2L of SR 17 in BC3 with constant 33.3 g/L CR ZVI & variable IPW GAC dose, continually mixed for 1-hr at 1000 RPM at pH 3.0 with pre-treatment CO2 purging

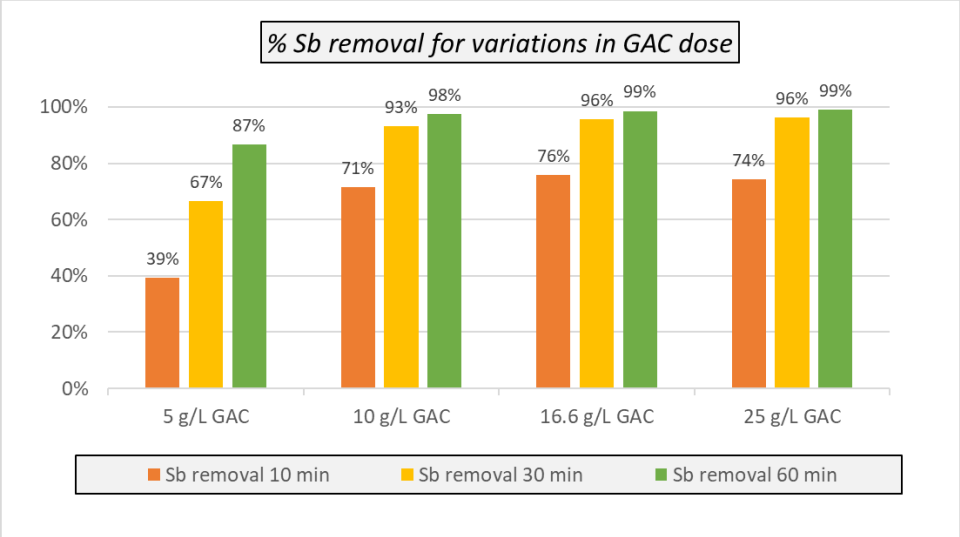

Figure 5.16 Comparison of Sb removal for varying GAC doses with ME treatment conditions of 2L of SR 17 in BC3 with constant 33.3 g/L CR ZVI & variable IPW GAC dose, continually mixed for 1-hr at 1000 RPM at pH 3.0 with pre-treatment CO2 purging

5.2.2 Effects of pH variations on As/Sb removal

pH optimization was of particular interest since the pH of the liquid matrix has notable effects on the kinetics of the ME process. ME treatment was previously run mostly at pH 3.0 which was repeatedly proven to be the most efficient operational pH for As and Sb removal (i.e., fastest removal kinetics) (Walters, 2022; Malik, 2020; Rifkin, 2021; Pinochet-Troncoso, 2023). Considerations for post-treatment effluent pH correction also generated inquiries into the amount of base which would be required to adjust the acidity of ME-treated effluent to an environmentally safe pH for discharge to a POTW (i.e., 6 to 9). Thus, higher pH values were tested to determine whether they could be suitable for ME treatment and also minimize base requirements for post-treatment pH adjustment.

5.2.2.1 Effects of pH variations: 20 g/L active media

ME treatment efficiency was investigated with respect to operational pH using 20 g/L ZVI: GAC (2:1, by mass) with LC Plus and IPW. ME treatment conditions are summarized in Table 5.6:

Table 5.6 ME treatment conditions for varying pH (20 g/L dose) experiment

V	SR	Reactor	Dose	pH	Agitation	Purging	Length

2 L	17	BC 3	20 g/L (2:1, LC Plus and IPW)	variable	Continuous mixing at ~1000 RPM	pre-treatment, CO_2 at ~ 1 LPM	30-min cycles

There was a poor removal achieved across all pH tested. These results indicated that 20 g/L of large particle Fe/C media was insufficient to achieve desired levels of treatment within 30 minutes of treatment (Figure 5.17 and Figure 5.18). It is to be noted that this dose (20 g/L) was acceptable for previous ME experimentation using fine particle sizes (i.e., LC Plus fines and PAC) which could achieve 95% As removal in 30-minutes (Pinochet-Troncoso, 2023). Despite this experiment's poor treatment, trends in ME performance with respect to pH were observed with pH 4 yielding optimal As treatment and pH 3.5 yielding the next best. The Sb removal results were slightly different with pH 4 still yielding the fastest removal of Sb but pH 3 being the next best operating condition for Sb removal.

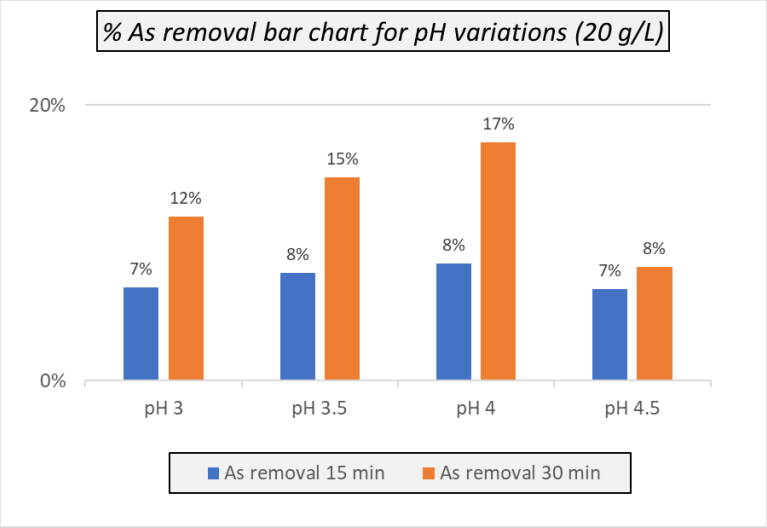

Figure 5.17 Comparison of As removal for varying pH (20 g/L dose) with ME treatment conditions of 2L of SR 17 in BC3 with 20 g/L LC Plus ZVI & IPW GAC (2:1) dose, continually mixed for 30-minutes at 1000 RPM at variable pH with pre-treatment CO_2 purging

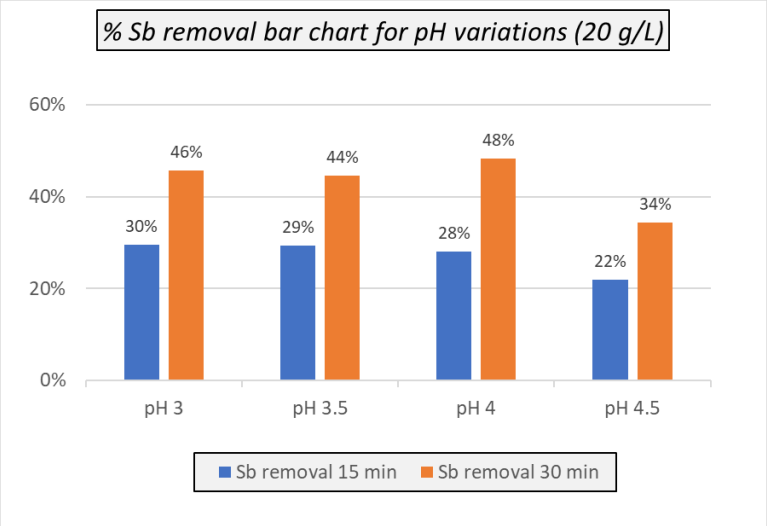

Figure 5.18 Comparison of Sb removal for varying pH (20 g/L dose) with ME treatment conditions of 2L of SR 17 in BC3 with 20 g/L LC Plus ZVI & IPW GAC (2:1) dose, continually mixed for 30-minutes at 1000 RPM at variable pH with pre-treatment CO2 purging

5.2.2.2 Effects of pH variations: 50 g/L active media

Repeating the pH variation experiment with a larger dose of coarse particle active media (50 g/L) yielded very consistent results. ME treatment conditions are summarized in Table 5.7:

Table 5.7 ME treatment conditions for varying pH (50 g/L dose) experiment

V	SR	Reactor	Dose	pH	Agitation	Purging	Length
2 L	17	BC 3	50 g/L (2:1, CR and IPW)	variable	Continuous mixing at ~1000 RPM	pre-treatment, CO2 at ~ 1 LPM	1-hr cycles

Results of these measurements showed a more noticeable effect of the operational pH and As/Sb removal (Figure 5.19 and Figure 5.20). pH 3 resulted in the fastest As/Sb removal and pH 4.5 the slowest. All pH tested achieved greater than 85% As removal within 1-hour, indicating the ME process can be sufficiently carried out at a range of pH (3 to 4.5). There was some variation in Sb treatment speed after 10-minutes, but 30- and 60- minute treatment resulted in the same direct correlation as As. These results affirmed pH 3.0 is optimal for ME treatment but the decrement of ME treatment efficiency for contact times of about 30 minutes is relatively limited.

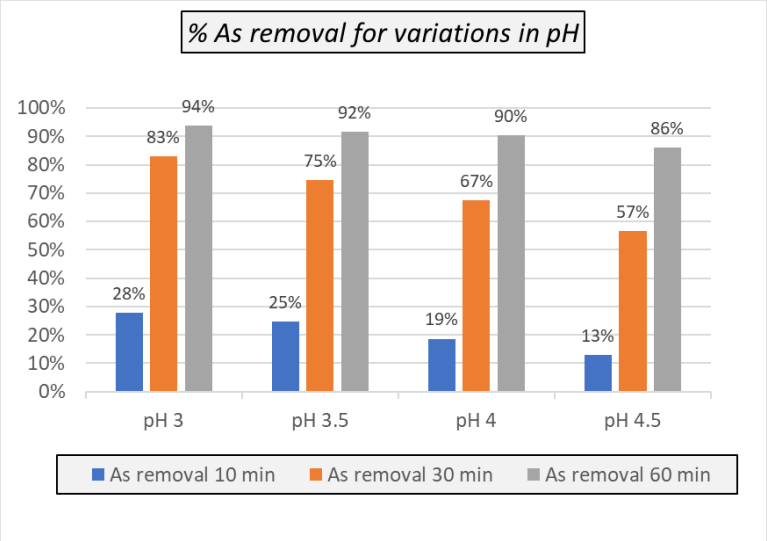

Figure 5.19 Comparison of As removal for varying pH (50 g/L dose) with ME treatment conditions of 2L of SR 17 in BC3 with 50 g/L CR ZVI & IPW GAC (2:1) dose, continually mixed for 1-hr at 1000 RPM at variable pH with pre-treatment CO2 purging

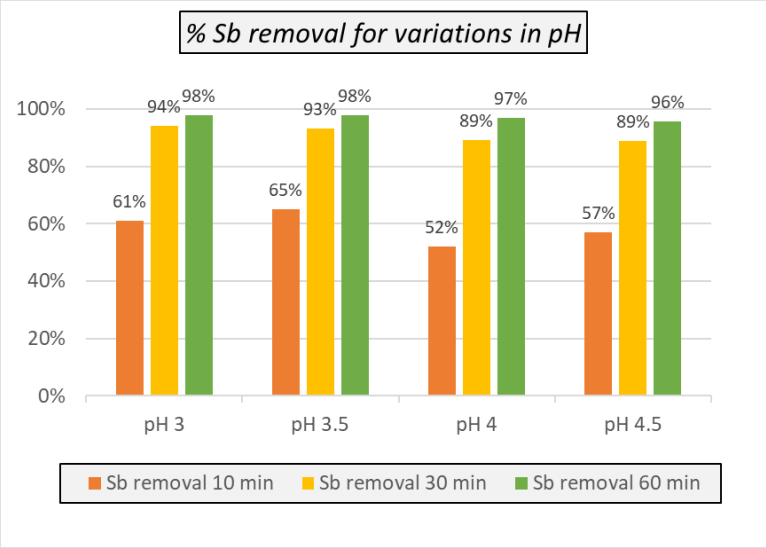

Figure 5.20 Comparison of Sb removal for varying pH (50 g/L dose) with ME treatment conditions of 2L of SR 17 in BC3 with 50 g/L CR ZVI & IPW GAC (2:1) dose, continually mixed for 1-hr at 1000 RPM at variable pH with pre-treatment CO2 purging

Logarithmic plots of normalized As and Sb concentrations (Figure 5.21 and Figure 5.22) show in more detail the trend of decreasing rate of As removal at increasing pHs; for Sb, there were only slight differences between pH 3 and pH 3.5 treatment.

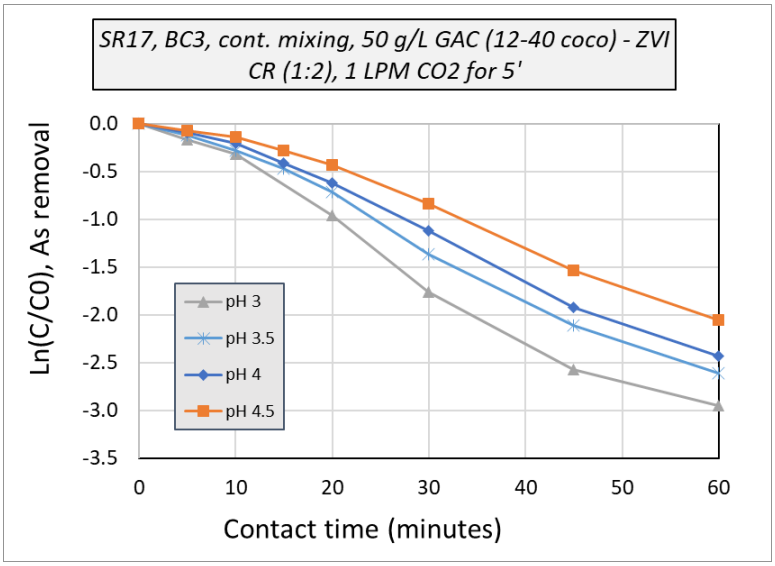

Figure 5.21 Comparison of As log-normalized removal for varying pH (50 g/L dose) with ME treatment conditions of 2L of SR 17 in BC3 with 50 g/L CR ZVI & IPW GAC (2:1) dose, continually mixed for 1-hr at 1000 RPM at variable pH with pre-treatment CO2 purging

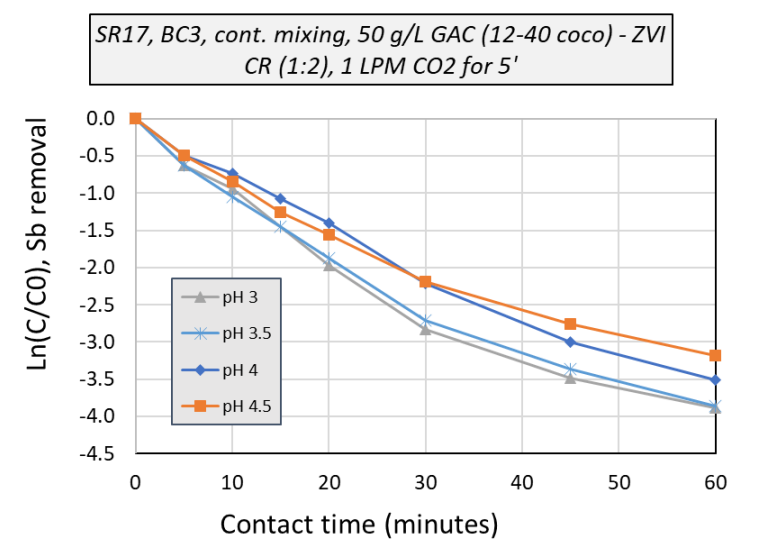

Figure 5.22 Comparison of Sb log-normalized removal for varying pH (50 g/L dose) with ME treatment conditions of 2L of SR 17 in BC3 with 50 g/L CR ZVI & IPW GAC (2:1) dose, continually mixed for 1-hr at 1000 RPM at variable pH with pre-treatment CO2 purging

When the active media dosage was increased from 20 g/L to the typical dose of 50 g/L, the redox potential decreased from -400 mV to -600 mV. These observations confirm that the ME process is accelerated by a reductive environment and that the degree of reduction is critical to the speed of As and Sb removal. There was little variation in redox potentials between the four-pH tested (Figure 5.23).

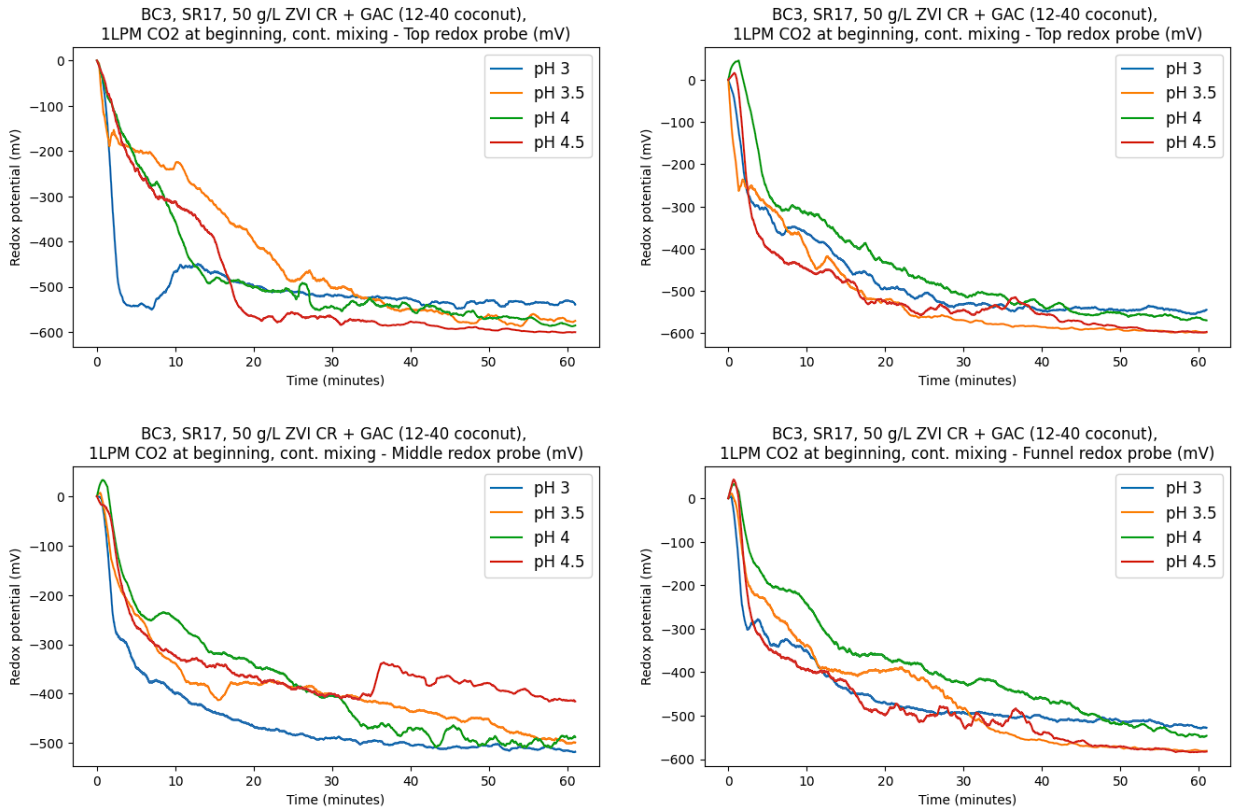

Figure 5.23 Comparison of redox potentials, by probe for varying pH (50 g/L dose) with ME treatment conditions of 2L of SR 17 in BC3 with 50 g/L CR ZVI & IPW GAC (2:1) dose, continually mixed for 1-hr at 1000 RPM at variable pH with pre-treatment CO_2 purging

5.2.3 Effects of variations of mixing conditions: axial flow and mixing intensity

Effects of alternative mixing regimes were explored to better understand the effects of axial flow and mixing intensity on ME treatment hydrodynamics. These experiments were motivated by the hypothesis that the ME treatment reactor may fail to achieve full suspension of the active media via mechanical mixing. It was also hypothesized that a more evenly distributed suspension of active media during ME treatment would maximize the interparticle contact time and result in improved removal of As and Sb. Mixing, and particle suspension, is affected by:

- Impellers: type (shape), pitch (angle), diameter, placement, number
- Mixer: mixing shaft diameter and length, impeller off-bottom distance, mixing intensity
- Reactor shape: degree of pitch and height of conical/funnel reactor bottom

These variables, and others, impact the degree of mixing, and type of mixing, achieved during ME treatment. A key requirement to achieve particle suspension is imposing sufficient force to the bulk liquid (via mechanical mixing) to exceed the media's settling velocity. Particle suspension is classified as partial, off bottom, and full (Figure 5.24).

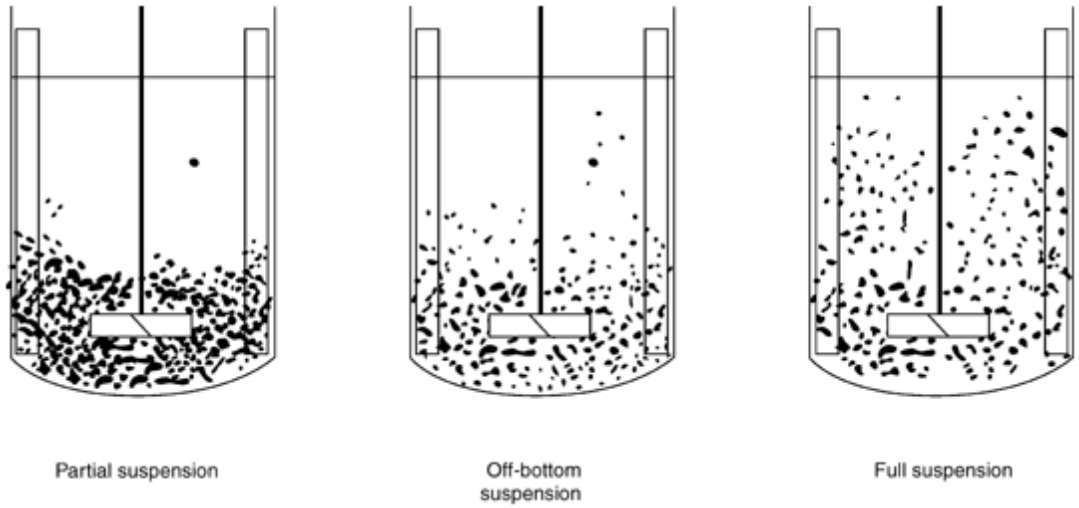

Figure 5.24 Differentiating degree of mixing based on particle suspension (Dynamix Agitators, 2020)

Particle suspension is often best achieved by axial flow mixing, where the bulk liquid flows parallel to the mixing axis (i.e., shaft) which fully mixes all particles. Axial flow can be facilitated by up or down flow mixing, referring to the direction of the imposed force; axial flow is most typically achieved by pumping liquid down by angled blades (Paul Mueller Company, 2018). The typical mixing mode as designed by prior researchers applied up flow mixing, as determined by the impeller pitch which pushes the liquid and particles up through the reactor (Pinochet-Troncoso, 2023). However, due to the high number of impellers fixed to a mixing shaft, the ME treatment mixing mode appeared to create discrete flow cells which may have inhibited particles from being fully mixed and integrated within the LFG condensate. The hydrodynamics of the mechanical mixing design warrant further investigation and optimization.

5.2.3.1 Variations in axial flow pattern: up v. down flow

Effects of axial flow were investigated by comparing ME treatment efficiency for up and down flow directions. Up flow mixing was the control condition that was the typical mixing mode used in all prior experimentation. Down flow mixing was achieved by designing an alternate mixing shaft with impellers turn upside down to instead push flow down towards the reactor bottom rather than lift the reactor's contents up. It was hypothesized that improving the uniformity of particle suspension during ME treatment mixing would remedy discrepancies in redox measurements throughout the column reactor and would potentially improve the quality of ME treatment. Supplementary doses for subsequent cycles were combined (i.e., ZVI and GAC, 2:1) based on results from the variable top-off experiment which showed that top-offs with both ZVI and GAC were the most effective at sustaining treatment across cycles (Section 5.3.3). ME treatment conditions are summarized in Table 5.8:

Table 5.8 ME treatment conditions for varying axial flow patterns experiment

V	SR	Reactor	Dose	pH	Agitation	Purging	Length
2 L	19	BC 3	50 g/L (2:1, CR and IPW) with 1 g/L combined top-offs	3	Continuous mixing at ~1000 RPM	pre-treatment, CO_2 at ~ 1 LPM	1-hr cycles

By a small margin, ME treatment in up flow mixing regime yielded better results, removing greater than 90% As for three cycles of treatment (Figure 5.25). The advantage of the up-flow conditions over down flow mixing is hypothesized to be caused by possible active media packing in the case of down flow mixing, especially given the column reactors conical bottom geometry that may impede media suspension. Conversely, upflow mixing is hypothesized to mobilize the media more efficiently and suspend them more evenly throughout the column reactor, yielding better treatment.

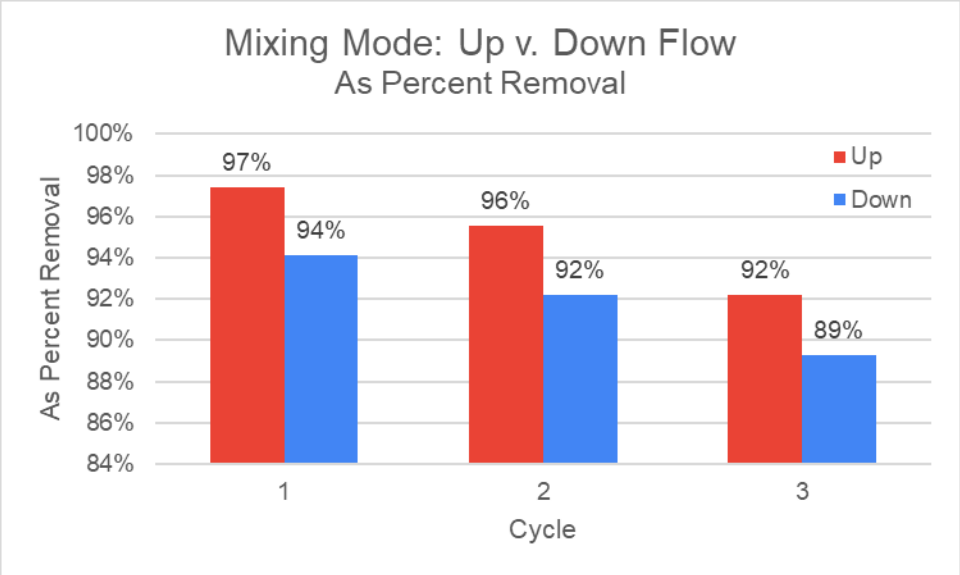

Figure 5.25 Comparison of As removal for varying axial flow patterns with ME treatment conditions of 2L of SR 19 in BC3 with 50 g/L CR ZVI & IPW GAC (2:1) dose and 1 g/L combined top-offs, continually mixed for 3- 1-hr cycles at 1000 RPM at pH 3.0 with pre-treatment CO2 purging

Another interesting metric to compare ME treatment is acid consumption throughout each experiment. Table 5.9 shows the volume of acid required to maintain pH 3 throughout each cycle. The maintenance of a constant pH in the up-flow cycles required consistently more acid than down flow cycles to maintain pH 3, which correlates to the activity of the media and the degree of treatment achieved.

Table 5.9 Comparing sulfuric acid (1 M) required to maintain pH 3 for 1-hr treatment cycles for varying axial flow patterns.

Cycle	**Volume acid (mL)**	
	Up flow	Down flow
1	57	46
2	39	31
3	33	25.5

5.2.3.2 Variations in mixing speed

ME treatment's response to varying mixing speed was investigated for four different rotation speeds, defined as 1, 10, 25, and 50% of the nominal mixer capacity. Previous researchers chose a

mixing speed for ME treatment that appeared to be approximately 25% of the JJ-1 mixer's capacity of 3000 RPM (Pinochet-Troncoso, 2023). These speeds were denoted by marks on the mixer's knob and 10% mixing capacity was tested as the control, the speed at which ME treatment was conducted for prior mechanical mixing. These mixing speeds were later translated from nominal percentage of mixer's capacity to RPM using a tachometer. ME treatment conditions are summarized in Table 5.10:

Table 5.10 ME treatment conditions for varying mixing intensities experiment

V	SR	Reactor	Dose	pH	Agitation	Purging	Length
2 L	17	BC 3	50 g/L (2:1, CR and IPW)	3	Continuous mixing at variable speeds	pre-treatment, CO_2 at ~ 1 LPM	1-hr cycles

Figure 5.26 shows the As removal results for the tested mixing intensities. Mixing intensity of 1% of the nominal maximum rotation rate resulted in no visible media suspension achieved, beyond a few particles of GAC. Subsequently, 1% mixing intensity resulted in negligible removal within 1-hour of treatment (i.e., 13%). Mixing intensities of 10, 25, and 50% all achieved visible suspension of the active media, and all achieved greater than 90% As removal within 1-hour of ME treatment. These results indicate that particle suspension and inter-particle Fe/C interactions are required to achieve ME treatment. However, 10% mixing intensity resulted in the best As removal (i.e., 87% in 30-minutes) followed by 25 and 50% intensity, respectively. Thus, mixing intensity greater than 10% of the mixer's nominal capacity resulted in decreased treatment efficiency. These results indicate that particle collisions are best facilitated at mixing intensities which are high enough to achieve particle suspension, but low enough to enable sufficient collision contact time between ZVI and GAC.

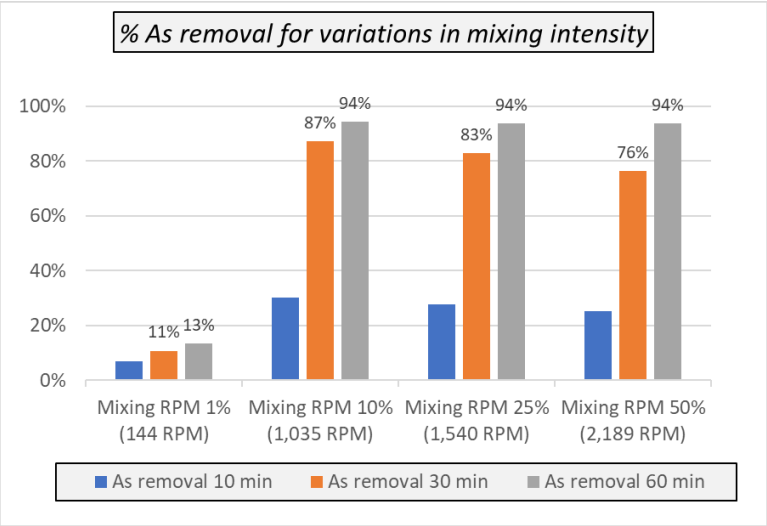

Figure 5.26 Comparison of As removal for varying mixing intensities with ME treatment conditions of 2L of SR 17 in BC3 with 50 g/L CR ZVI & IPW GAC (2:1) dose, continually mixed for 1-hr at variable RPM at pH 3.0 with pre-treatment CO2 purging

Trends in As removal at varying rotation rates of the mixing unit were supported by similar trends observed for Sb removal (Figure 5.27). This confirms that the 10% setting of the nominal maximum rotation rate can be the optimal speed for the ME reactor examined in this study.

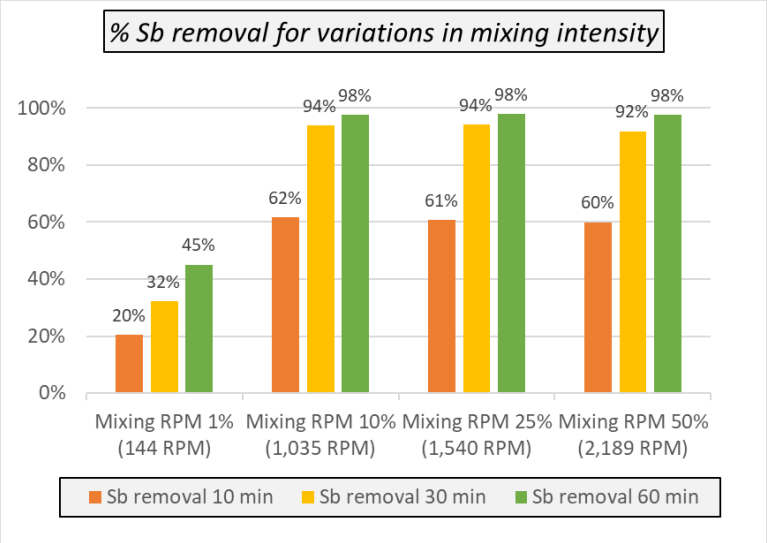

Figure 5.27 Comparison of Sb removal for varying mixing intensities with ME treatment conditions of 2L of SR 17 in BC3 with 50 g/L CR ZVI & IPW GAC (2:1) dose, continually mixed for 1-hr at variable RPM at pH 3.0 with pre-treatment CO2 purging

Results shown in Figure 5.26 and Figure 5.27 are reinterpreted further in Figure 5.28 and Figure 5.29 which show the logarithmic plots of the normalized As and Sb concentrations measured at

varying rotation speeds. These figures demonstrate that the 10% relative mixing intensity achieved the fastest As removal while little effect in Sb removal was seen for 10, 25, and 50 % nominal mixing intensities.

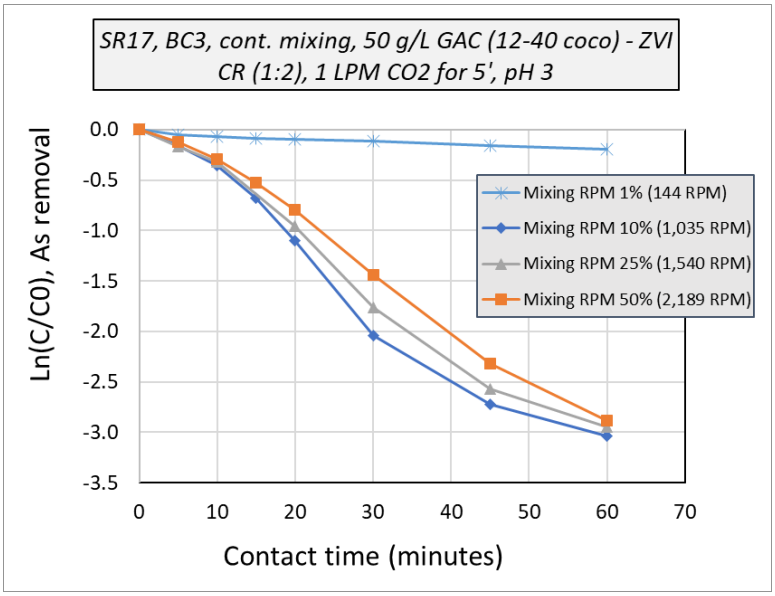

Figure 5.28 Comparison of As log-normalized removal for varying mixing intensities with ME treatment conditions of 2L of SR 17 in BC3 with 50 g/L CR ZVI & IPW GAC (2:1) dose, continually mixed for 1-hr at variable RPM at pH 3.0 with pre-treatment CO2 purging

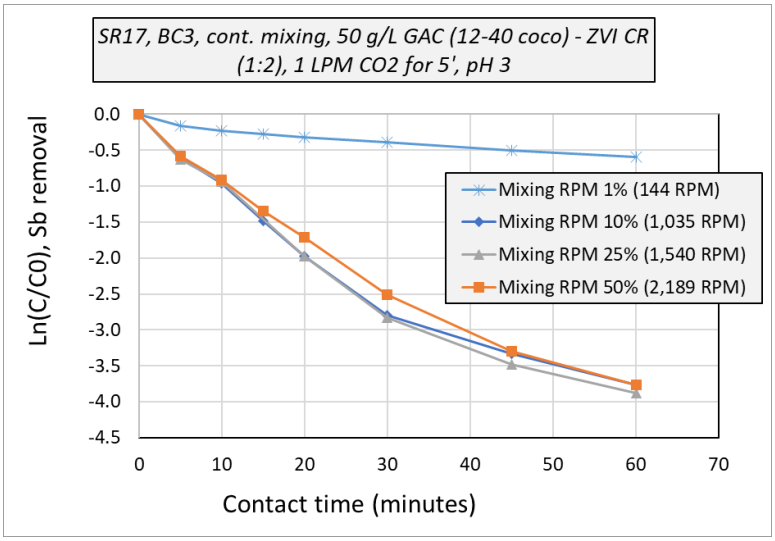

Figure 5.29 Comparison of Sb log-normalized removal for varying mixing intensities with ME treatment conditions of 2L of SR 17 in BC3 with 50 g/L CR ZVI & IPW GAC (2:1) dose, continually mixed for 1-hr at variable RPM at pH 3.0 with pre-treatment CO2 purging

Redox potential measurements showed that 10% nominal mixing intensity consistently resulted in the lowest redox potentials (Figure 5.30). 1% mixing intensity is very obviously offset from the other mixing intensities tested. The 25 and 50% mixing intensities measured similar redox potentials to 10%, correlating with their similar degrees of treatment achieved.

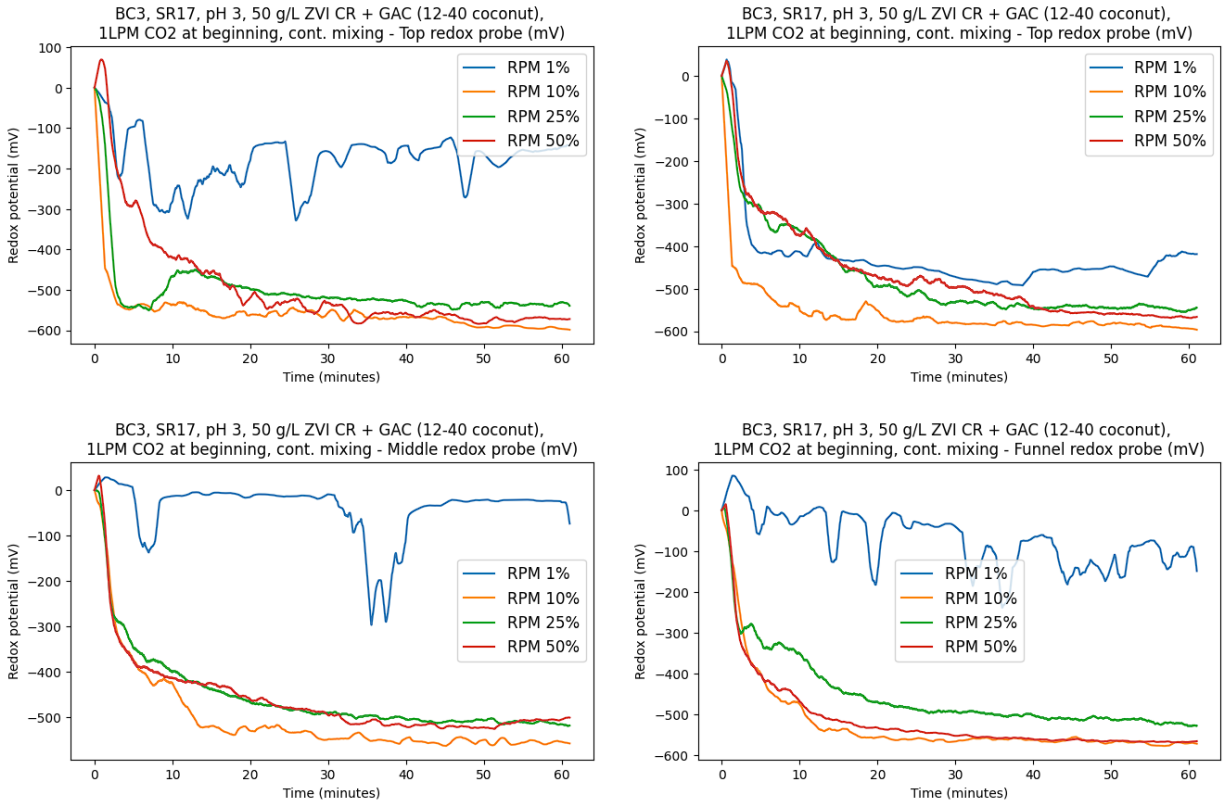

Figure 5.30 Comparison of redox potentials, by probe for varying mixing intensities with ME treatment conditions of 2L of SR 17 in BC3 with 50 g/L CR ZVI & IPW GAC (2:1) dose, continually mixed for 1-hr at variable RPM at pH 3.0 with pre-treatment CO2 purging

5.3 ME treatment cycling

5.3.1 Delayed cycling

5.3.1.1 10 cycles, 2-hr to overnight delays, no top-offs

Delays between treatment cycles were performed to investigate the impact of intermitted treatment, with the active media exposed to the ambient gas phase when no influent to be treated is present in the reactors, on ME treatment efficiency. Delays between the sequential rounds of ME treatment using the same media ranged from two hours to overnight (approximately 14

hours). Overnight delays took place between cycles 3 to 4 and cycles 7 to 8. All other cycles were conducted with a two-hour delay between the end of one cycle and the beginning of the next. This experiment consumed 20 L of LFG condensate sample, expending the remainder of SR 17. ME treatment conditions are summarized in Table 5.11:

Table 5.11 ME treatment conditions for cycles with 2-hr delays and no top-offs experiment

V	SR	Reactor	Dose	pH	Agitation	Purging	Length	Other
2 L	17	BC 3	50 g/L ZVI:GAC (2:1, CR and IPW)	3	Continuous mixing at ~1000 RPM	pre-treatment, CO2 at ~ 1 LPM	1-hr cycles	2-to-14-hour delays between cycles

Results of these cycles indicate that there was a consistent decrease of the efficiency of ME treatment and the number of cycles (Figure 5.31 and Figure 5.32). As the number of cycles with the same active media increased, the removal of As gradually worsened. For 1-hour ME treatment cycles with 2-hour delays, greater than 80% As removal was observed for the first three cycles. This trend was previously observed for cycling experiments in February 2023 with SR 16 for 30-minute cycles and large particle media reutilization (Pinochet-Troncoso, 2023).

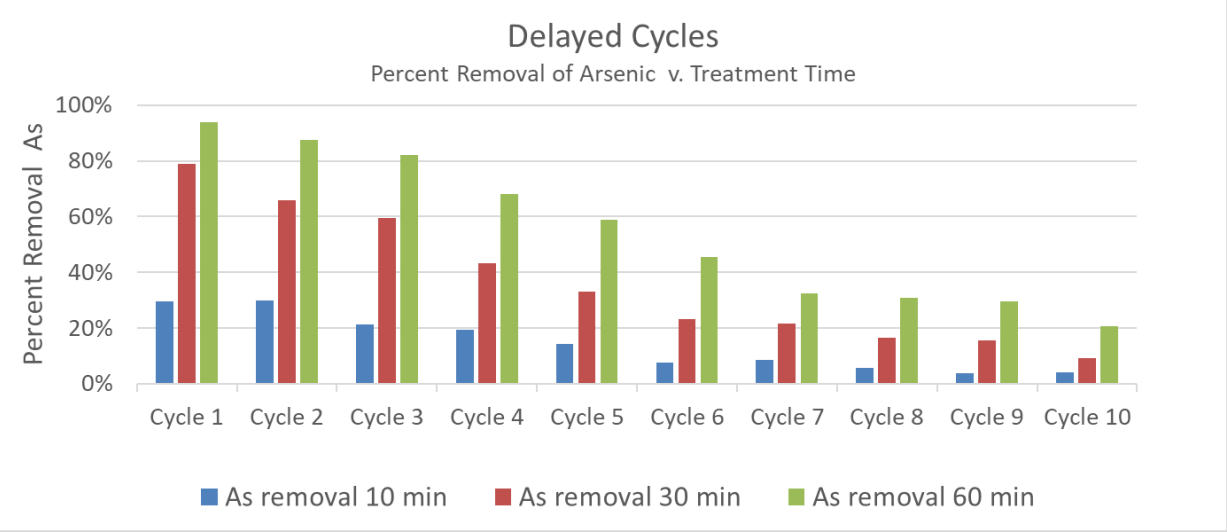

Figure 5.31 Comparison of As removal for cycles with 2-hr delays and no top-offs with ME treatment conditions of 2L of SR 17 in BC3 with 50 g/L CR ZVI & IPW GAC (2:1) dose, continually mixed for 10- 1-hr cycles, with 2-hour to overnight delays, at 1000 RPM at pH 3.0 with pre-treatment CO2 purging

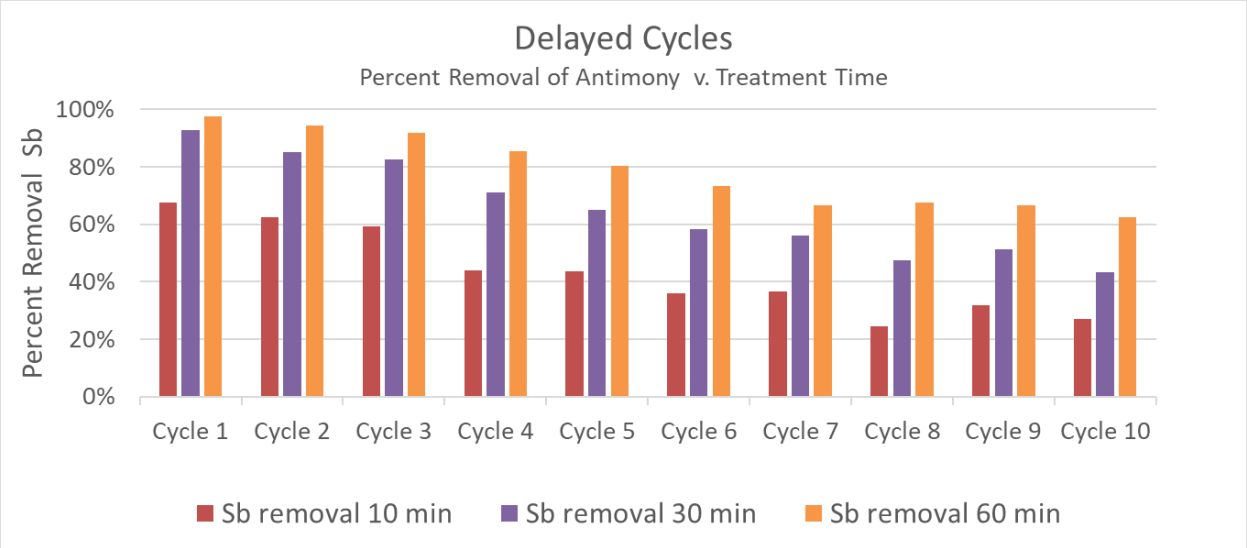

Figure 5.32 Comparison of Sb removal for cycles with 2-hr delays and no top-offs with ME treatment conditions of 2L of SR 17 in BC3 with 50 g/L CR ZVI & IPW GAC (2:1) dose, continually mixed for 10- 1-hr cycles, with 2-hour to overnight delays, at 1000 RPM at pH 3.0 with pre-treatment CO2 purging

From the first to second cycle, As removal decreased by 6% and then by 5% from the second to third delayed cycles (Table 5.12). After the first overnight delay, the amount of As removal decreased by 14% which was a greater reduction in treatment than for the two prior delayed cycles. This may indicate that the length of delay between treatment cycles may affect the extent of the inter-cycle decrease in As removal. This is likely due to the continued oxidation of ZVI during treatment delays. These data however show that exposures of the active media to ambient gas phase during the inter-cycle periods does not result in an immediate failure of their performance. In addition, given the relatively small volume of the reactors used in these experiments and the lack of their complete isolation from ambient air, the decrease of performance in repetitive cycles, with or without inter-cycle delays, may be less pronounced in pilot- and full-scale operations where larger and more gas-tight reactors will be used.

Table 5.12 Comparison of inter-cycle decrease in As removal for cycles with 2-hr delays and no top-offs.

Cycles	1 to 2	2 to 3	3 to 4	4 to 5	5 to 6	6 to 7	7 to 8	8 to 9	9 to 10
Inter-cycle decrease in As % removal	6%	5%	14%	9%	13%	13%	2%	1%	9%

Logarithmic plots of the normalized As and Sb concentrations confirm the finding that delayed repetitive cycles affect ME treatment efficiency (Figure 5.33 and Figure 5.34). For later cycles (i.e., Cycles 7 to 9), the differentiation between As/Sb removal is less clear which indicates that the degree of As/Sb treatment is similar for these cycles.

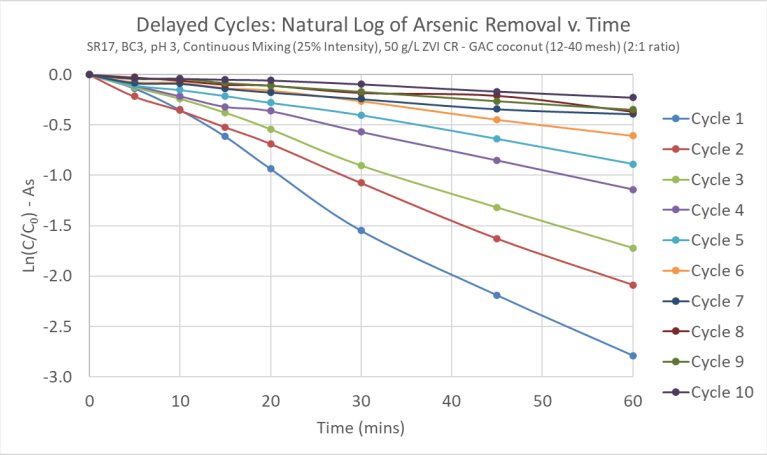

Figure 5.33 Comparison of As log-normalized removal for cycles with 2-hr delays and no top-offs with ME treatment conditions of 2L of SR 17 in BC3 with 50 g/L CR ZVI & IPW GAC (2:1) dose, continually mixed for 10- 1-hr cycles, with 2-hour to overnight delays, at 1000 RPM at pH 3.0 with pre-treatment CO2 purging

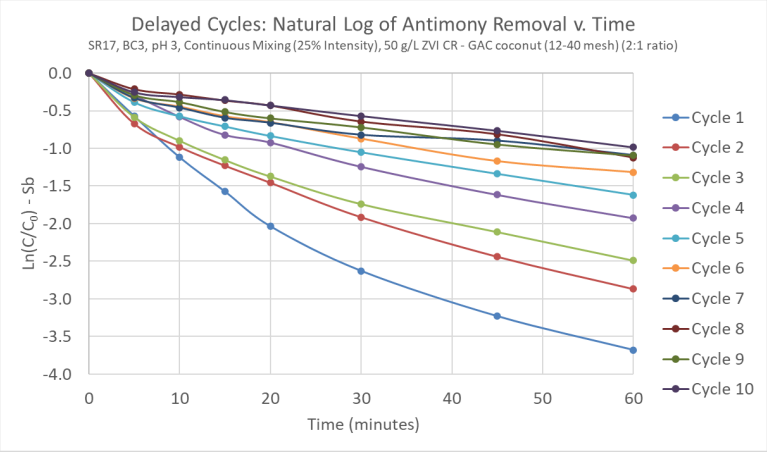

Figure 5.34 Comparison of Sb log-normalized removal for cycles with 2-hr delays and no top-offs with ME treatment conditions of 2L of SR 17 in BC3 with 50 g/L CR ZVI & IPW GAC (2:1) dose, continually mixed for 10- 1-hr cycles, with 2-hour to overnight delays, at 1000 RPM at pH 3.0 with pre-treatment CO2 purging

The reduction in inter-cycle treatment can also be quantified by calculating the apparent rate of removal for As and Sb. Figure 5.35 shows the reduction in apparent rate of removal for As and Sb versus treatment cycle. The kinetics can be related to required treatment time for batch treatment in the presence of a first-order reaction (Benjamin & Lawler, 2013):

$$\frac{C}{C_0} = \exp(-kt)$$

The negative is disregarded since the apparent rate of removal "k" includes a negative. Taking the natural log of this expression yields:

$$ln\frac{C}{C_0} = \ln(\exp(-kt))$$

Which further simplifies to:

$$ln\frac{C}{C_0} = kt$$

Finally, the treatment time can be isolated by:

$$t = \frac{ln\frac{C}{C_0}}{k}$$

Equation 1 Estimation for required contact time based on apparent first-order kinetics for batch mode treatment

Thus, the time required to achieve a given degree of treatment is dependent on the apparent first-order rate of removal. For greater rates of removal, less time is required to achieve a desired degree of treatment (e.g., 90% removal). Conversely, for lower rates of removal, more time is required to achieve a desired degree of treatment. This can be applied to cyclical treatment where the kinetics change cycle-to-cycle. For the data generated in the experiment described in this section, Figure 5.35 shows the reduction in the apparent rate of removal against the number of treatment cycles conducted. Similar to the previous figures, Figure 5.35 shows a plateau in treatment from Cycles 7 onwards, where there is little change in the apparent kinetics despite the continuation of cycling.

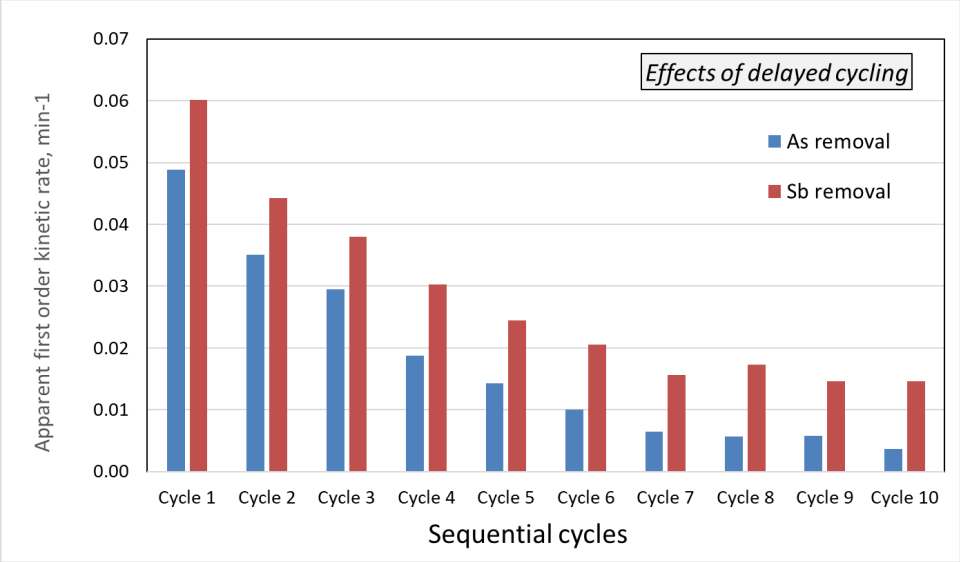

Figure 5.35 Comparison of apparent first order kinetics removal rate for cycles with 2-hr delays and no top-offs with ME treatment conditions of 2L of SR 17 in BC3 with 50 g/L CR ZVI & IPW GAC (2:1) dose, continually mixed for 10- 1-hr cycles, with 2-hour to overnight delays, at 1000 RPM at pH 3.0 with pre-treatment CO2 purging

Using the derived formula (Equation 1), the required contact time to achieve a treatment target of 90% As and Sb removal (i.e., C/Co = 0.1) for ME treatment cycles with delays was estimated and shown in Figure 5.36. Required contact time for As is greater than Sb based on As's slower removal kinetics (Figure 5.35). This estimation indicates that the required treatment time to achieve treatment targets increases with an increasing number of treatment cycles.

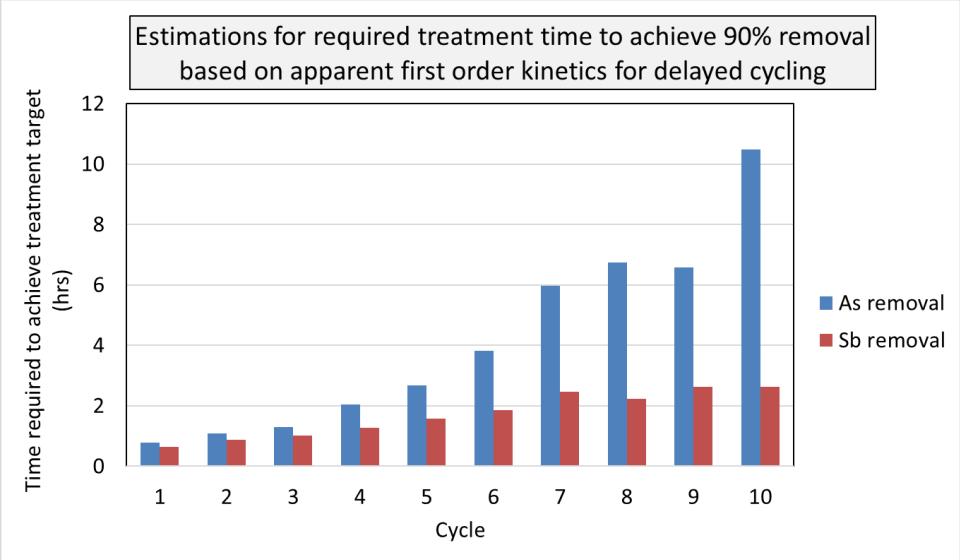

Figure 5.36 Estimations for required treatment (contact) time to achieve 90% As/Sb removal based on apparent first order kinetics for delayed cycling

5.3.1.2 2 cycles, 2-hr delays, 1 g/L GAC top-offs

Delayed cycles experiments were expanded to examine effects of top-offs of the active ZVI/GAC media as a means to extend their useful life. Two cycles of ME treatment were conducted with a 21-hour delay and a 1 g/L GAC top-off was added for the second cycle. Some samples of the gas phase were taken in this experiment to determine the formation of As volatiles. Results of these measurements are not in the scope of this thesis, and they have been reported elsewhere. Nitrogen was used as a purging gas in this experiment because carbon dioxide gas that was typically employed for purging the column can interfere with the arsine detection method. Using Nitrogen as a purging gas in this experiment did not appear to affect the effectiveness of ME treatment. ME treatment conditions are summarized in Table 5.13:

Table 5.13 ME treatment conditions for cycle with 21-hr delay and 1 g/L GAC top-off experiment

V	SR	Reactor	Dose	pH	Agitation	Purging	Length	Other
2 L	18	BC 3	50 g/L ZVI:GAC (2:1, CR and IPW) and 1 g/L GAC top-off	3	Continuous mixing at ~1000 RPM	continuous, N2 at ~ 1 LPM	1-hr cycles	21-hr delay between cycles

Arsenic removal efficiencies were greater than 90% after 1 hour of treatment for both cycles, with the second cycle removing As slightly faster at 10 and 30 minutes of the contact time than the As removal in the first cycle (Figure 5.37). Sb removal was negligible from the first cycle to the second, despite the delay (Figure 5.38). These results confirmed the previous findings that "topping off" of the active media in subsequent cycles of ME treatment with small amounts of active media increases the overall useful life of the ZVI/GAC materials.

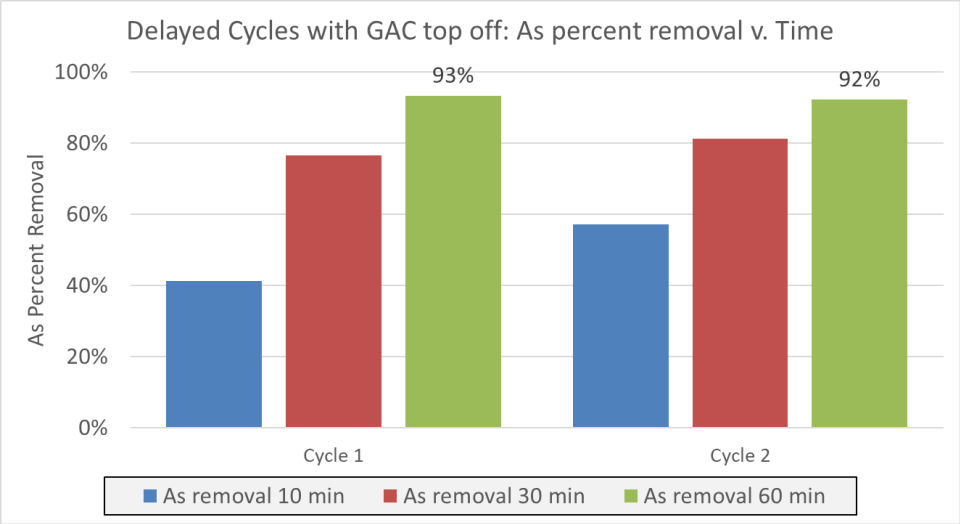

Figure 5.37 Comparison of As removal for cycle with 21-hr delay and 1 g/L GAC top-off with ME treatment conditions of 2L of SR 18 in BC3 with 50 g/L CR ZVI & IPW GAC (2:1) dose and 1 g/L GAC top-off, continually mixed for 2- 1-hr cycles, with a 21-hr delay, at 1000 RPM at pH 3.0 with pre-treatment N2 purging

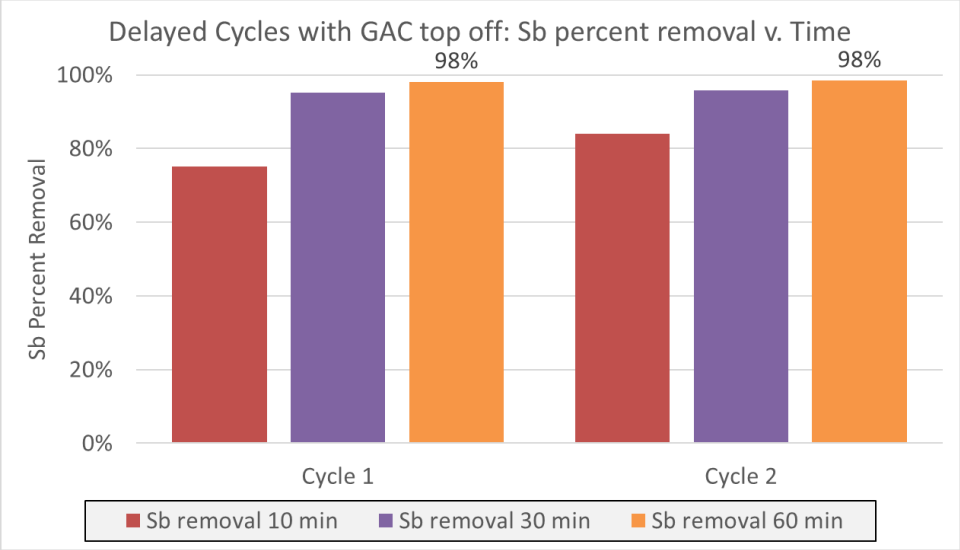

Figure 5.38 Comparison of Sb removal for cycle with 21-hr delay and 1 g/L GAC top-off with ME treatment conditions of 2L of SR 18 in BC3 with 50 g/L CR ZVI & IPW GAC (2:1) dose and 1 g/L GAC top-off, continually mixed for 2- 1-hr cycles, with a 21-hr delay, at 1000 RPM at pH 3.0 with pre-treatment N2 purging

5.3.2 Examination of effects of an extended number of cycling

An experiment was conducted to continue exploring the limits to cycling the same active media for multiple consecutive cycles of ME treatment, utilizing 1 g/L IPW GAC top-offs. ME treatment conditions are summarized in Table 5.14. The transition from one cycle to the next took approximately 15 minutes. Four days of cycling (at 6 per day, and 2 on the last day), with three overnight delays, were required to complete 20 consecutive cycles of ME treatment. Comprehensive sampling was conducted for every third cycle (i.e., C1, C4, C7, etc.) to quantify trends in removal versus time. Otherwise, effluent was sampled only after 60-minutes of ME treatment. However, the pH probe used in these experiments may have become fouled during this cycle and the data presented below may need to be reproduced in future measurements.

Table 5.14 ME treatment conditions for an extended number of cycles experiment

V	SR	Reactor	Dose	pH	Agitation	Purging	Length
2 L	18	BC 3	50 g/L ZVI:GAC (2:1, CR and IPW) with 1 g/L GAC top-offs	3	Continuous mixing at ~1000 RPM	pre-treatment, CO2 at ~1 LPM	20, 1-hr cycles

As observed in other ME experiments, there was a clear trend of decreasing of As/Sb removal efficiency with the number of cycles (Figure 5.39 and Figure 5.40). Removal of As was less than expected for the first four cycles of treatment. This may to be attributed to either insufficient precision of ICP-MS quantification due to the sometimes-experienced instabilities of the calibration of the ICP-MS instrument employed in this study, as well as the age of the used condensate sample whose treatability deteriorates with storage time. Prior cycles with SR 19 determined 89, 91, and 85 % As removal after 30-minutes of ME treatment with top-offs, for Cycles 1-3, respectively (Section 5.1.6.2). Furthermore, previous cycles with SR 18 yielded 93 and 92% As removal after two cycles, with a 21-hour delay (Section 5.3.1.2). These experiments different based on:

- flushing gas employed (N2 versus CO2)
- sample (SR 18 versus 19)
- degree of pH control (diligent calibration practices)
- treatment time (30 versus 60 minutes)
- delays between treatment cycles

Thus, an exploration into the effects of top-off composition on cycling was conducted, to better optimize the performance of media cycling.

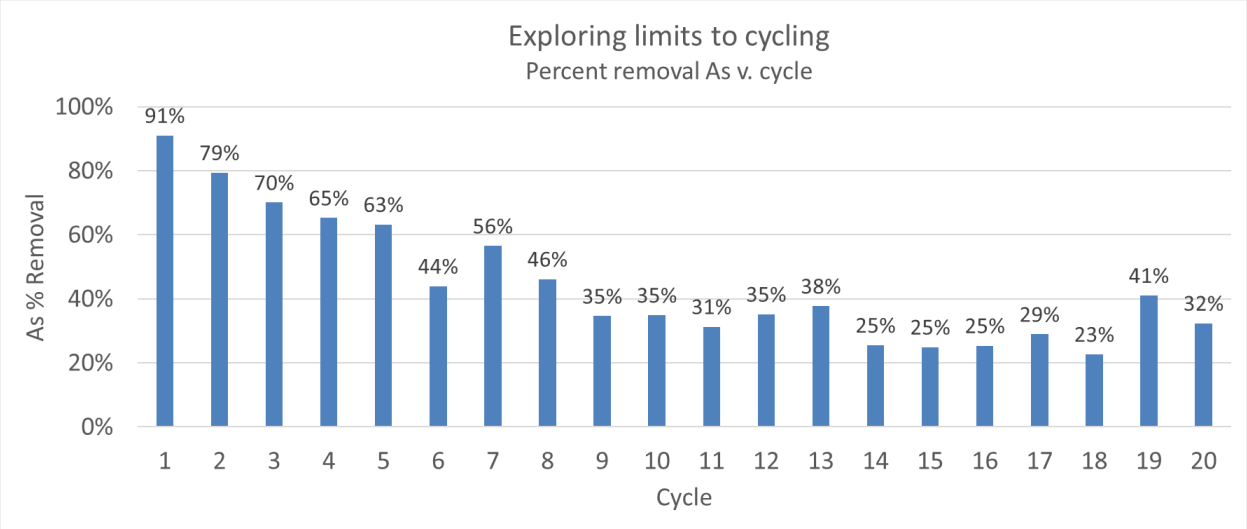

Figure 5.39 Comparison of As removal for an extended number of cycles with ME treatment conditions of 2L of SR 18 in BC3 with 50 g/L CR ZVI & IPW GAC (2:1) dose and 1 g/L GAC top-offs, continually mixed for 20- 1-hr cycles, with minimal delays, at 1000 RPM at pH 3.0 with pre-treatment CO2 purging

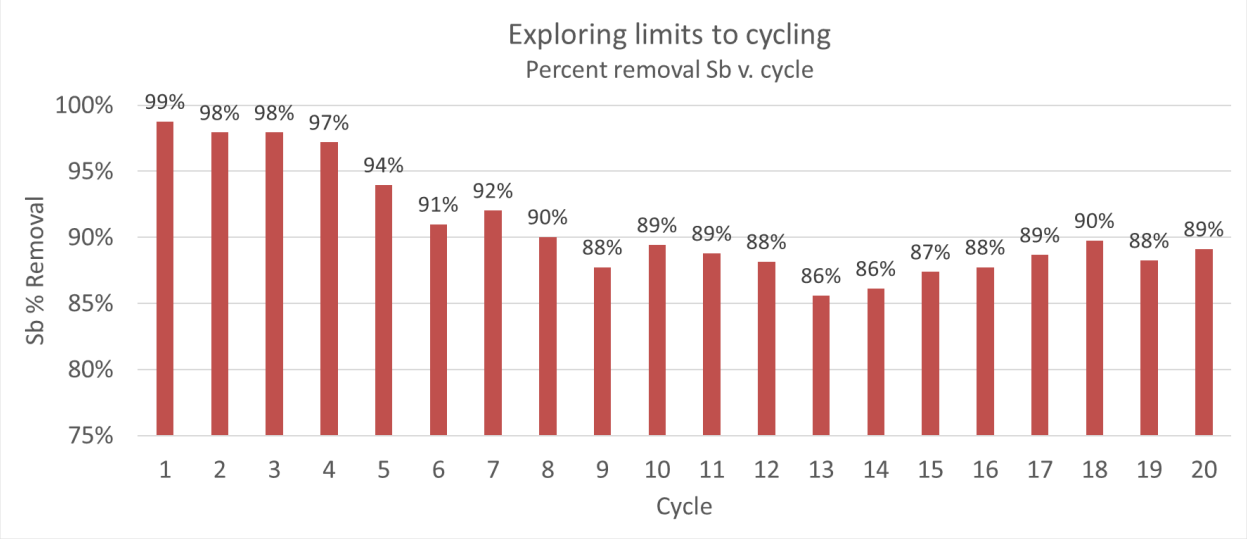

Figure 5.40 Comparison of Sb removal for an extended number of cycles with ME treatment conditions of 2L of SR 18 in BC3 with 50 g/L CR ZVI & IPW GAC (2:1) dose and 1 g/L GAC top-offs, continually mixed for 20- 1-hr cycles, with minimal delays, at 1000 RPM at pH 3.0 with pre-treatment CO2 purging

5.3.3 Variations of the top-offs compositions

Previous results indicated that the use of 1 g/L GAC top-offs was somewhat insufficient for achieving greater than 90% As removal for multiple cycles of treatment (Section 5.3.2). As a result, other top-off compositions were tested to determine their suitability for multi-cycle ME

treatment. 8 cycles of ME treatment were conducted for three compositions of 1 g/L top-offs: GAC only, ZVI only, and ZVI & GAC (2:1, i.e., "combined" top-off). ME treatment conditions are summarized in Table 5.15:

Table 5.15 ME treatment conditions for cycles with variable top-offs experiment

V	SR	Reactor	Dose	pH	Agitation	Purging	Length
2 L	19	BC 3	50 g/L ZVI:GAC (2:1, CR and IPW) with variable 1 g/L top-offs	3	Continuous mixing at ~1000 RPM	pre-treatment, CO2 at ~1 LPM	8, 1-hr cycles

Across all variables tested, ME treatment efficiency decreased consistently with an increased number of cycles. Results indicated that a combined top-off, of ZVI and GAC, improved cycling performance the most for As removal (Figure 5.41).

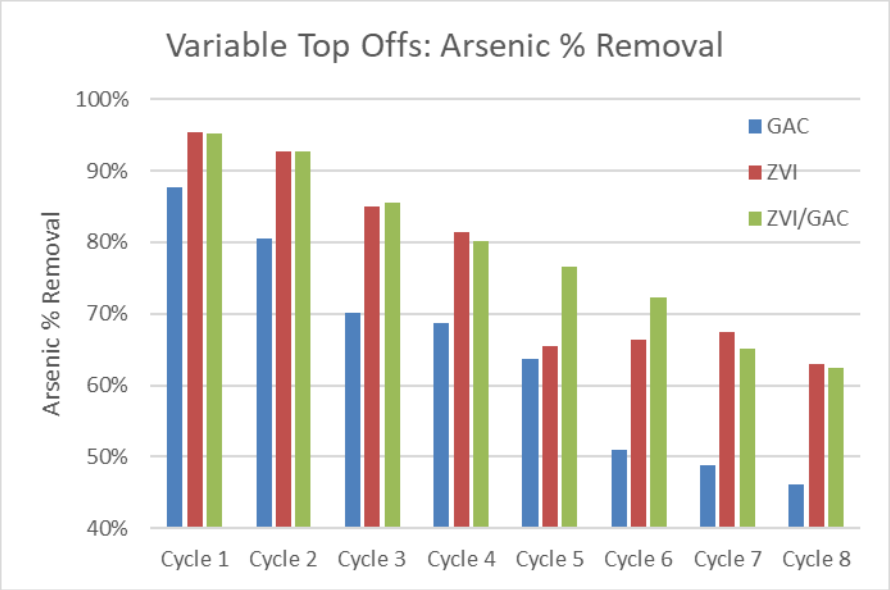

Figure 5.41 Comparison of As removal for cycles with variable top-offs with ME treatment conditions of 2L of SR 19 in BC3 with 50 g/L CR ZVI & IPW GAC (2:1) dose and variable 1 g/L top-offs, continually mixed for 8- 1-hr cycles at 1000 RPM at pH 3.0 with pre-treatment CO2 purging

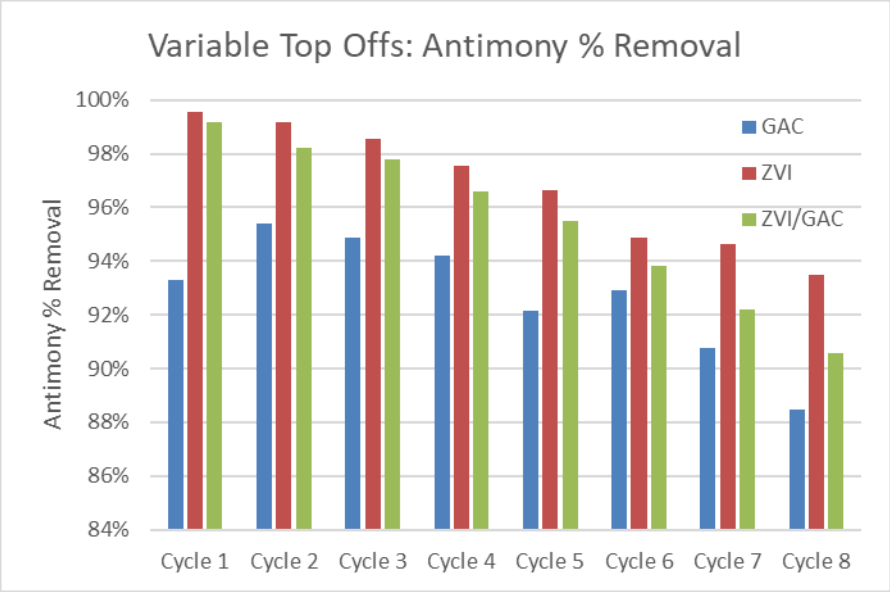

Figure 5.42 Comparison of Sb removal for cycles with variable top-offs with ME treatment conditions of 2L of SR 19 in BC3 with 50 g/L CR ZVI & IPW GAC (2:1) dose and variable 1 g/L top-offs, continually mixed for 8- 1-hr cycles at 1000 RPM at pH 3.0 with pre-treatment CO2 purging

There were only slight differences between the performance of ZVI only and the combined top-offs; however, after four cycles, the combined top-off resulted in better treatment until Cycle 7. The GAC only top-off cycles' treatment was lower than expected. Cycle 1 of the GAC only treatment should have yielded the same treatment as the other two variables tested, since ME treatment conditions for the first cycle was consistent across all top-offs tested (i.e., 50 g/L CR and IPW, 2:1). Beyond the first cycle, the GAC only top-off cycles had notably worse As/Sb removal, as compared to ZVI only and the combined top-offs. It was hypothesized that that the SR 19 sample used for the GAC top-off experiment hindered removal since it had been stored half-full, and thus had been more oxidized than the other SR 19 bottles utilized for this experiment. These cycle results were anomalous as the first cycle of 50 g/L ME treatment consistently resulted in greater than 90% As removal. Sb removal trends differed from As in that the ZVI only top-offs resulted in the best sustained ME treatment over multiple cycles (Figure 5.42).

Redox potentials measured in this experiment indicated that the combined top-offs resulted in the most reducing conditions measured, making it the preferred option over the ZVI only top-offs

(Figure 5.43). The ZVI only experiment resulted in nearly the same average ORP across the first four cycles. After cycle four, combined top-offs maintained a lower ORP than ZVI only top-offs. The average redox potential across GAC top-off cycles may indicate that mixing was insufficient to achieve the desired treatment, for example, by not sufficiently lowering the mixing shaft.

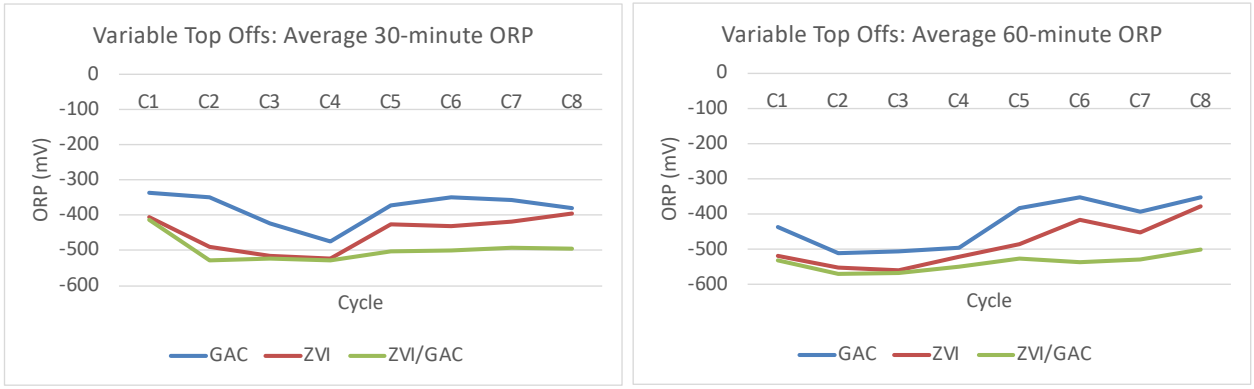

Figure 5.43 Comparison of redox potentials, by probe for cycles with variable top-offs with ME treatment conditions of 2L of SR 19 in BC3 with 50 g/L CR ZVI & IPW GAC (2:1) dose and variable 1 g/L top-offs, continually mixed for 8- 1-hr cycles at 1000 RPM at pH 3.0 with pre-treatment CO2 purging

Correlating Fe release to As removal, across all cycles 60-minute data, indicated that there was general agreement between the ZVI only and ZVI/GAC experiments (Figure 5.44). The GAC only decreased treatment is visible through the equivalent amount of ZVI released, as compared to the other two top-offs, with reduced As removal.

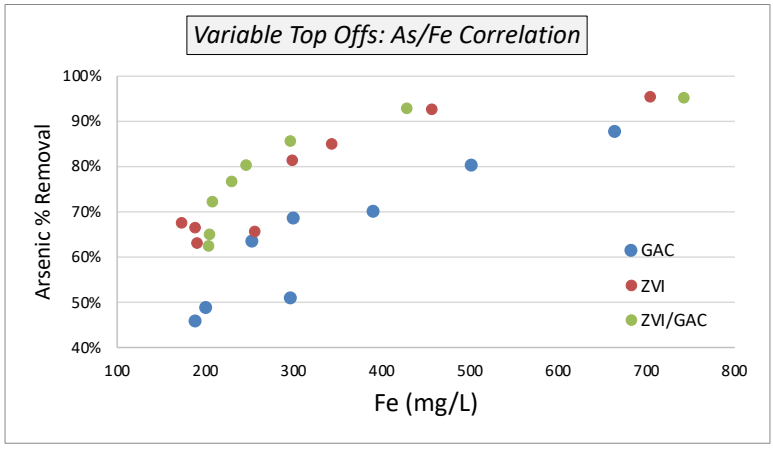

Figure 5.44 Comparison of As removal versus Fe release for cycles with variable top-offs with ME treatment conditions of 2L of SR 19 in BC3 with 50 g/L CR ZVI & IPW GAC (2:1) dose and variable 1 g/L top-offs, continually mixed for 8- 1-hr cycles at 1000 RPM at pH 3.0 with pre-treatment CO2 purging

Acid consumption to maintain pH 3.0 was tracked throughout each cycle of treatment (Figure 5.45). Across the three tested variables, the amount of acid required to maintain pH 3.0 decreased with the number of treatment cycles. This may indicate the presence of a gradual decrease of the catalytic action in the ZVI/GAC system with the number of cycles of using the active media. Specific mechanisms of this effect need to be established in further experiments.

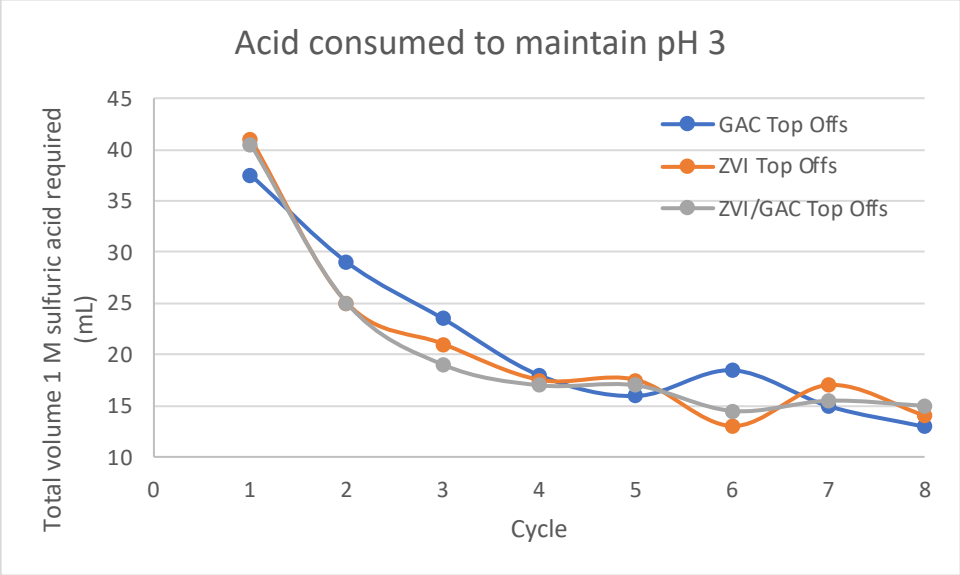

Figure 5.45 Comparison of acid required to maintain pH 3.0 for cycles with variable top-offs with ME treatment conditions of 2L of SR 19 in BC3 with 50 g/L CR ZVI & IPW GAC (2:1) dose and variable 1 g/L top-offs, continually mixed for 8- 1-hr cycles at 1000 RPM at pH 3.0 with pre-treatment CO2 purging

5.3.4 Typical up flow cycles

To confirm the repeatability of As/Sb removal in typical ME treatment conditions, three cycles of ME treatment were conducted with SR 18. ME treatment conditions are summarized in Table 5.16:

Table 5.16 ME treatment conditions for cycles with upflow mixing and 1 g/L GAC top-offs experiment.

V	SR	Reactor	Dose	pH	Agitation	Purging	Length
2 L	18	BC 3	50 g/L ZVI:GAC (2:1, CR and IPW) with 1 g/L GAC top-offs	3	Continuous mixing at ~1000 RPM	pre-treatment, CO_2 at ~1 LPM	3, 1-hr cycles

The first cycle of treatment yielded As removal rates consistent with the first ME treatment cycles observed in the prior experiments (Figure 5.46). The two subsequent cycles resulted in As removal 80% or greater. Decreased As removal for the subsequent cycles is hypothesized to be linked to the age of the SR 18 sample at time of experiment. Sb removal was very consistent for all three treatment cycles, with removal seemingly not as impaired by sample age.

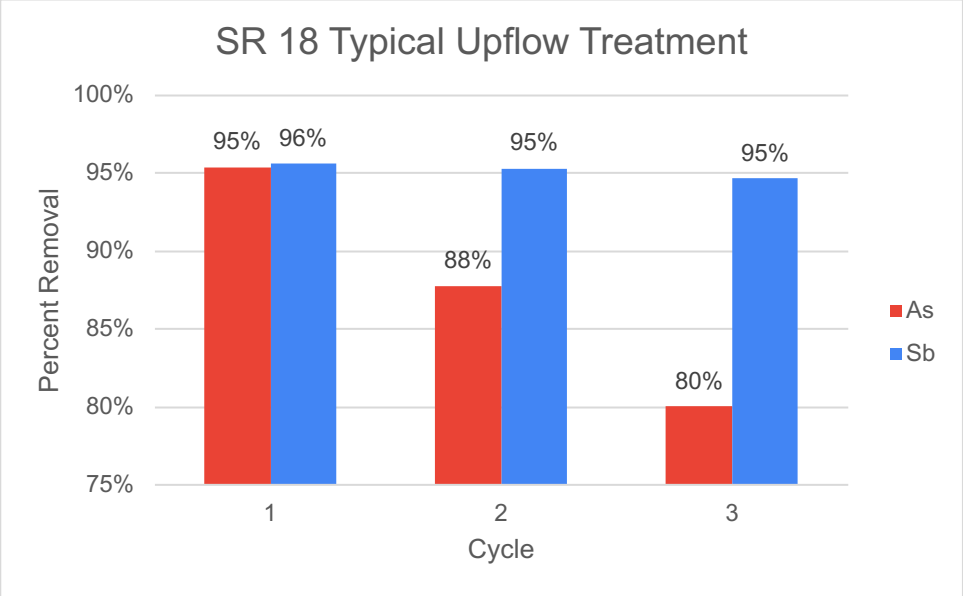

Figure 5.46 Comparison of As removal for cycles with upflow mixing and 1 g/L GAC top-offs with ME treatment conditions of 2L of SR 18 in BC3 with 50 g/L CR ZVI & IPW GAC (2:1) dose and 1 g/L GAC top-offs, continually mixed for 3- 1-hr cycles at 1000 RPM at pH 3.0 with pre-treatment CO_2 purging

The redox potential was consistently measured at approximately -450 mV across all three cycles, after 60-minutes of ME treatment (Figure 5.47). From 30- to 60-minutes of ORP treatment, each cycle, ORP lowered by approximately 50 mV.

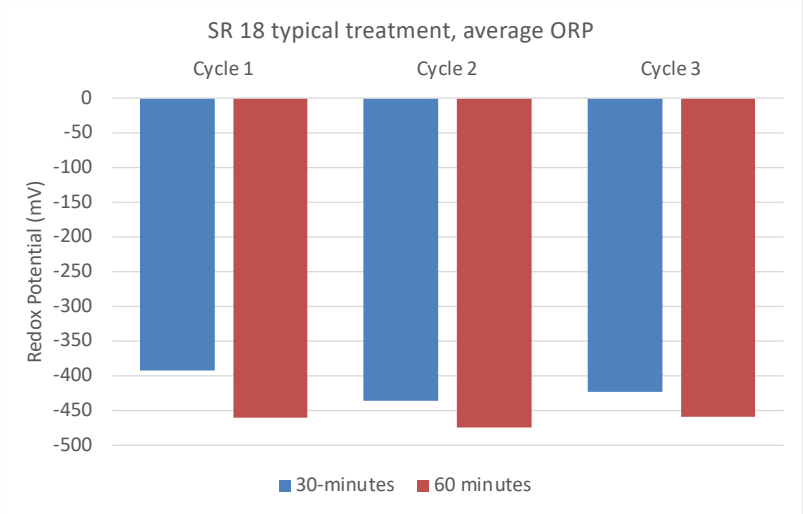

Figure 5.47 Comparison of average redox potentials, by cycle for cycles with upflow mixing and 1 g/L GAC top-offs with ME treatment conditions of 2L of SR 18 in BC3 with 50 g/L CR ZVI & IPW GAC (2:1) dose and 1 g/L GAC top-offs, continually mixed for 3- 1-hr cycles at 1000 RPM at pH 3.0 with pre-treatment CO2 purging

5.3.5 Variations in pH

To confirm and expand the findings concerning the effects of pH on As removal in ME treatment (Section 5.2.2), ME treatment cycles were conducted at four pH values. In these experiments, it was assumed that the degree of Fe dissolution was both determined by operational pH, making the exploration into pH greater than 3.0 of particular interest to confirm whether such an acidic environment was necessary for cyclical ME treatment. Top-off doses were combined (2:1 ZVI and GAC) and increased from 1 to 2 g/L, based on Variations of the top-offs experimental results. ME treatment conditions are summarized in Table 5.17:

Table 5.17 ME treatment conditions for cycles with variable pH experiment

V	SR	Reactor	Dose	pH	Agitation	Purging	Length
2 L	19	BC 3	50 g/L ZVI:GAC (2:1, CR and IPW) with 2 g/L combined top-offs	variable	Continuous mixing at ~1000 RPM	pre-treatment, CO_2 at ~1 LPM	6, 1-hr cycles

Consistent treatment greater than 80% As removal was achieved for four consecutive cycles by both pH 3.0 and 4.0 (Figure 5.48). pH 3.5 was only viable for two cycles of treatment to remove greater than 80% As. pH 4.5 yielded slightly less treatment than pH 4.0 until cycle four. pH 3.0

was affirmed to yield the best As removal treatment across multiple ME cycles with pH 4.0 being the next best operational pH. Sb removal trends differed slightly, with pH 4.5 yielded the most consistent Sb removal across multiple cycles of treatment (Figure 5.48).

All told, variations of pH from 3.0 to 4.5 did not result in dramatic changes of As/Sb removal in the sequence of six consecutive ME cycles. This is an important finding that may have significant implications for pilot- and full-scale implementation of ME treatment, both in terms of the stringency of pH controls and amount of acid used for the process. Effects of pH on extent of As volatilization are also highly important. They will be addressed in further experiments.

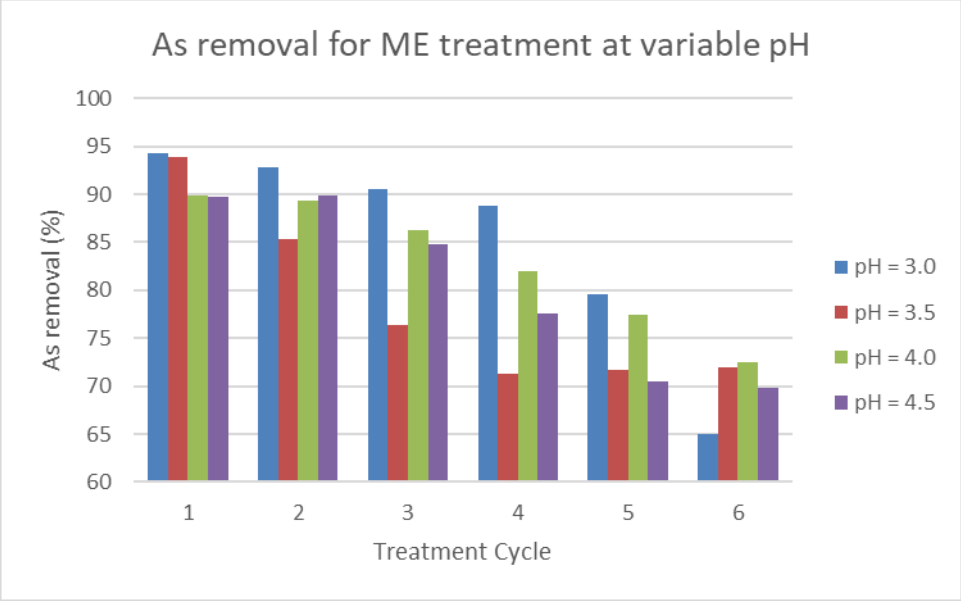

Figure 5.48 Comparison of As removal for cycles with variable pH with ME treatment conditions of 2L of SR 19 in BC3 with 50 g/L CR ZVI & IPW GAC (2:1) dose and 1 g/L combined top-offs, continually mixed for 6- 1-hr cycles at 1000 RPM at variable pH with pre-treatment CO2 purging

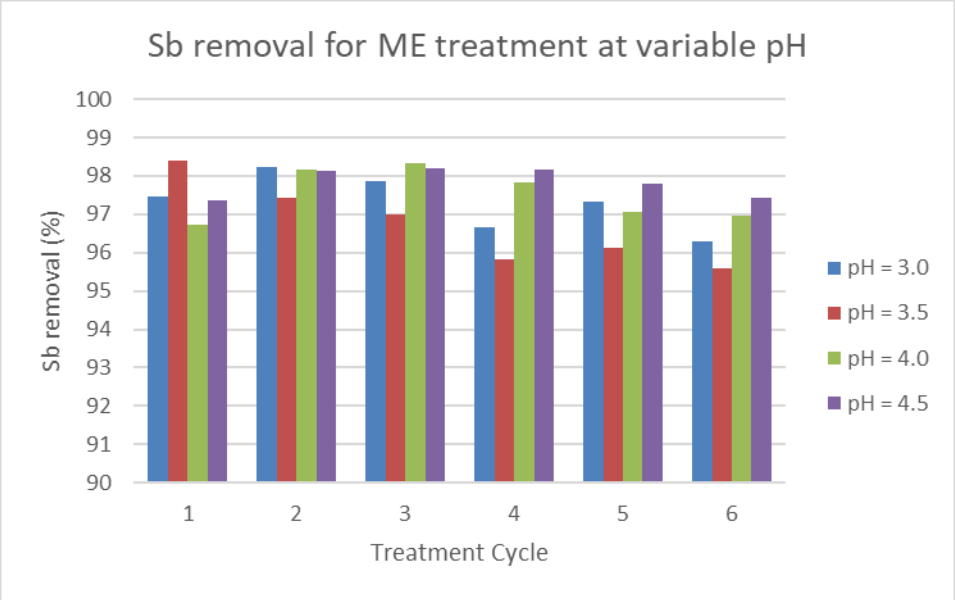

Figure 5.49 Comparison of Sb removal for cycles with variable pH with ME treatment conditions of 2L of SR 19 in BC3 with 50 g/L CR ZVI & IPW GAC (2:1) dose and 1 g/L combined top-offs, continually mixed for 6- 1-hr cycles at 1000 RPM at variable pH with pre-treatment CO2 purging

5.3.6 Comparing efficiencies of ME treatment using alternative top-off compositions and doses

Similar to the experiments conducted in Section 5.3.3, typical ME treatment experiments were conducted with varying top-off conditions for a total of three treatment cycles. Combined (ZVI/GAC) top-offs were compared against GAC only. Additionally, the combined top-off dose was increased from 1 to 2 g/L to investigate the effect of an increased top-off dose on improving the performance of ME treatment media for multiple treatment cycles. The 1 g/L GAC top-off experiment was conducted with SR 18 whereas the two combined top experiments were conducted with SR 19. ME treatment conditions are summarized in Table 5.18:

Table 5.18 ME treatment conditions for cycles with variable top-off compositions and doses experiment

V	SR	Reactor	Dose	pH	Agitation	Purging	Length
2 L	variable	BC 3	50 g/L ZVI:GAC (2:1, CR and IPW) with variable top-offs	3.0	Continuous mixing at 1000 RPM	pre-treatment, CO2 at ~1 LPM	3, 1-hr cycles

Figure 5.50 compares the performance of the different top-off compositions and based on this data, the 1 g/L combined top-offs yielded the best sustained performance of ME treatment media for 1-hr treatment cycles. The first treatment cycle indicates a degree of experimental variability with As removal ranging from 94 to 97 % across the three experiments conducted. Despite some differences in the experimental conditions (i.e., top-offs, SRs), all three experiments confirmed that ME treatment at the typically used pH 3.0 with 50 g/L active media dose (2:1) removed greater than 80% of As for at least three cycles of ME treatment. The reduced treatability of the SR 18 experiment is hypothesized to be attributed to length of sample storage time. Supplementary doses extend the useful life of active media and optimization of active media top-offs is still an area of exploration.

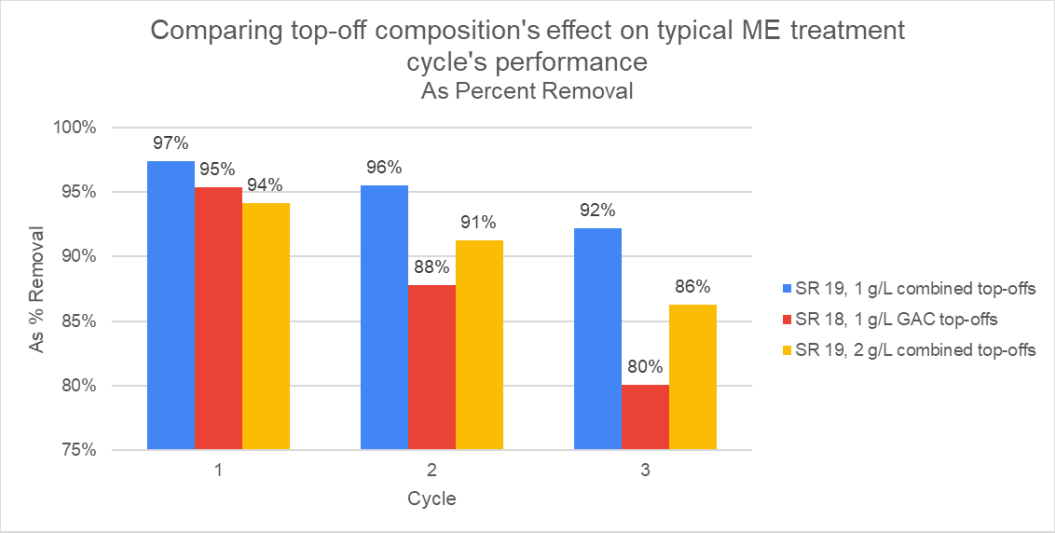

Figure 5.50 Comparison of As removal for cycles with variable top-off compositions and doses with ME treatment conditions of 2L of variable SR in BC3 with 50 g/L CR ZVI & IPW GAC (2:1) dose and variable top-offs, continually mixed for 3- 1-hr cycles at 1000 RPM at pH 3.0 with pre-treatment CO2 purging

5.4 Iron as a predictor of As removal in ME treatment

Previously, in-situ oxidation-reduction potential (ORP) measurements have been the primary surrogate parameter of interest that can be used to predict the efficiency of As removal by ME treatment. In-situ ORP measurements are easy to implement, at least in principle, and they can be used to track the progress of ME treatment in the sense of the development of its reducing environment due to the reactions induced by ZVI and GAC. As a result, ORP changes during ME treatment can be correlated with the degree of As and Sb removal by ME treatment.

Prior work in our group has shown that in situ measured ORPs could be correlated with ME treatment efficiency but the correlations were not sufficiently precise and achieved only via binning ORP into quantiles of expected As removal (Pinochet-Troncoso, 2023). Experimental ORP data also showed that at the beginning of ME treatment, there was a characteristic decrease in ORP values that corresponded to the initial activation of ZVI/GAC treatment media, with ensuing generation of a reducing environment. After this activation phase (approximately 5 minutes), ORP was observed to be relatively constant. Thus, one of the primary benefits of in-situ ORP measurements is to characterize the development of the reductive environment that is needed for efficient ME treatment.

In this thesis, ORP measurements made with commercially available ORP electrodes were observed to be insufficiently stable. There were issues with their calibration and stability during ME treatment, and in many cases sudden failures. When efforts were made to calibrate them more consistently and use higher-quality ORP probes, they still were observed to drift from their calibration from the beginning to end of a given ME treatment experiment, calling their accuracy into question. Another challenge with ORP calibration is that most standard calibration solutions provide highly oxidative conditions, for instance +256 mV. The ME process predominantly occurs in highly reductive conditions, with ORP reaching the potentials as low as -700 mV. Thus, calibrating ORP probes with these standards that generate ORP potentials >+200 mV may not be optimal. ORP was also observed to vary within probe location on the column reactor. Thus, a more

reliable surrogate parameter was desired to track ME treatment efficiency, especially one which could directly and unambiguously correlate to a given degree of As removal.

As ME treatment progresses, the ZVI media is continually interacting with various solutions components, notably with the protons, with resultant oxidation of Fe(0) to Fe(II) and release of Fe solutes. Measurements of Fe concentrations in the reactor can thus provide an estimation of the extent of ZVI phase reactions which, on the other hand, also remove As from the solution.

Testing this hypothesis based on the analytical data for concurrently measured As and Fe concentrations indicated the presence of a clear trend between the amount of dissolved Fe released during ME treatment and resultant As removal. Thus, measurements of dissolved Fe concentration became the subject of further investigation which aims to quantify Fe release to track ME treatment progress.

Due to the high concentrations of Fe in ME treatment effluent, the ICP-MS procedure that was used for trace level analyses had to be improved. This included changes of the sample dilution factors from 200 to 500 to better quantify Fe, with a tradeoff of potentially reducing the accuracy of measurements for As and Sb due to higher dilution.

Examination of the Fe/As correlations was mostly focused on comparing the change in Fe concentrations during ME treatment with the simultaneously occurring As removal. The quantitation of the change rather of the absolute values of the Fe concentrations was necessary since different LFG condensate samples were found to have different initial Fe concentrations. Trends in the Fe/As correlations were also found to depend on the pH and the treatment cycle number.

For instance, the first cycle of ME treatment consistently yielded the highest Fe dissolution rates and As removals. This trend changed somewhat during the subsequent ME treatment cycles that used the same ZVI/GAC media, with applicable increments of their doses, as described in the prior sections of this thesis.

The changes in the As removal vs. Fe release correlations is hypothesized to be attributed to the initial in-situ activation of ZVI media during the first treatment cycle. Given that the ZVI phase is activated during the first cycle, this process does not take place in the subsequent treatment cycles which tend to mobilize comparatively lower Fe concentration; the latter cycles tend to result in largely similar As removal vs. Fe release correlations. Likewise, ME treatment at pHs higher than 3.0 tended to result in comparatively lower Fe release but similar As removal efficiencies (Figure 5.52). This also resulted in some changes of As removal vs. Fe release correlations. These points are explained in more detail below.

Figure 5.51 shows the correlations between As removal and Fe release for seven "typical" ME treatment experiments. Their conditions were as follows: 2L LFG condensate, BC reactor, 50 g/L CR ZVI and IPW GAC initial active media dose, continuous mixing, pH 3.0, pre- and post-treatment CO_2 flush. The LFG condensate SR18 and SR19 samples were used. ZVI/GAC dose increments (top-offs) in Cycles 2 and 3 were also variable, in dose and composition. Despite these differences in the experimental conditions, the observed trends show the applicability of the concept of tracking the efficiency of ME treatment via the quantitation of Fe release. As mentioned above, these trends are cycle dependent where the first treatment cycle yields the greatest degree of Fe dissolution and As removal. Subsequent cycles of ME treatment yield less Fe dissolution and As removal yet the overall As removal vs. Fe release correlations are quite similar.

This proves the applicability of the notion of correlating As removal vs. Fe release, especially in the context of determining specific thresholds of expected levels of As removal vs. ranges of Fe release. This is shown in the tables that include average As removals and their standard deviations. Some variability in the As/Fe trends, most prominently observed for Cycles 2 and 3, can also be attributed to limitations in ICP-MS quantification. The analytical aspects of the quantitation of Fe in ME treatment are outside the scope of this thesis. Their findings will be presented elsewhere.

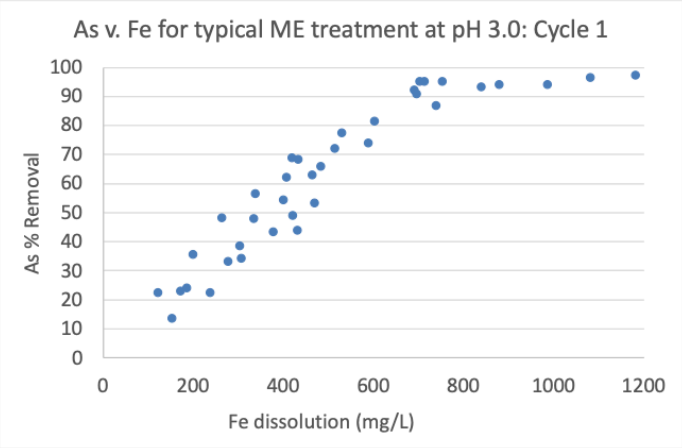

As v. Fe for typical ME treatment at pH 3.0: Cycle 1		
Range of Fe dissolution (mg/L)	Average As removed (%)	Standard Deviation (%)
100 - 200	24	8
200 - 300	35	11
300 - 400	44	9
400 - 500	59	9
500 - 600	75	3
600 - 700	88	6
700 - 800	93	4
800 - 1000	94	0
1000 - 1200	97	1

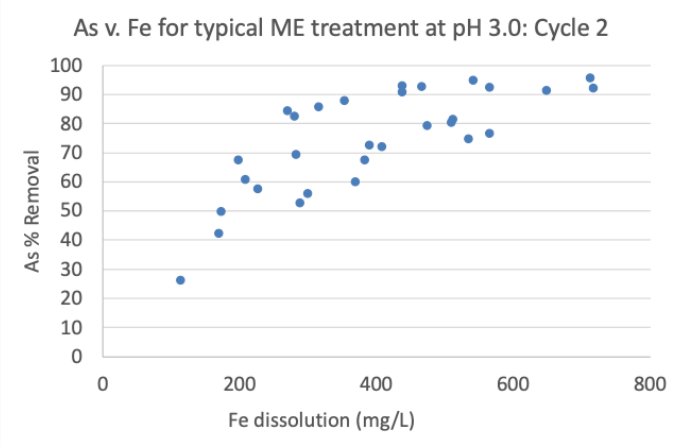

As v. Fe for typical ME treatment at pH 3.0: Cycle 2		
Range of Fe dissolution (mg/L)	Average As removed (%)	Standard Deviation (%)
100 - 200	46	17
200 - 300	68	13
300 - 400	72	13
400 - 500	86	9
500 - 600	83	8
600 - 700	91	--
700 - 800	94	2

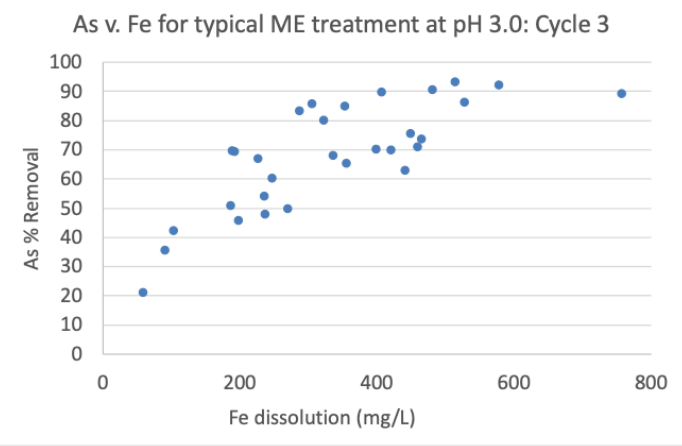

As v. Fe for typical ME treatment at pH 3.0: Cycle 3		
Range of Fe dissolution (mg/L)	Average As removed (%)	Standard Deviation (%)
0 - 100	28	10
100 - 200	56	13
200 - 300	60	13
300 - 400	76	9
400 - 500	76	10
500 - 600	91	4
600 - 700	--	--
700 - 800	89	--

Figure 5.51 As removal/Fe release correlations for typical ME treatment at pH 3.0 for Cycles 1 - 3, with tabulated average As removal for ranges of Fe released

To demonstrate the dependence of the As/Fe correlation on the cycle number, one set of data for a representative treatment experiment is shown below. The first cycle of treatment is different from that for the subsequent cycles, with greater Fe release corresponding to comparable levels of As. As aforementioned, this is hypothesized to be attributed to the activation phase of ME treatment. The activation phase proceeds via the dissolution of the surface scales (rusts) that are formed naturally on ZVI surfaces prior to the introduction of ZVI in the ME reactor. The stripping of the preformed scales results in higher Fe release during the first cycle, compared with the further phases of ME treatment. Subsequent cycles (2 and 3) follow a very similar trend and nearly achieve the same treatment plateau as Cycle 1. A plateau in As removal during the second and third cycles occurred after approximately 600 mg/L of Fe was observed to be released.

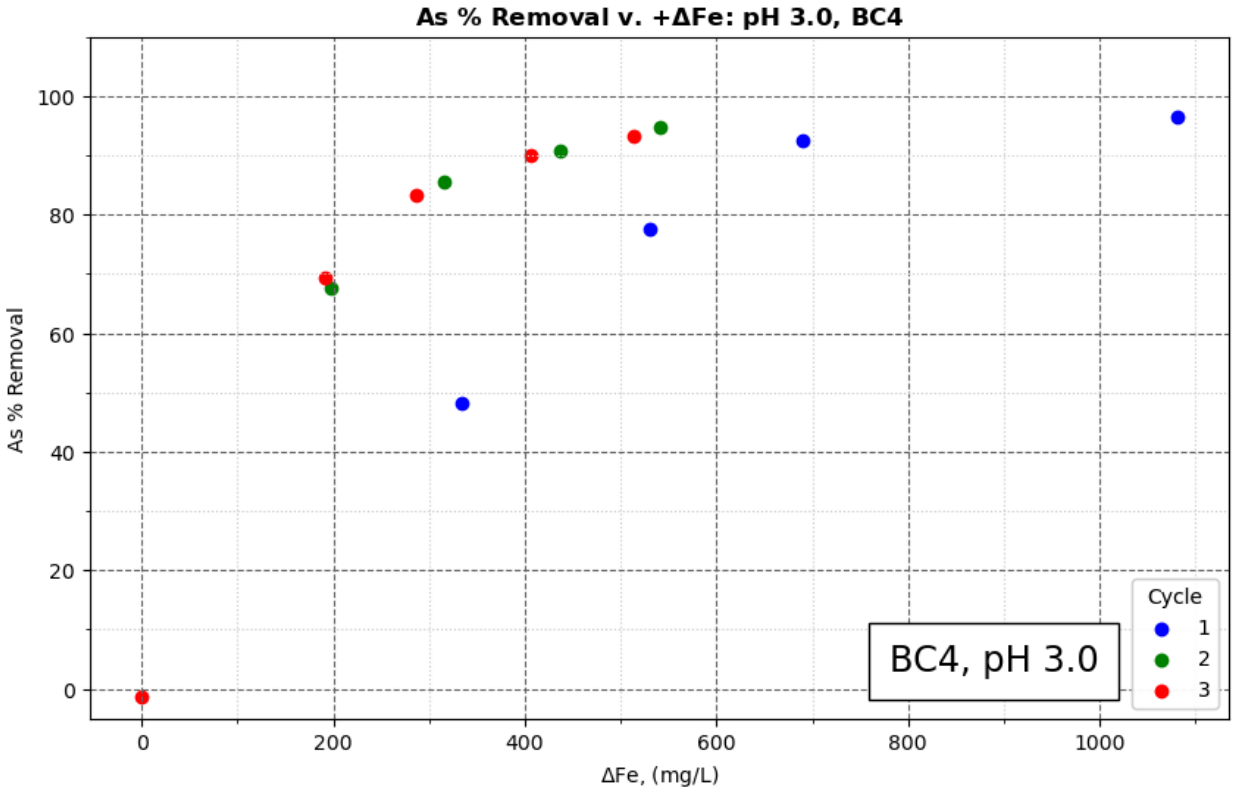

Figure 5.52 As removal/Fe release correlations for three cycles of typical ME treatment at pH 3.0 in BC4: 2L, SR 19, BC4, 50 g/L CR ZVI & IPW GAC with 2 g/L combined top-offs, pH 3.0 (1M H2SO4), pre-treatment CO2 purging, continuous mixing at 1000 RPM (10-19-2023)

Figure 5.53 compares the dissolution of Fe to As removal for ME treatment at four operational pH values across six cycles of treatment. It shows the dependence of the As/Fe correlations on pH. pH 3.0 yielded the greatest Fe dissolution and As removal. pH 3.5 and pH 4.0 yielded the next greatest Fe dissolution, respectively, and pH 4.5 yielded notably less Fe dissolution for comparatively similar As removal.

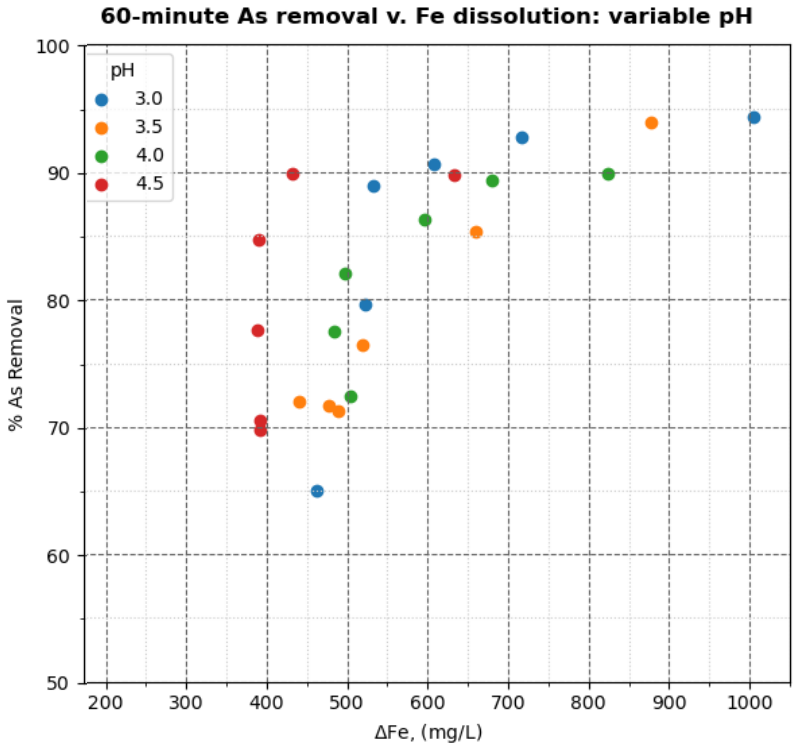

Figure 5.53 As removal/Fe release correlations for variable pH experiment for 6 cycles of typical ME treatment: 2L, SR 19, BC3, variable pH

These preliminary results show that correlating As removal to Fe release observed during ME treatment offers an actionable option that can be used to predict ME treatment efficency, with correlations being both pH and cycle dependent. Concentrations of dissolved Fe can be quickly and precisely determined using, for instance, the standard phenanthroline spectrophotometric method. This method is applicable for conditions typical for ME treatment, including field

conditions when ME treatment is deployed using pilot- and full-scale reactions, a continuing area of research of our group. These findings will be reported elsewhere.

6 Conclusions and suggestions for future work

The following section summarizes conclusions drawn from this thesis' experimental findings and provides suggestions for future work. This thesis reports ME treatment's capability to consistently remove the overwhelming majority (>90%) of organic As from LFG condensate. This provides a reliable treatment process for LFG-to-RNG operations that need to have a viable waste (LFG condensate in this case) management approach to prevent major complications in their long-term operations. This study also demonstrates that the active media used to drive ME treatment can be cycled/reused to remove at least 80% of As or greater from at least 4 consecutive cycles of batch treatment. Another finding of this study is that measurements of Fe release in ME treatment can be used for rapid estimation of the degree of ME treatment achieved.

6.1 Material characterization conclusions

Physical properties of ME treatment media were investigated through sieving, BET analysis, and settling time observations. Samples of ZVI products were procured from Höganäs, a trusted metal powder vendor. A research grade GAC product was compared against a commercially available GAC product of the same specified mesh size. Sieving characterized media based on particle size; resultant ZVI particle size distributions were applied to estimate specific surface areas which showed that finer particles yield higher specific surface areas, and the converse. Particle size distributions were used to size screens to retain media within the reactor during draining, thus minimizing media losses which is an important design consideration for recycling treatment media. BET analyses were conducted to estimate the specific surface area, pore volume, and pore sizes for two GAC products with the same 12-40 specified mesh size. Relevant experiments results indicated slight differences between the two GAC products. Settling tests and observations were conducted to define the required settling time between batch treatment. Larger sized media settled well during settling tests in water (within 15 seconds) and after the conclusion of ME

treatment cycles (within 5 minutes) indicating their suitability to quickly transition to the next consecutive batch ME treatment cycles which reutilizes the same media.

Rates of ME treatment media activation were compared with pH drift experiments. The effect of increasing catalyst (GAC) dose on ME treatment activation via proton consumption was investigated and results showed that GAC dose strongly affects the activation of ZVI. This effect can be highly important for probing the fundamental mechanisms of ME treatment and its optimization needs to be explored in more detail.

ME treatment performance was compared for various ZVI and GAC products. An acceptable replacement to Höganäs' LC Plus ZVI was required due to the product's discontinuation. Another set of extensive experiments examined the performance of an alternative material to replace the previously utilized expensive, research-grade Thermo Scientific GAC product. Höganäs' CR ZVI product had a similar particle size distribution, appearance, and performance to the previously utilized LC Plus product. While the Thermo Scientific GAC better catalyzed ZVI's oxidation and yielded faster ME treatment kinetics, the commercially available IPW GAC was determined to be a suitable, less-expensive replacement to achieve ME treatment targets. Thus, most of this thesis' experimental work optimized the ME treatment process with Höganäs CR ZVI and IPW 12-40 mesh GAC.

6.2 ME treatment optimization conclusions

An initial ME treatment active media dose of 50 g/L ZVI/GAC (2:1) was confirmed to be the optimal dose for 60-minutes of treatment using CR ZVI and IPW GAC. Similarly, 16.6 g/L GAC was confirmed as the optimal GAC dose to sufficiently catalyze 33.3 g/L ZVI and meet ME treatment goals. In agreement with the pH drift results, increasing doses of GAC resulted in increased ME treatment kinetics, and thus, increased As removal efficiency.

An operational pH of 3.0 was confirmed to yield the fastest ME kinetics. A correlation between increasing pH and decreasing ME kinetics was also observed. However, the increase of the system

pH from 3 to as high as 4.5 did not result in a failure of ME treatment although longer contact times may be required to remove a target fraction (e.g., 90%) of arsenic from the condensate.

An upflow axial mixing regime was confirmed to yield better performance over downflow mixing for the current geometry of ME treatment reactors. This is hypothesized to be due to a compaction of the active media into the conical reactor bottom with downflow mixing, hindering the media's suspension and interparticle interactions. Effects of flow direction and mixing intensity are to be quantified further for larger reactors that will be used in pilot- and full-scale ME applications.

An investigation into mixing speed determined approximately 1,000 RPM to be the optimal mixing intensity for ME treatment facilitated by mechanical mixing and showed a decrement of ME kinetics for greater speeds; additionally, particle suspension was determined to be required for ME treatment facilitated by mechanical mixing. The optimal mixing speed/intensity for pilot- and full-scale reactors may differ from that used in the experiments reported in this study.

6.3 ME treatment cycling conclusions

The first cycle of ME treatment for 50 g/L ZVI and GAC consistently removed greater than 90% of As despite experimental differences such as sample round or ZVI type (Table 6.1).

Table 6.1 Comparison of As removal for the first cycle of ME treatment for ME treatment conditions of 2L of LFG condensate sample, 60-minutes treatment length, IPW GAC, and 50 g/L ZVI and GAC (2:1)

Experiment	Variable	SR	Reactor	Length (mins)	ZVI	GAC	Initial Dose (g/L)	ZVI:GAC	Cycle 1 As Removal
Variable active media doses (2:1)	50 g/L	17	BC3	60	LC Plus	IPW	50	2:1	94%
Variable GAC dose	16.6 g/L GAC	17	BC3	60	CR	IPW	50	2:1	94%
Variable pH	pH 3.0	17	BC3	60	CR	IPW	50	2:1	94%
Variable flow pattern	Up flow	19	BC3	60	CR	IPW	50	2:1	97%
Variable mixing speed	1000 RPM	17	BC3	60	CR	IPW	50	2:1	94%

Delayed cycles without top-offs resulted in a consistent decrease in ME treatment efficiency. With top-offs of the active ZVI/GAC media, delayed cycle media exhibited only minor decreases in ME efficiency treatment, or ME kinetics even increased in the second treatment cycle. These results indicated that media *do not fail* while exposed to ambient gas phase over extended periods of time (e.g., up to 21 hours) which is beneficial for field conditions where LFG condensate supply may be

interrupted. The inclusion of an equalization basin for the LFG condensate treatment process will provide operational flexibility for batch mode treatment.

While there were still decreases in As removal kinetics for treatment cycles with ZVI/GAC top-offs, small supplementary doses of active media improved media performance across multiple cycles of treatment. Top-off composition affects ME treatment cycles' kinetics and combined top-offs of ZVI and GAC may yield the best sustained performance of treatment media.

Operational pH was further investigated and was confirmed to impact ME kinetics with pH 3.0 yielding the fastest sustained kinetics. However, there was no critical difference observed between ME performance for pH 3.0 to 4.5.

LFG condensate sample age is known to reduce As treatability by the ME treatment approach. Cycles treating fresh LFG condensate sample will likely perform better than those included in this thesis.

Cycles of ME treatment for 50 g/L CR ZVI and IPW GAC (2:1) consistently removed greater than 90% of As for at least 2 consecutive cycles of treatment, despite experimental differences such as sample round, pH, delays, or top-off composition (Table 6.2).

Cycles of ME treatment for 50 g/L CR ZVI and IPW GAC (2:1) *at pH 3.0* often removed greater than 80% for at least 4 consecutive cycles of treatment (i.e., ZVI and Combined "Varying top-offs" experiments, pH 3.0 "Varying pH" experiment) (Table 6.2).

Table 6.2 Comparison of As removal for cycles of ME treatment for ME treatment conditions of 2L of LFG condensate sample and 50 g/L CR ZVI and IPW GAC (2:1)

						As removal, by cycle									
Experiment	Variable	SR	Reactor	Length (mins)	Top Offs	1	2	3	4	5	6	7	8	9	10
Varying GAC types	IPW GAC	19	BC2	30	1 g/L GAC	89%	91%	85%							
Varying axial flow patterns	Up flow	19	BC3	60	1 g/L combined	97%	96%	92%							
Varying axial flow patterns	Down flow	19	BC3	60	1 g/L combined	94%	92%	89%							
Delayed cycles, no top offs	N/A	17	BC3	60	--	94%	88%	82%	68%	59%	46%	32%	31%	29%	20%
Delayed cycles, with top off	N/A	18	BC3	60	1 g/L GAC	93%	92%								
Extended number of cycles	N/A	18	BC3	60	1 g/L GAC	91%	79%	70%	65%	63%	44%	56%	46%	35%	35%
Varying top offs	GAC	19	BC3	60	1 g/L GAC	88%	80%	70%	69%	64%	51%	49%	46%		
Varying top offs	ZVI	19	BC3	60	1 g/L ZVI	95%	93%	85%	81%	66%	66%	68%	63%		
Varying top offs	Combined	19	BC3	60	1 g/L combined	95%	93%	86%	80%	77%	72%	65%	62%		
Varying top offs, continued	1 g/L GAC	18	BC3	60	1 g/L GAC	95%	88%	80%							
Varying top offs, continued	1 g/L combined	19	BC3	60	1 g/L combined	97%	96%	92%							
Varying top offs, continued	2 g/L combined	19	BC3	60	2 g/L combined	94%	91%	86%							
Varying pH	pH = 3.0	19	BC3	60	2 g/L combined	94%	93%	91%	89%	80%	65%				
Varying pH	pH = 3.5	19	BC3	60	2 g/L combined	94%	85%	76%	71%	72%	72%				
Varying pH	pH = 4.0	19	BC3	60	2 g/L combined	90%	89%	86%	82%	77%	72%				
Varying pH	pH = 4.5	19	BC3	60	2 g/L combined	90%	90%	85%	78%	70%	70%				
					Average	93%	90%	84%	76%	70%	62%	54%	50%	32%	28%

6.4 Iron as a treatment predictor conclusions

Trends between As removal and Fe release observed during ME treatment are cycle and pH dependent. However, in all cases, they are predictive of As removal. Typical ranges of Fe release may be developed for correlation with specific As removal goals. This is an ongoing area of exploration with the potential to offer a reliable metric for tracking ME treatment in field conditions.

6.5 Suggestions for future work

Gas phase analysis and As mass balance: Improved gas-phase analytical methods need to be implemented and further experimentation must be conducted to capture and quantify evolved As-containing volatiles formed during ME treatment. This requires a gas-tight bench scale ME treatment reactor and precise control of gas conveyance. Quantifying the degree of As volatilization during ME treatment for a variety of treatment conditions through cryo-trapping and adsorption of applicable media (e.g., silver impregnated silica, Fe amended GAC) or other gas phase analyses (e.g., gas chromatography) is a critical component required to quantify the As mass balance in complete detail. In addition to improved gas phase analysis for As, structural analyses

(e.g., EXAFS, XPS) and high-precision quantification of Fe by microwave digestion need to be performed to determine the nature of retention of As by ZVI/GAC during ME treatment.

Operational pH: We posit that volatilization of As may potentially be suppressed by the operating pH for ME treatment and use of a carrier gas. The degree of As volatilization should be investigated at increasing pHs (e.g., 3.0 to 4.5).

Extending media cycling: Further optimization of supplementary doses and exploration of alternative catalysts should be conducted to increase the recycling capabilities of active media. Since GAC has been shown to retain the majority of removed As, and since ORP measurements have consistently shown that the reductive ME environment is maintained for many cycles of treatment, cycling efficiency may be limited by available GAC surface area, or the fouling of ZVI/GAC surfaces during ME treatment. GAC is non-selective and likely retains many more constituents present in LFG condensate than As and Sb alone. The effectiveness of larger top-off doses should be further explored, specifically doses with greater amounts of GAC.

Media regeneration: Media regeneration, for instance by strong acids applied to the ZVI phase, should be investigated to extend the useful life of ME treatment media, potentially reducing media costs and hazardous waste generated.

Optimizing mixing regime: The current mixing regime needs to be further optimized to best facilitate active media particle suspension and inter-particle interactions. Applicable variables include mixing speed and impeller design. Decreasing the required mixing intensity to facilitate ME treatment may reduce energy requirements for mixing. It may also minimize the breakage of GAC (i.e., pulverization/powderization).

ME treatment media: Further investigations into the performance of other commercially available ZVI/GAC active media products, based on cost and ME treatment kinetics, may help optimize practical operations of ME technology.

Fe as a precise predictor of As removal: Correlations between iron release and As removal should be explored further to better develop the parameter as a precise and reliable treatment

predictor for varying ME treatment conditions. Iron can be quickly quantified utilizing the Phenanthroline standard method. Additionally, the availability and performance of in-situ Fe sensors should be explored for real-time tracking of Fe release during ME treatment.

Fundamental modeling of ME treatment: Finally, it is clearly necessary to ascertain the fundamental mechanisms of ME treatment and develop a high-level model of its performance in practically important conditions. This will help design and optimize ME treatment for variable treatment conditions (e.g., dose, pH, treatment media dose and surface areas, activation and mixing conditions) and LFG condensate properties.

7 Appendix

7.1 Sample round composition quantified by UW ICP-MS analysis

Table 7.1 averages the initial concentrations of As, Sb, and Fe determined by the UW ICP-MS analyses and reports the standard deviation for samples analyzed. Experiments which experienced ICP-MS calibration drift were excluded and re-run. Variability between Fe samples may be attributed to Fe contaminated glassware used for sample preparation, exceedance of ICP-MS Fe calibration range, and/or natural variability of LFG condensate Fe concentration, similarly seen in the certified laboratory's Fe determinations (Table 4.1). The UW's quantification of LFG condensate initial Sb concentrations trended higher, likely attributed to element carryover during ICP-MS analysis runs.

Table 7.1 Sample round composition quantified by UW ICP-MS analysis

Sample Round	Samples	As (mg/L)		Sb (mg/L)		Fe (mg/L)	
		Avg.	Std. Dev.	Avg.	Std. Dev.	Avg.	Std. Dev.
SR 17	9	18.1	0.5	1.9	0.1	--	--
SR 18	4	17.4	0.4	3.4	0.1	265	64
SR 19	53	13.2	1.2	3.1	0.3	64	78

7.2 Confirmation of UW ICP-MS analysis with KCEL

Aqueous samples were sent to the King County Environmental Laboratory (KCEL) to confirm ICP-MS analyses conducted by the UW and determine other analytes of interest. The KCEL laboratory is accredited by the Washington State Department of Ecology (WDOE) (King County, 2024). Samples were primarily comprised of untreated LFG condensate and ME treatment effluent.

7.2.1 September 2023 samples

7.2.1.1 SR 19 initial concentrations

The average concentration of KCEL analyzed SR 19 samples was 13.1 ± 0.3 mg/L As and 2.4 ± 0.1 mg/L Sb. This can be interpreted either as the laboratory having an inter-sample analysis error of

about 2% for As and 3% for Sb. KCEL's range of reported SR 19 initial concentrations was 12.5 to 13.4 mg/L As and 2.33 to 2.54 mg/L Sb.

7.2.1.2 Comparison of analyte quantification

Figure 7.1 compares UW and KCEL-determined As, Sb and Fe concentrations by ICP-MS analysis. A trend line with a slope of 1 and intercept at the origin (0,0) is included on each plot to visualize a perfect agreement between the UW's and KCEL's analyses.

The comparison shows the presence of a good agreement between the As data obtained by the UW and KCEL measurements, with some deviation as explained in more detail below. This is shown as the grouping of concentrations which intersects at approximately 2,000 µg/L As and continues to about 13,000 µg/L As. On the As plot, there is a grouping of data with a greater skew from the KCEL determined concentrations. This is seen where KCEL reports approximately 1,000 µg/L As and the UW reports about 3,000 µg/L As. The disagreement between UW and KCEL concentrations has been attributed to the drift in the UW's ICP-MS calibration.

Similar trend skew in Sb concentrations were observed between the KCEL and UW datasets. The UW's ICP-MS analysis tended to yield comparatively higher concentrations of Sb (approximately 3,000 µg/L) than KCEL (approximately 2,500 ug/L). This is hypothesized to be attributable to Sb carryover within the ICP-MS instrument (Nelms, 2018).

The UW and KCEL data for Fe concentrations are well correlated, although the UW measurements typically result in lower Fe concentrations. This is most likely due to the constraints of the RTT ICP-MS instrument and the method used by the UW group. The latter method was developed to primarily measure trace levels of analytes.

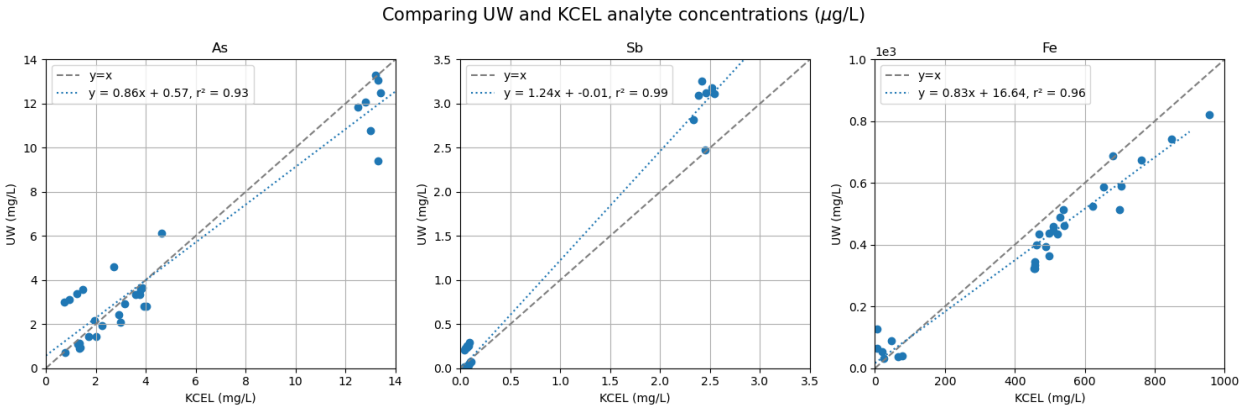

Figure 7.1 Comparison of ICP-MS analyses between the UW and KCEL for As, Sb, and Fe

Figure 7.2 compares the UW and KCEL data by the experiment round, rather than as an entire dataset. It is to be noted here the UW's ICP-MS method processes a blank sample (Blank) which is comprised of nitric acid and ultrapure water. Based on the examination of the variations in the ICP-MS calibration shown in the plot, the blank used for Experiment A set of samples may have been contaminanted, or some other factor impacted instrument calibration. It is relevant to mention here that the UW data for Experiment A were generated on 08-28-2023 and the remaining experiments (B-D) were generated 09-01-2023. The observed difference between the Experiment A and other data indicates a variability in ICP-MS calibration between analysis runs. Note that Experiment A's initial As concentration was nearly the same as the KCEL determined concentration (i.e., approximately 13.5 mg/L). However, the UW ICP-MS resulted were skewed relatively higher at lower concentrations of As resulting in percent removal calculations which underrepresent the true amount of As removed by ME treatment. Since the time at which these experiments performed, the the UW ICP-MS method was modified, increasing the ICP-MS samples' nitric acid concentration to 5% to improve analyte solubility and extended the flush time between the subsequent samples.

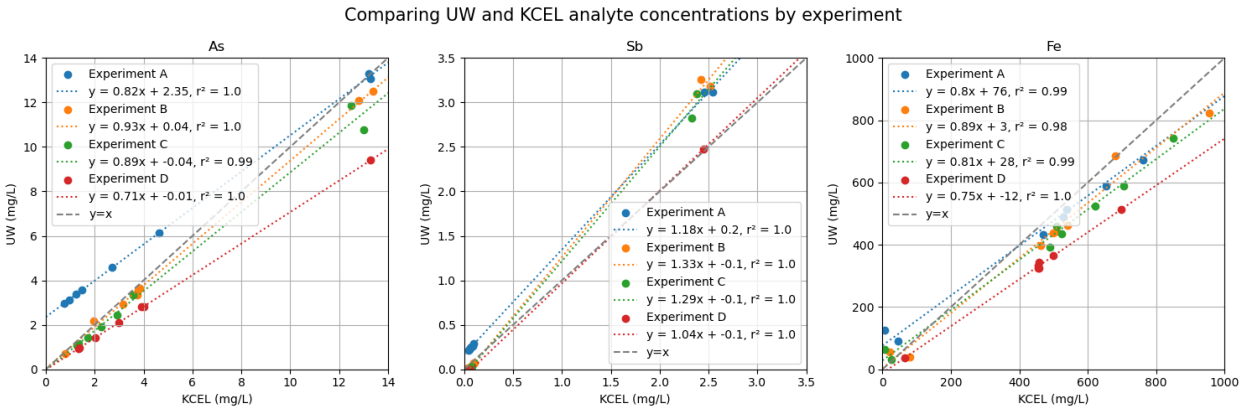

Figure 7.2 Comparison of ICP-MS analyses between the UW and KCEL for As, Sb, and Fe, separated by experiment

7.2.1.3 Comparison of analyte percent removals determined based on UW and KCEL experimental data

Determining the percent removal of As and Sb achieved by ME treatment is the most frequently used calculation to gauge ME performance. Despite the comparatively lower precision of the ICP-MS measurements using the UW equipment, the analyte's percent removal results are very similar to those determined using KCEL data for the same samples (Figure 7.3). Still, there are some differences between the UW and KCEL analyses. The instability of in the performance of the UW ICP-MS instrument did not significantly affect the As removal trends (other than that for Experiment A). However, due to a drift in the ICP-MS calibration, many Sb concentrations UW determined for 60-minutes of ME treatment were reported as negative which resulted in greater than 100% removal while the KCEL Sb data show correct removal rates. Still, both sets of the Sb analytical data show a near complete (>95%) removal of Sb by ME treatment.

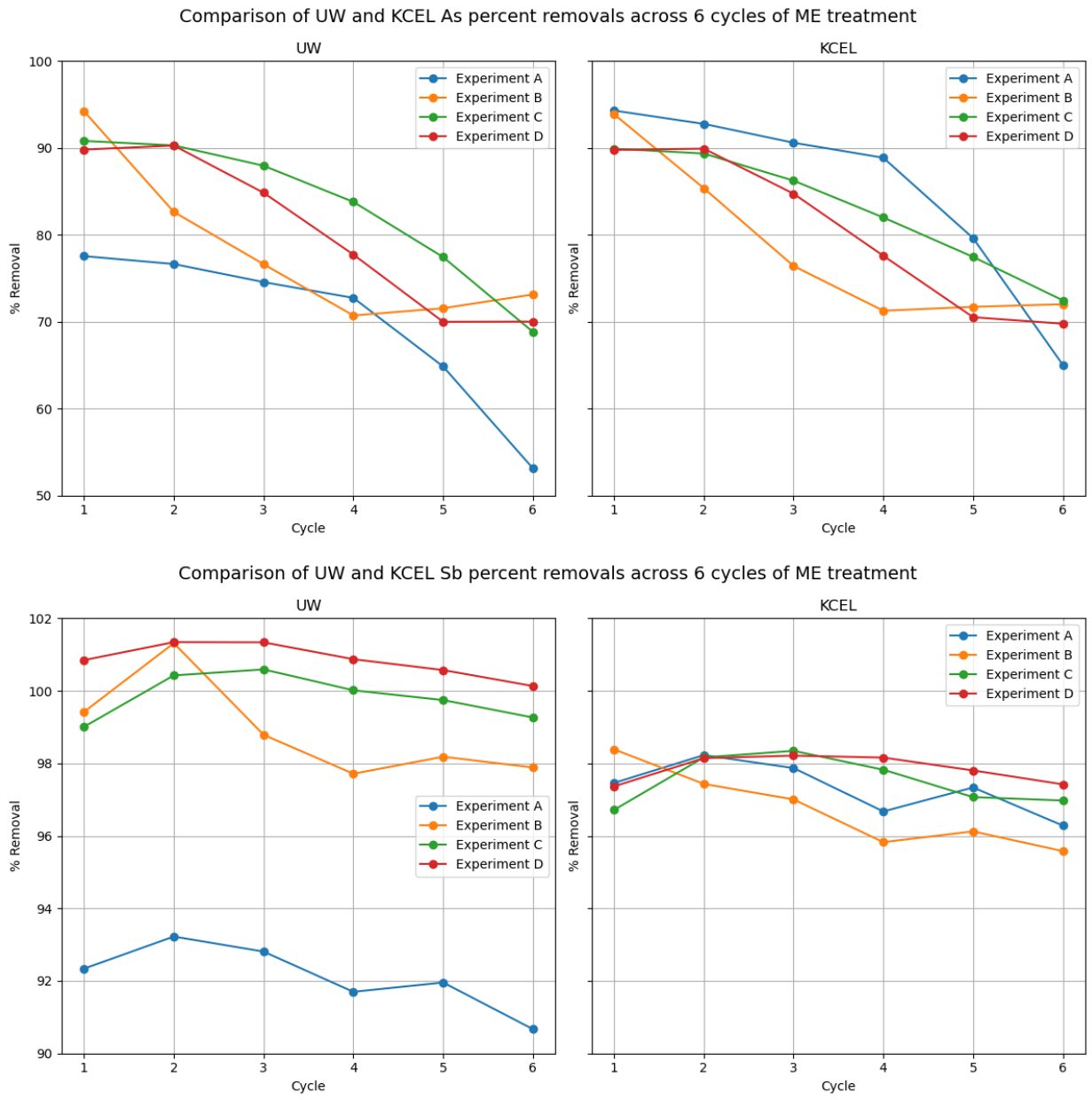

Figure 7.3 Comparison of UW and KCEL percent removals of As and Sb as determined by ICP-MS analyses (September 2023)

The UW data on dissolved Fe had some differences from those of KCEL. On average, the UW's quantification of Fe tended to yield ca. 100 mg/L less than KCEL's. KCEL specifies their minimum detection limit (MDL) for each analyte, but it is unclear what their ICP-MS's upper detection limit (or MaxDL) is. The accuracy of the analytical data for iron release will become increasingly important as Fe release thresholds are expected to be used as a method of predicting the attainment of sufficient ME treatment.

In conclusion, it can be observed that despite the comparatively lower accuracy of determinations of As and Sb using the UW ICP-MS equipment, the great majority of the reported As percent removal calculations were accurate. This suggests that despite the UW's As calibration drift, the removal trends could still be trusted for largely all experiments.

7.2.2 December 2023 samples

Effluent samples from three ME treatment experiments were sent to KCEL for analysis in December 2023. BC4 ME treatment conditions are summarized in Table 7.2 and Table 7.3. These experimental findings will be more fully reported elsewhere. ME treatment conditions for Typical ME treatment (BC3)", as specified in Figure 7.6 and Figure 7.7, are summarized in Table 5.8.

Table 7.2 ME treatment conditions for cycles in BC4 with copper catalysis experiment

V	SR	Reactor	Dose	pH	Agitation	Purging	Length
2 L	19	BC 4	50 g/L ZVI:GAC (2:1, CR and IPW) with 2 g/L combined top-offs and 500 mg/L Cu each cycle	3.0	Continuous mixing at 1000 RPM	pre-treatment, CO2 at ~1 LPM	3, 1-hr cycles

Table 7.3 ME treatment conditions for typical ME treatment cycles in BC4 experiment

V	SR	Reactor	Dose	pH	Agitation	Purging	Length
2 L	19	BC 4	50 g/L ZVI:GAC (2:1, CR and IPW) with 2 g/L combined top-offs	3.0	Continuous mixing at 1000 RPM	pre-treatment, CO2 at ~1 LPM	3, 1-hr cycles

7.2.2.1 Comparison of analyte quantification

Figure 7.4 compares UW and KCEL-determined As, Sb, Fe, and Cu concentrations. A trend line with a slope of 1 and intercept at the origin (0,0) is included on each plot to visualize a perfect agreement between the UW's and KCEL's analyses.

The comparison shows the presence of a good agreement between As data obtained by the UW and KCEL. However, there is a subset of the data which skews farther from KCEL's findings. This phenomenon was also seen in previous KCEL correlations and attributed to drift in the UW's ICP-MS calibration and/or element carryover. This is further explored in Figure 7.5, where the data is

separated by ICP-MS analysis run. The comparison for the Sb data shows that the UW tended to yield higher Sb concentrations, by about 20% (per the regression slope). The UW slightly under-quantified Fe concentrations. However, there was a very good agreement between the UW's and KCEL's Fe determinations although the UW Fe data deviate somewhat more from those of KCEL at higher Fe concentrations. The UW under-quantified Cu (which was an ancillary element in these analyses), but there was good agreement between the two labs' findings.

As previously concluded in the September KCEL investigation (Section 7.2.1), the UW and KCEL data are well correlated, although the UW measurements tend to result in lower Fe concentrations. This is most likely due to the constraints of the RTT ICP-MS instrument and the method used by the UW group; the method was developed to primarily measure trace levels of analytes.

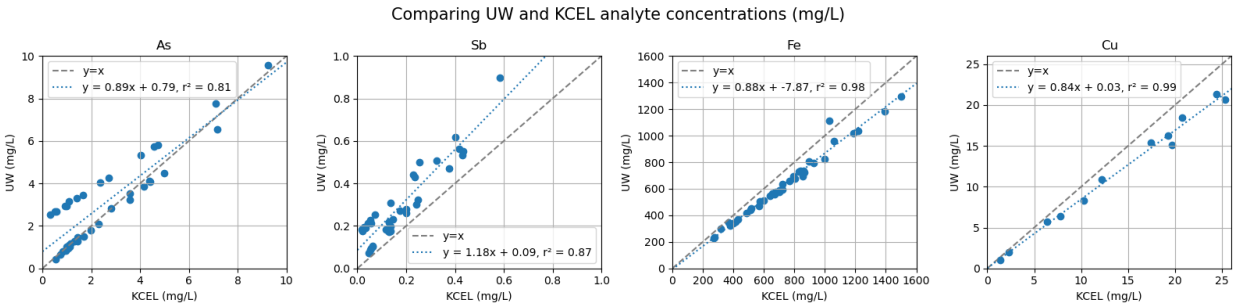

Figure 7.4 Comparison of ICP-MS analyses between the UW and KCEL for As, Sb, Fe, and Cu

Figure 7.5 shows the variability in ICP-MS calibration between runs, similarly observed in Figure 7.1. There are two separate trends in As and Sb correlation for the two separate ICP-MS runs, indicating variability in the UW's instrument calibration. However, the corelation between UW and KCEL Fe data appears to be independent of ICP-MS run.

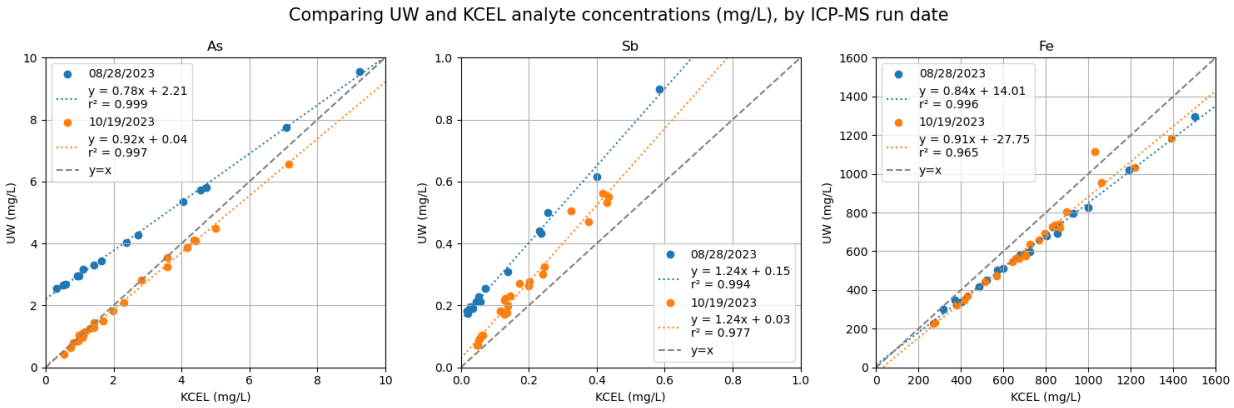

Figure 7.5 Comparison of ICP-MS analyses between the UW and KCEL for As, Sb, and Fe, separated by analysis run

7.2.2.2 Comparison of As and Sb percent removals determined using UW and KCEL data

Figure 7.6 shows that the samples for two BC4 experiments, analyzed at ICP-MS on 10/19/2023, were accurately measured and yielded near-same percent removal trends for As. However, the 08/28/2023 ICP-MS run for the BC3 typical ME treatment experiment significantly underrepresented As removal by ME treatment due to the aforementioned challenges with quanitfying low level analyte concentrations.

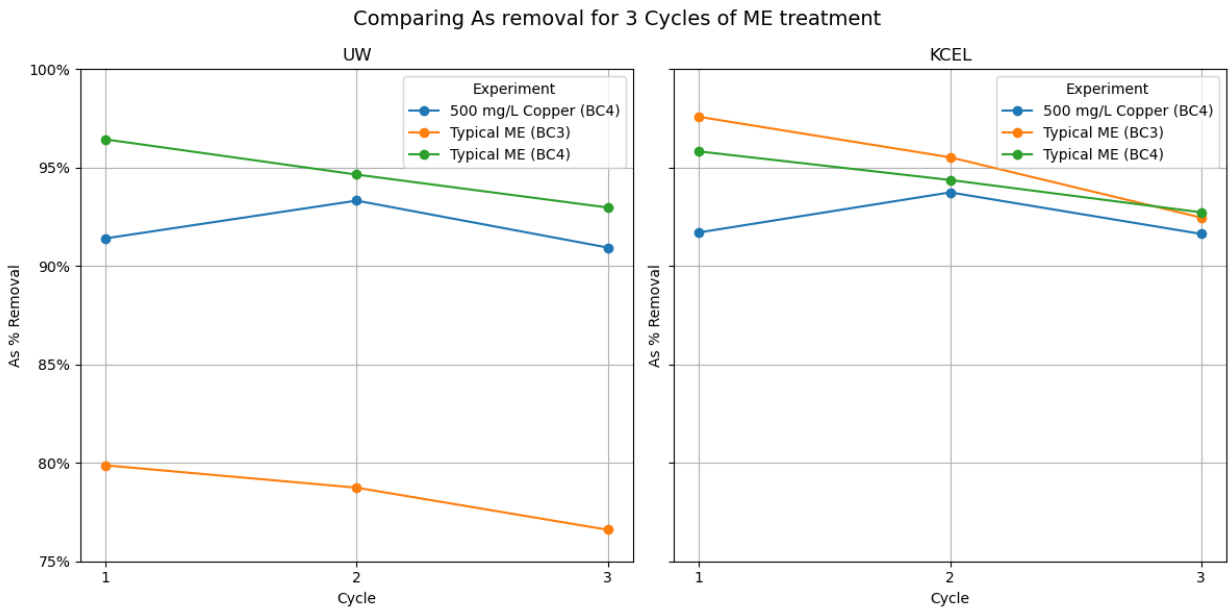

Figure 7.6 Comparison of UW and KCEL percent removals of As as determined by ICP-MS analyses (December 2023)

Figure 7.7 shows that the samples for two BC4 experiments, analyzed at ICP-MS on 10/19/2023, were accurately measured and yielded near-same percent removal trends for Sb. The UW only slightly underestimated Sb removal for these BC4 exeriments. However, similar to As, the 08/28/2023 ICP-MS run for the "Typical ME (BC3)" experiment underestimed Sb removal by ME treatment due to the aforementioned challenges with quanitfying low level analyte concentrations.

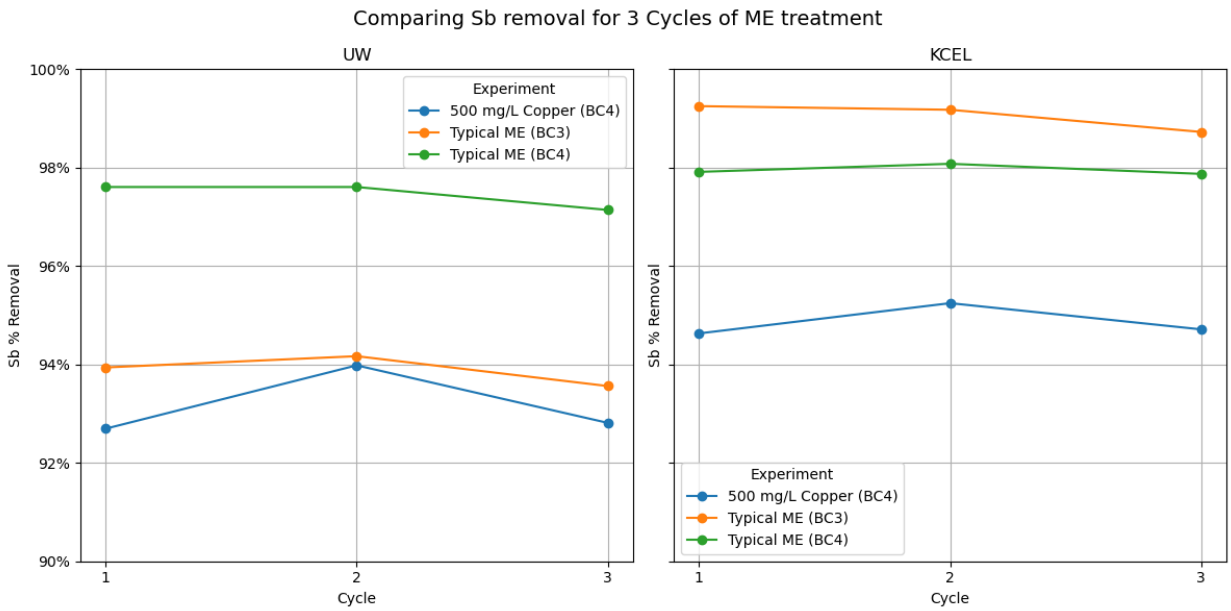

Figure 7.7 Comparison of UW and KCEL percent removals of Sb as determined by ICP-MS analyses (December 2023)

7.2.2.3 Summary of findings

- The UW's 10/19/2023 ICP-MS run had an excellent correlation with KCEL's As determinations. The UW's 08/28/2023 ICP-MS run had a high r-squared but was skewed higher than KCEL's As determinations. Alternatively, the UW tends to consistently under quantify analytes such as Fe and Cu. Despite being skewed slightly lower, the UW's determinations are well-correlated to KCEL's determinations with r-squared values of 0.98 and 0.99 for Fe and Cu, respectively.
- The UW's data is consistently well-correlated with KCEL's findings, but often skews higher for As and Sb. Thus, the UW's correlation to KCEL's ICP-MS analyte determinations sometimes have differences. For example, the 08/28/2023 run incurred an issue with determining low levels of analytes (As & Sb), a phenomenon which was previously observed in the September 2023 KCEL comparative analysis. The outcome of this overdetermination of analytes is an underestimation of As and Sb removal. While the UW calculated As removal of 80%, 79%, and 77% for Cycles 1-3 of typical ME treatment

(analyzed 08/28), KCEL's data reported analyte removals which were much greater: 98%, 96%, and 92%, respectively. This data confirms that the typical ME treatment bench tested at the UW achieves greater than 90% removal of As for at least three cycles of treatment.

- The UW has improved their ICP-MS methodology by increasing the wash time between samples to at least 90 seconds and by increasing the concentration of nitric acid in the wash solution from 1 to at least 2% HNO_3 (v/v). To improve the accuracy of determination of Fe concentrations in ME effluent samples, the UW's ICP-MS sample dilution factor was increased from 200 to 500. Both the 08/28 and 10/19 UW ICP-MS runs were performed with sample dilutions of 500. The 10/19/2023 ICP-MS run showed excellent agreement for As between the two labs.

8 References

ACTenviro. (2024, February 3). *Solid Waste Incineration*. ACTenviro. https://www.actenviro.com/solid-waste-incineration/

Agusa, T., Fujihara, J., Takeshita, H., & Iwata, H. (2011). Individual variations in inorganic arsenic metabolism associated with AS3MT genetic polymorphisms. *International Journal of Molecular Sciences*, *12*(4), 2351–2382. https://doi.org/10.3390/ijms12042351

American Cancer Society. (2023, June 1). *Arsenic and Cancer Risk*. https://www.cancer.org/cancer/risk-prevention/chemicals/arsenic.html

ARI. (n.d.). *How is RNG Created?* Adsorption. https://www.adsorption.com/how-is-rng-created/

Arsenic. (1977). National Academy of Sciences. https://www.ncbi.nlm.nih.gov/books/NBK231016/

Benjamin, M. M., & Lawler, D. F. (2013). *Water quality engineering: physical/chemical treatment processes*. John Wiley & Sons.

Bounab, N., Duclaux, L., Reinert, L., Oumedjbeur, A., Boukhalfa, C., Penhoud, P., & Muller, F. (2021). Improvement of zero valent iron nanoparticles by ultrasound-assisted synthesis, study of Cr(VI) removal and application for the treatment of metal surface processing wastewater. *Journal of Environmental Chemical Engineering*, *9*(1), 104773-. https://doi.org/10.1016/j.jece.2020.104773

Bio Energy Washington. (2023, September 21). *Community Meeting* [Webinar]. Bio Energy Washington. https://us02web.zoom.us/rec/share/zxTjCIbeWkxxffZN2laqKzfOrmwCPXlGQ663hqMZf8qo8PVu2AfW0bMxiuDtiJM.zvWq-nwCFW5M5cZB

Briggs, J., Vogt, W. G., & Peterson, E. R. (1988). *Disposal Options for Landfill Gas Condensate*. SCS Engineers. https://scsengineers.com/wp-content/uploads/2015/05/Briggs-Vogt-Peterson_Disposal_Options_for_LFG_Condensate.pdf

Briggs, Jeffrey. (1988). *Municipal landfill gas condensate*. U.S. Environmental Protection Agency, Hazardous Waste Engineering Research Laboratory.

Brookshire, Ron. (1995, May 1). *How To Control LFG, Leachate And Condensate*. Waste 360. https://www.waste360.com/leachate/how-to-control-lfg-leachate-and-condensate

Challenger, F. (1947). Biological Methylation. *Chemical Reviews*, *36*(3), 315–361. https://doi.org/10.1021/cr60115a003

Chen, P.-A., Wang, H. P., Kuznetsov, A. M., Masliy, A. N., Liu, S., Chiang, C.-L., & Korshin, G. V. (2023). XANES/EXAFS and quantum chemical study of the speciation of arsenic in the condensate formed in landfill gas processing: Evidence of the dominance of As-S species. *Journal of Hazardous Materials*, *445*, 130522–130522. https://doi.org/10.1016/j.jhazmat.2022.130522

Cullen, W. R. (2005). The toxicity of trimethylarsine: an urban myth. *Journal of Environmental Monitoring*, *7*(1), 11-. https://doi.org/10.1039/b413752n

Cullen, W. R., & Reimer, K. J. (1989). Arsenic speciation in the environment. *Chemical Reviews*, *89*(4), 713–764. https://doi.org/10.1021/cr00094a002

de Oliveira, F. D. G., Robey, N. M., Smallwood, T. J., Spreadbury, C. J., & Townsend, T. G. (2022). Landfill gas as a source of anthropogenic antimony and arsenic release. *Chemosphere (Oxford)*, *307*, 135739–135739. https://doi.org/10.1016/j.chemosphere.2022.135739

Duckworth, O. W., & Harrington, J. M. (2012). Student Presentations of Case Studies to Illustrate Core Concepts in Soil Biogeochemistry. *Journal of Natural Resources and Life Sciences Education*, *41*(1), 35–43. DOI: 10.17226/9003

Dynamix Agitators. (2020, April 16). *Solid Suspension Mixing – Product Settlement and Separation Challenge? Consider Proper Mixer Configuration*. Dynamix Agitators. https://dynamixinc.com/product-settlement-and-separation-challenge-consider-proper-mixer-configuration/

Elemental Analysis Core. (n.d.). *ICP-MS as a Technique*. Oregon Health & Science University. https://www.ohsu.edu/elemental-analysis-core/icp-ms-technique#:~:text=Mass%20Spectrometer%20(MS)%20separates%20the,concentration%20of%20each%20chosen%20element.

Energy Information Administration. (2023, August 16). *U.S. energy facts explained*. EIA. https://www.eia.gov/energyexplained/us-energy-facts/

Energy Information Administration. (n.d.). *Glossary - R*. EIA. https://www.eia.gov/tools/glossary/index.php?id=R

Environmental Protection Agency. (2003, July). *Arsenic Treatment Technology Evaluation Handbook for Small Systems*. Environmental Protection Agency. https://cfpub.epa.gov/safewater/arsenic/arsenictradeshow/Pubs/handbook_arsenic_treatment-tech.pdf

Environmental Protection Agency. (2023, November 22). *National Overview: Facts and Figures on Materials, Wastes and Recycling*. Environmental Protection Agency. https://www.epa.gov/facts-and-figures-about-materials-waste-and-recycling/national-overview-facts-and-figures-materials

Environmental Protection Agency. (2024, July). *Inductively Coupled Plasma – Mass Spectrometry* (Method 6020B). Environmental Protection Agency. https://www.epa.gov/sites/default/files/2015-12/documents/6020b.pdf

European Commission. (n.d.). *Methane emissions*. European Commission. https://energy.ec.europa.eu/topics/oil-gas-and-coal/methane-emissions_en

Facility Engineering & Science Section, King County Solid Waste Division. (2019, April 1). *2018 Annual Report Cedar Hills Regional Landfil*l. King County Department of Natural Resources and Parks: Solid Waste Division.

Frankenberger, W. T. (William T.). (2002). *Environmental chemistry of arsenic*. Marcel Dekker.

Frohne, T., Rinklebe, J., Diaz-Bone, R. A., & Du Laing, G. (2011). Controlled variation of redox conditions in a floodplain soil: Impact on metal mobilization and biomethylation of arsenic and antimony. *Geoderma*, *160*(3), 414–424. https://doi.org/10.1016/j.geoderma.2010.10.012

Höganäs. (2021). *CR-15: Reduced iron powder*. Höganäs. https://www.hoganas.com

Höganäs. (2023). *CleanER ™ - PRB*. Höganäs. https://www.hoganas.com

Hughes, M. F. (2002). Arsenic toxicity and potential mechanisms of action. *Toxicology Letters*, *133*(1), 1–16. https://doi.org/10.1016/S0378-4274(02)00084-X

IARC Working Group on the Evaluation of Carcinogenic Risks to Humans. (2012). Arsenic, Metals, Fibres and Dusts [Monograph]. *IARC Monographs on the Evaluation of Carcinogenic Risks to Humans, No. 100C, Arsenic and Arsenic Compounds*. https://www.ncbi.nlm.nih.gov/books/NBK304380/

IEA. (2020). *The outlook for biogas and biomethane to 2040*. IEA. https://www.iea.org/reports/outlook-for-biogas-and-biomethane-prospects-for-organic-growth/the-outlook-for-biogas-and-biomethane-to-2040

King County. (n.d.). *Facts about arsenic*. King County. https://kingcounty.gov/en/legacy/depts/health/environmental-health/toxins-air-quality/arsenic-lead/about-arsenic#:~:text=Arsenic%20has%20a%20long%20history,quantities%20in%20semi%2Dconductor%20manufacturing.

King County. (2024). *Environmental Lab*. King County. https://kingcounty.gov/en/legacy/depts/dnrp/wlr/sections-programs/environmental-lab

Kösters, J., Diaz-Bone, R. A., Planer-Friedrich, B., Rothweiler, B., & Hirner, A. V. (2003). Identification of organic arsenic, tin, antimony and tellurium compounds in environmental samples by GC-MS. *Journal of Molecular Structure*, *661*, 347–356. https://doi.org/10.1016/j.molstruc.2003.09.005

Landfill Methane Outreach Program. (2023a, August 3). *LMOP National Map*. Environmental Protection Agency.

Landfill Methane Outreach Program. (2023b, November 16). *Frequent Questions about Landfill Gas*. Environmental Protection Agency. https://www.epa.gov/lmop/frequent-questions-about-landfill-gas

Landfill Methane Outreach Program. (2024a, February 12). *Basic Information about Landfill Gas*. Environmental Protection Agency. https://www.epa.gov/lmop/basic-information-about-landfill-gas

Landfill Methane Outreach Program. (2024b, February 12). *Benefits of Landfill Gas Energy Projects*. Environmental Protection Agency. https://www.epa.gov/lmop/benefits-landfill-gas-energy-projects#four

Landfill Methane Outreach Program. (2024c, January). *LFG Energy Project Development Handbook*. Environmental Protection Agency. https://www.epa.gov/system/files/documents/2024-01/pdh_full.pdf

Liu, S., Kuznetsov, A. M., Han, W., Masliy, A. N., & Korshin, G. V. (2022). Removal of dimethylarsinic acid (DMA) in the Fe/C system: roles of Fe(II) release, DMA/Fe(II) and DMA/Fe(III) complexation. *Water Research (Oxford)*, *213*, 118093-. https://doi.org/10.1016/j.watres.2022.118093

Malik, S. (2020). *Comparison of Physiochemical Methods to Remove Arsenic from Landfill Leachate and Gas Condensate*. [Master's thesis, University of Washington] ProQuest Dissertations Publishing.

Marconi, P., & Rosa, L. (2023). Role of biomethane to offset natural gas. *Renewable and Sustainable Energy Reviews*, 187, 113697-. https://doi.org/10.1016/j.rser.2023.113697

Mirfendereski, T. (2023, November 22). 'He's just so sick:' Landfill employees concerned about arsenic exposure amid King County violations. King 5. https://www.king5.com/article/news/investigations/investigators/landfill-employees-concerned-about-arsenic-exposure-amid-king-county-violations/281-f8152860-0049-474f-b49a-24f163a17f38

Mohan, D., & Pittman, C. U. (2007). Arsenic removal from water/wastewater using adsorbents—A critical review. *Journal of Hazardous Materials*, *142*(1), 1–53. https://doi.org/10.1016/j.jhazmat.2007.01.006

Mudhoo, A., Sharma, S. K., Garg, V. K., & Tseng, C.-H. (2011). Arsenic: An Overview of Applications, Health, and Environmental Concerns and Removal Processes. *Critical Reviews in Environmental Science and Technology*, *41*(5), 435–519. https://doi.org/10.1080/10643380902945771

Paul Mueller Company. (2018, January 31). *How to Choose the Right Impeller*. Paul Mueller Company. https://de.paulmueller.com/akademie/how-to-choose-the-right-impeller

Nelms, S. (2018, November 16). *How to Improve Your ICP-MS Analysis, Part 1 Contamination*. Thermo Fisher Scientific. https://www.thermofisher.com/blog/analyteguru/how-to-improve-your-icp-ms-analysis-part-1-contamination/

Nowicki, H. (2016, February 1). *The basics of activated carbon adsorption*. Water Technology. https://www.watertechonline.com/wastewater/article/15549902/the-basics-of-activated-carbon-adsorption

Panico, A. (2023). [Master's thesis, Università degli Studi di Napoli Federico II].

Parris, G. E., & Brinckman, F. E. (1976). Reactions which relate to environmental mobility of arsenic and antimony. II. Oxidation of trimethylarsine and trimethylstibine. *Environmental Science & Technology*, *10*(12), 1128–1134. https://doi.org/10.1021/es60122a010

Particle Technology Labs. (n.d.). *BET Specific Surface Area*. Particle Technology Labs. https://particletechlabs.com/analytical-testing/bet-specific-surface-area/

PerkinElmer. (n.d.). *NexION 2000B ICP Mass Spectrometer*. PerkinElmer. https://www.perkinelmer.com/product/nexion-2000b-icp-ms-configuration-n8150044

Phidgets. (2023, June 26). *PH/ORP Sensor Guide*. Phidgets. https://www.phidgets.com/docs/PH/ORP_Sensor_Guide

Pinel-Raffaitin, P., Le Hecho, I., Amouroux, D., & Potin-Gautier, M. (2007). Distribution and Fate of Inorganic and Organic Arsenic Species in Landfill Leachates and Biogases. *Environmental Science & Technology*, *41*(13), 4536–4541. https://doi.org/10.1021/es0628506

Pinochet-Troncoso, I. (2023). *Optimization of Microelectrolysis Treatment to Remove Arsenic from Landfill Gas Condensate and Correlations Between Changes of Redox Potential and Arsenic Removal* [Master's thesis, University of Washington]. ProQuest Dissertations Publishing.

Puget Sound Clean Air Agency. (2019). *Regulation I*. Puget Sound Clean Air Agency. https://www.epa.gov/sites/default/files/2017-02/documents/sip-wa-approved-regulations-pscaa-table7.pdf

Rifkin, G. (2021). *Arsenic in Landfill Gas Condensates and Gas Treatment Solids: A Study of Removal by Alternative Treatment Approaches and Mobilization* [Master's thesis, University of Washington]. ProQuest Dissertations Publishing.

Sharma, A., Jelemenský, M., Paulen, R., & M. Fikar. (2016). Estimation of membrane fouling parameters for concentrating lactose using nanofiltration. *Computer Aided Chemical Engineering, 38,* 151-156. https://doi.org/10.1016/B978-0-444-63428-3.50030-8.

Thayer, J. (2002). Biological methylation of less-studied elements. *Applied Organometallic Chemistry*, *16*(12), 677–691. https://doi.org/10.1002/aoc.375

Upadhyay, M. K., Shukla, A., Yadav, P., & Srivastava, S. (2019). A review of arsenic in crops, vegetables, animals and food products. *Food Chemistry*, *276*, 608–618. https://doi.org/10.1016/j.foodchem.2018.10.069

Waga Energy. (n.d.). *Everything about landfill gas*. Waga Energy. https://waga-energy.com/en/everything-about-landfill-gas/

Walters, S. (2022). *A study of removal techniques for arsenic species in landfill gas condensate.* [Master's thesis, University of Washington]. ProQuest Dissertations Publishing.

Wang, P., Sun, G., Jia, Y., Meharg, A. A., & Zhu, Y. (2014). A review on completing arsenic biogeochemical cycle： Microbial volatilization of arsines in environment. *Journal of Environmental Sciences (China)*, *26*(2), 371–381. https://doi.org/10.1016/S1001-0742(13)60432-5

Wasatch Integrated Waste Management District. (n.d.). *Davis Landfill*. Wasatch Integrated. https://www.wasatchintegrated.org/davis-landfill/

Waste Management. (2015). *Columbia Ridge Landfill & Green Energy Plant* [Fact sheet]. Waste Management. https://www.wmsolutions.com/pdf/factsheet/CLRFactSheet_Final.pdf

Waste Management. (n.d.a). *Columbia Ridge Landfill and Green Energy Plant*. WM Northwest. https://www.wmnorthwest.com/landfill/columbiaridge.htm

Waste Management. (n.d.b). *Landfill doubling renewable energy output for Seattle.* https://www.wm.com/about/wm-monday/seattle_energy.jsp

Yokogawa. (2014, March). *Basics of ORP*. Yokogawa. https://www.yokogawa.com/us/library/resources/white-papers/basics-of-orp/

Zhao, R., Novak, J. T., & Douglas Goldsmith, C. (2013). Treatment of organic matter and methylated arsenic in landfill biogas condensate. *Waste Management (Elmsford)*, *33*(5), 1207–1214. https://doi.org/10.1016/j.wasman.2013.01.013

Zhulin Carbon. (n.d.). *Density of activated carbon*. Zhulin Activated Carbon. https://www.activatedcarbon.net/Resources/density-of-activated-carbon/